POLITECNICO DI TORINO

Master's Degree Program

in Environmental and Land Engineering

Master Thesis

Assessment of Microplastics Variation in a Sequence Batch Reactor

Supervisors

Prof. Silvia Fiore

Prof. Amparo Bes Piá

Prof. José Antonio Mendoza Roca

Candidate

Stefano Castelluccio

July 2020

Acknowledgements

My research would not have been possible without the economic support of the Erasmus Agreement between Politecnico di Torino and Universitat Politecnica de Velencia.

I'm extremely grateful to my supervisor Silvia Fiore for her unwavering guidance and support throughout the different phases of my research. I would also like to extend my deepest gratitude to Amparo Bes Piá and José Antonio Mendoza Roca for their invaluable knowledge, their trust in my work and my abilities. Moreover, I would like to thank them for the formative opportunity of working at Universitat Politècnica de Valencia.

The completion of my research would not have been possible without the support of Clara Bretas Alvim. I very much appreciate her valuable contribution, her practical and sometimes ingenious suggestions, her experience and her patience. I also had great pleasure of working with Eva Ferrer Polonio and I want to thank her for her helpful advices and her extensive knowledge and experience. Thanks should also go to my colleagues at Universitat Politècnica de Valencia for their constant support.

Finally, I cannot begin to express my thanks to Claudia, who transformed my research into an amazing experience.

Summary

Table of figures

1 Introduction

Microplastics (MPs) are any synthetic solid particle or polymeric matrix, with regular or irregular shape and size ranging from 1 μm to 5 mm, of either primary or secondary manufacturing origin, which are insoluble in water (Frias and Nash, 2019).

Plastic materials generally have low density, low thermal and electric conductivity, and corrosion resistance, characteristics that make them extremely versatile (Frias and Nash, 2019). These properties, paired with manufacturing ease and low cost, allowed plastic materials to rapidly revolutionize a variety of technological applications. At the same time, the rise in plastics production (Figure 1.1) and consumption has gradually become a global threat to the environment. Over the last decade, the focus on the issue of microplastics as a novel pollutant has seen a large increase in investments on a global scale, resulting in an exponential growth of microplastics literature (Frias and Nash, 2019).

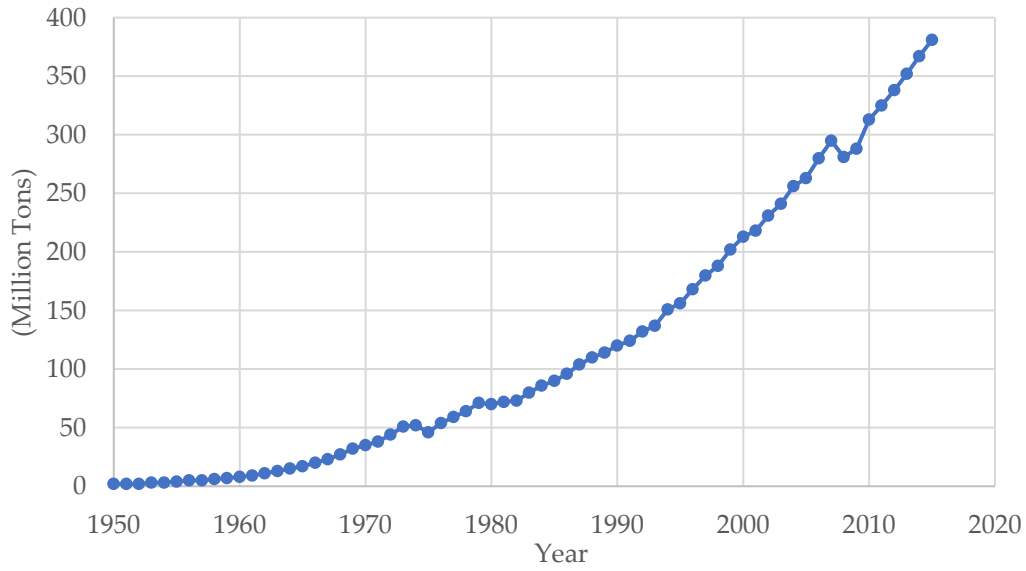

Figure 1.1 Global plastics production trend (EPRO, 2016)

MPs are found worldwide in all types of habitats, from water to sediments, from urban to remote areas and from continents to oceans (Ngo et al., 2019). The most concern has been raised by aquatic ecosystems. Ingested MPs can cause damage to organisms because of their sharp ends, leading to inflammation (Sun et al., 2019). Moreover, the physical and chemical properties of microplastics facilitate the sorption of hydrophobic contaminants to the particle surface. Through ingestion MPs can expose organisms

to toxic contaminants such as heavy metals, polycyclic aromatic hydrocarbons (PAHs) and polychlorinated biphenyls (PCBs) (Carbery et al., 2018; Li et al., 2019; Avio et al., 2015). Moreover, MPs may leach plastics additives, since these chemicals are incorporated and not chemically bound to the polymeric structure (Hermabessiere et al., 2017). MPs in marine environments have been linked to a significant reduction in the indices of energy intake and reproductive health. Strong negative effects on fish fecundity and offspring growth at the larval stage have been shown (Sussarellu et al., 2016). The negative impacts of MPs on animals are also possible at higher levels of the food chain due to trophic transfer (Carbery et al., 2018; Ngo et al., 2019).

There are two main ways to classify MPs (Figure 1.2). The first one refers to the formation process. Microplastics directly manufactured in small-sized particles are defined as primary. An example is the microspheres used in toothpastes or body cleansing products. MPs originated from the fragmentation of larger plastic objects, like microfibers released by synthetic clothes during washing, are defined as secondary (GESAMP, 2015; Shim et al., 2018). MPs can also be classified according to their shape. The most common are fibers (significantly longer than wider), fragments (irregular pieces), spheres and films.

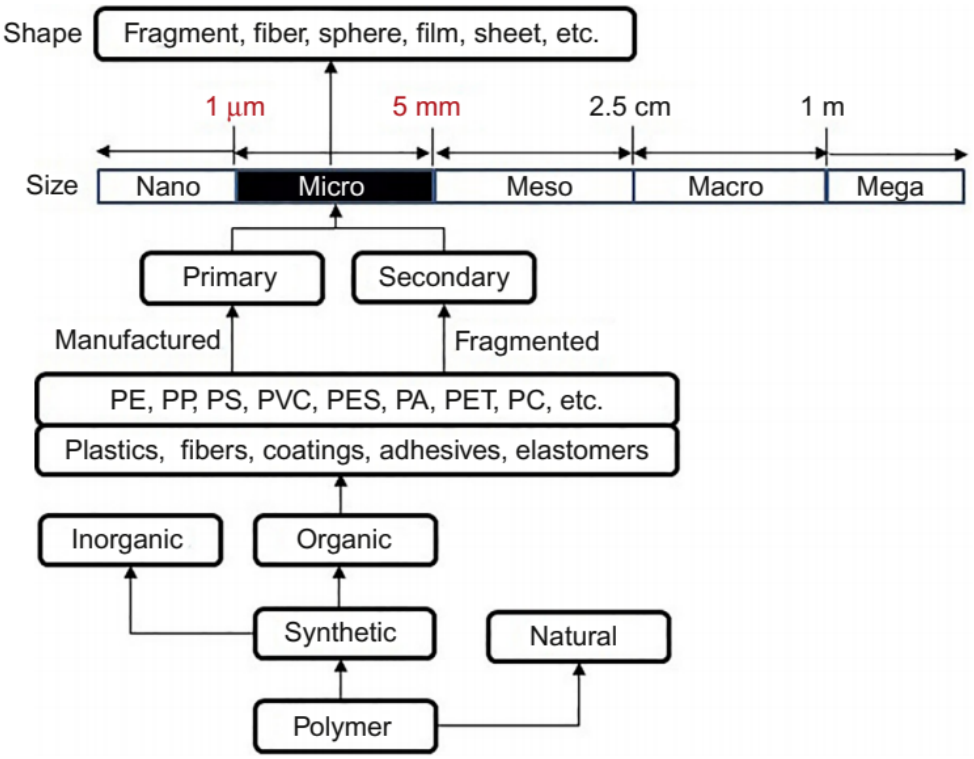

Figure 1.2 Schematic diagram of microplastics definition and classifications (Shim et al., 2018)

There are many known sources of MPs. Firstly, tiny plastic debris can be originated from the wear or breakdown of larger products like tires, artificial turf, packaging or other plastic items (Kole et al., 2017). The second source is domestic, including microfibers released from textiles during washing (Hernandez et al., 2017) and microspheres contained in personal care products and cosmetics (Cocca et al., 2018; Zitko and Hanlon, 1991). Several countries, including the US, Canada and the UK have banned the use of plastic microspheres in some consumer products (Conkle et al., 2018). There is also an industrial source due to plastic particles used in manufacturing processes such as molding or air-blasting technology (Ngo et al., 2019; Cole et al., 2011). Finally, landfills are a potential source of MPs. The plastics buried in landfills can slowly fragment and enter the leachate (He et al., 2019). Some microplastics can reach directly natural waters, but most of them are directed to wastewater treatment plants (WWTPs) through the sewage system. Siegfried et al. (2017) presented a modeling approach for quantifying the transport of microplastics into the marine environment. The model considers the contributions from tire and road wear particles, laundry of textiles, household dust, and personal care products, which account for 42%, 29%, 19% and 10% of the total respectively (Figure 1.3). However, the complexity of sources and pathways for MPs to enter WWTPs has not been understood completely. Investigating the topic could help reduce future pollution.

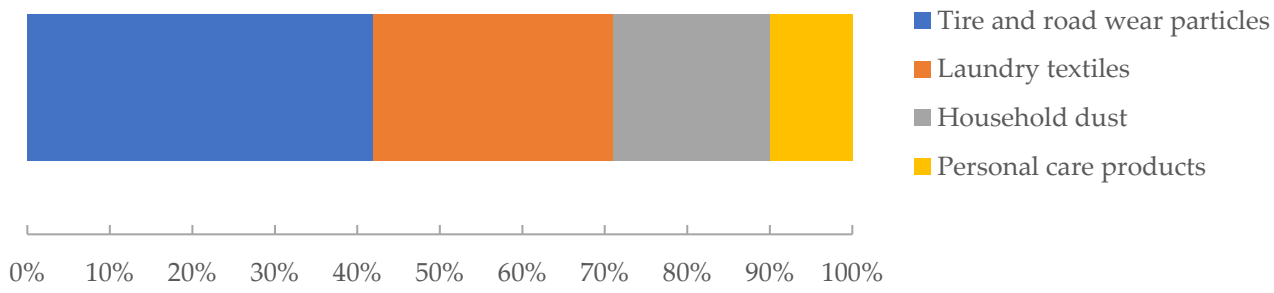

Figure 1.3 Microplastics sources (Siegfried et al., 2017).

1.1 Approach and goals

WWTPs are the ultimate barrier preventing MPs from being discharged into natural waters. For this reason, it's important to assess the distribution and fate of microplastics entering WWTPs. The first aim of this study is to evaluate MPs behavior in secondary treatment. The primary focus is to observe the variation in concentration of plastic microfibers (MPFs) in a secondary sludge sample from a municipal WWTP. The second aspect is to quantify the distribution of the entering MPFs into the waste activated sludge (WAS) and the effluent (treated wastewater). A laboratory-scale sequence batch reactor (SBR) was seeded with WAS from a municipal WWTP and fed with artificial wastewater. The SBR cycle was divided into four phases: feeding, aeration and stirring, settling, and effluent extraction. The SBR was monitored by analyzing both mixed liquor and effluent samples to evaluate the variation of MPFs concentration over time. Microfibers were selected as the focus of the research because some difficulties estimating the concentration of MPs with other shapes were encountered. Specifically, it has been challenging to reliably distinguish MPs fragments or sheets from residual organic structures. The choice of microfibers has been validated by an analysis of the published review articles on MPs composition. Fibers have been found to account for the majority of microplastics entering the WWTPs, ranging from 52,7% to 56,7% of the total (Sun et al., 2019; Ngo et al., 2019). MPs shape distribution varies widely between different WWTPs and in some cases microfibers represent under 20% of the total (Long et al., 2019). However, in most researches and our case study, MPFs account for more than 65% of the total (Ngo et al., 2019). The second aim is to assess the proportion between natural and synthetic fibers in the SBR. This evaluation is essential because the inclusion of the natural fibers would lead to misleading and overestimated results and, ultimately, to an incorrect assessment of the environmental threat posed by microplastics.

2 State of the art

WWTPs don't currently have treatment processes specifically designed for MPs removal (Ou and Zeng, 2018). Even though there is evidence of a significant MPs reduction in WWTPs (Carr et al., 2016), a portion of the entering MPs is still released to the environment (Murphy et al., 2016). Even in WWTPs where concentrations of MPs in the effluent are low, the total discharged amount is concerning due to extremely high volumes of wastewater treated. Concentrations of MPs in WWTPs influents ranged from 1.51×10^{1} to 1.83×10^{4} particles/L and from 8.25×10^{-3} to 4.47×10^{2} particles/L in the effluents (Magnusson and Norén, 2014; Simon et al., 2018). Sun et al. (2019) found that the average value of discharged MPs is 2 million particles/day. These discrepancies can be attributed to different levels of industrialization of the served area, seasonal changes, and especially different sampling and detection methods (Sun et al., 2019).

Furthermore, MPs characteristics influence their removal. The shape affects the interactions between MPs and both the treatment units and the present microorganisms. For example, the rough surfaces and sharp edges of the fragments help the colonization of bacteria, resulting in a more efficient removal through settling processes (Long et al., 2019). By contrast, fibers have a smooth surface and a high length-to-width ratio, leading to less resistance in the wastewater column and allowing them to pass through the small pores of the filtration units (Long et al., 2019; Talvitie et al., 2017a). This results in an increase, by percentage, in fibers over fragments in WWTPs effluents (Gies et al., 2018; Long et al., 2019). The density impacts the buoyancy, which is a crucial parameter in sedimentation and flotation processes (Ngo et al., 2019). Table 2.1 collects the densities of the polymers most commonly detected in WWTPs. Finally, a positive correlation between MPs size and removal efficiency has been shown, leading to WWTPs effluents generally having lower percentages of large microplastics compared to the influents (Talvitie et al., 2017b; Ziajahromi et al., 2017).

Polymer	Abbreviation	Density (kg/m^3)
Acrylic	–	1.09 – 1.20
Polyamide (nylon)	PA	1.02 – 1.16
Polyester	PES	1.24 – 2.30
Polyethylene	PE	0.89 – 0.98
Polyethylene terephthalate	PET	0.96 – 1.45
Polypropylene	PP	0.83 – 0.92
Polystyrene	PS	1.04 – 1.10
Polyvinyl chloride	PVC	1.16 – 1.58
Synthetic rubber	–	0.85 – 0.90

Table 2.1 Densities of polymers detected in WWTPs (Hidalgo-Ruz et al., 2012; Ngo et al., 2019)

2.1 MPs removal efficiency of WWTPs conventional treatments

The removal efficiency of MPs in a WWTP varies from 64,4% to 99,9%, depending on the specific treatments employed (Ngo et al., 2019; Sun et al., 2019). In most studies, the overall removal rate was above 88% and above 97% in WWTPs applying tertiary treatments (Ngo et al., 2019; Sun et al., 2019).

Preliminary and primary treatments are quite effective in MPs removal, especially reducing the fraction of large particles (Dris et al., 2015). Preliminary treatments have reported MPs removal efficiency between 35% and 59% (Sun et al., 2019). Primary treatments generally remove heavier MPs through sedimentation and lighter ones with dissolved air flotation technology and skimming of the surface. In the studies reviewed by Sun et al. (2019) primary treatments could eliminate between 24% and 95% of the entering MPs, accounting for a cumulative removal varying from 50% to 98% (Table 2.2). However, in a more recent study, Liu et al. (2019) calculated an MPs removal efficiency of just 41% after the primary treatment. The substantial variance in the results can be attributed to differences in the treatments employed and in the composition and density of the MPs (Ngo et al., 2019). Also, the lack of uniformity in the methods used for sampling and detection can lead to inconsistent results which are difficult to compare (Sun et al., 2019).

Secondary treatments typically include a biological treatment followed by clarification. Flocs formation and bacteria growth on the surface of MPs are likely to impact microplastics removal efficiency. Therefore, the use of flocculants could enhance MPs removal (Murphy et al., 2016). Nevertheless, the

exact interaction mechanisms between MPs and flocculants are still unclear (Rummel et al., 2017). Sun et al. (2019) found that secondary treatments could eliminate between 72% and 90% of the inflowing MPs, for a cumulative removal efficiency ranging from 86% to 99.8% (Table 2.2). However, in two more recent studies Liu et al. (2019) and Yang et al. (2019) measured an MPs removal efficiency of 28% and 38%, respectively. Once again, the differences in the results may be attributed to the absence of standardization in the sampling and detection methods (Sun et al., 2019), but also to discrepancies in retention times and nutrient levels in different WWTPs (Carr et al., 2016; Ngo et al., 2019). Most studies observed that fragments are eliminated more efficiently than fibers (Sun et al., 2019), but Talvitie et al. (2017b) highlighted the opposite trend. The membrane bioreactor technology combines an AS process with a membrane filtration (Bernardo and Drioli, 2010). MBRs have shown MPs removal rates ranging from 99.4% to 99.9%, the best among the currently available technologies in WWTPs (Lares et al., 2018; Talvitie et al., 2017a).

The MPs removal efficiency of tertiary treatments depends strongly on the employed technology. In Sun et al. (2019) review tertiary treatments could eliminate from 40% to 98.5% and cumulatively from 98% to 99.9% of the entering MPs (Table 2.2). Nevertheless, Liu et al. (2019) analyzed a WWTP that used chlorinated disinfection which removed only 17% of the MPs in the secondary effluent. This result highlights chlorinated disinfection as the least effective technology for MPs removal, leading to a cumulative removal efficiency of 64.4%. Disc filters displayed inconsistent removal efficiency, ranging from 40% to 98.5% (Hidayaturrahman and Lee, 2019; Sun et al., 2019). Finally, dissolved air flotation and rapid sand filtration showed to be very effective in treating secondary effluents, as they could eliminate respectively 95% and from 74% to 98% of the inflowing MPs (Hidayaturrahman and Lee, 2019; Talvitie et al., 2017a).

Stage	Specific Removal Efficiency		Cumulative Removal Efficiency	
	Min	Max	Min	Max
Preliminary	35%	59%	35%	59%
Primary	23%	95%	50%	98%
Secondary	72%	99.9%	86%	99.8%
Tertiary	40%	98.5%	98%	99.9%

Table 2.2 Specific and cumulative removal efficiency of WWTPs treatment stages (Sun et al., 2019)

The relatively low percentage of microplastics retained in the final effluent indicates that most MPs are sequestrated by the sewage sludge, but studies on MPs abundance in sludges are scarce (Rolsky et al., 2020). The concentration of MPs in WWTPs sludges varied between 2.5 and 113 particles/g dry weight (DW) (Lusher et al., 2018; Magni et al., 2019). The differences may result from different input sources, for example a correlation has been observed between industrial activities and MPs concentration in WWTPs sludges (Li et al., 2018). Furthermore, the concentration of MPs in WWTPs sludges can be affected by seasonal changes, as sustained precipitations can increase the number of microplastics originated from road dust (Lee and Kim, 2018). Finally, non-standardization in the methods used for sampling and collection can contribute to the differences in the results (Rolsky et al., 2020). Data show a higher concentration of MPs in primary sludges, especially the one produced by the skimming process (Lusher et al., 2018; Murphy et al., 2016). WWTPs sludge can be disposed of in landfills, incinerated, or used for land application as an agricultural amendment. Before being used or disposed of, sludge is pretreated. Still, concentrations as high as 15.4 particles/g DW have been found in sludges after the pretreatments (Mahon et al., 2016). One of the drawbacks of sludge disposal is that MPs are not permanently controlled, as they have been found in landfill leachates. The most concerns, however, have been raised by land application, which worsen the threat posed by MPs pollution in soil. Although the fate of MPs after land application has not been fully assessed, microplastics have been found in the soil up to 15 years after application retaining the characteristics of MPs in WWTPs sludge (Zubris and Richards, 2005). MPs can be a vector for contamination of heavy metals and hydrophobic pollutants, thanks to the high specific surface area. This problem could be exacerbated by the weathering of the MPs surface during the treatments endured (Li et al., 2019; Turner and Holmes, 2015) and by the favorable environment for pollutants adsorption encountered in sewage systems (Ngo et al., 2019). MPs in soil have been shown to affect the bulk density, water holding capacity, and the microbial activity (De Souza Machado et al., 2018), potentially undermining the positive aspects of biosolids land application (Rolsky et al., 2020).

2.2 Procedures for MPs detection in WWTPs

The detection process of microplastics in WWTPs is divided into three steps: collection of the sample, sample pretreatment and characterization. In the absence of standardized procedures, each phase can be performed with different techniques. The techniques used can vary depending on the sampling environment, sample characteristics and circumstances (Figure 2.1). A harmonization of the detection methods is urgently needed to compare results among different studies (Sun et al., 2019).

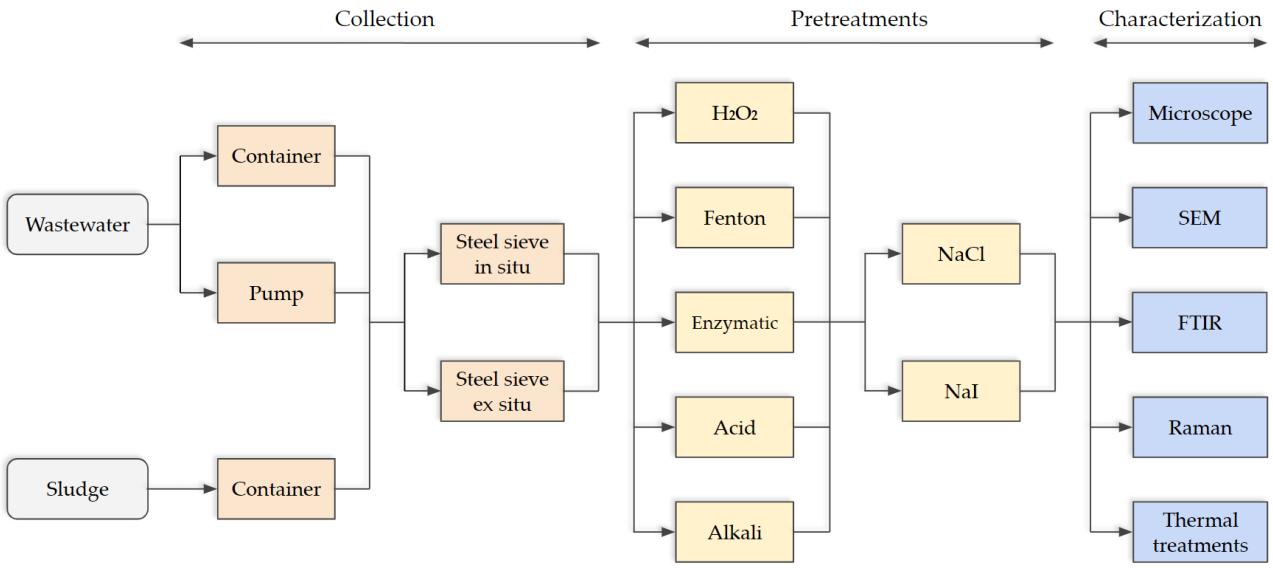

Figure 2.1 Description of microplastics detection in WWTPs: steps and major techniques.

2.2.1 Collection

Even though various methods have been used for MPs collection in wastewater, two are the most relevant. In the first one, water is collected with a container, which is very practical but allows for restricted sample volumes. This method is advised for collecting samples with a high content of solids and organic matter, such as WWTPs influents and sludges (Sun et al., 2019). In the second method water is collected with a pump and filtered in situ. The pumping and collection system has the advantage of increasing the sample volume considerably. However, the process must be performed with caution because the filtration is done in an environment much more exposed to cross-contamination than a laboratory (Bretas Alvim et al., 2020). The design of the sampling process must consider the problem of the representativeness of the sample. Sample representativeness can be compromised by the relatively low concentration of microplastics and, also, by its uneven temporal and spatial distribution, which depends on MPs characteristics and flow conditions (Prata et al., 2019a; Sun et al., 2019). To address this problem, it is important to increase the sampled volume, to carefully select the sampling depth and location, and to take composite samples. The use of automated samplers can ease the load of composite sampling (Simon et al., 2018; Talvitie et al., 2017b).

After the collection the sample is filtered, in situ or in laboratory, to concentrate microplastics in a lower volume. The sample is usually filtered through a sieve, then the captured material is rinsed with

distilled water and stored. The mesh size chosen influences decisively the amount and the size range of the MPs detected (Magnusson and Norén, 2014; Prata et al., 2019a). However, this choice is not uniform among different studies, varying from 1 µm to 500 µm (Sun et al., 2019). A standardization of mesh sizes used is needed to allow comparisons between different studies (Prata et al., 2019a). Another factor that can that the influence the filtration procedure is the morphology of MPs. Granules smaller than the mesh size can still be captured due to their sharp edges, whereas fibers longer then the mesh size can pass longitudinally through the sieve (Bretas Alvim et al., 2020; Sun et al., 2019).

2.2.2 Pretreatments

The stored sample still contains organic matter and inorganic solids; therefore, pretreatments steps are often required to prepare the sample for the characterization process. Once again, there is a lack of standardization for sample pretreatments, resulting in variable MPs recovery rates and difficulties in comparing data from different sources (Bretas Alvim et al., 2020; Rolsky et al., 2020).

Samples collected from WWTPs have a high organic content, especially influent and sludge samples. Therefore, the most important pretreatment step is a digestion protocol capable of removing organic matter. Organic matter can increase characterization uncertainties, because during the quantification process it can be confused for MPs, leading to an overestimation of MPs concentration (Prata et al., 2019a). Furthermore, organic matter can aggregate on the surface of MPs forming biofilms, which can interfere with the polymer identification (Bretas Alvim et al., 2020; Enders et al., 2017). The digestion protocol must be efficient in removing organic matter, but it is also crucial that the chemical and structural integrity of MPs is not affected. For this reason, the digestion temperature is a key factor, as some polymers start melting above 60 °C (Munno et al., 2018). Also, the duration of the digestion protocol can be relevant, due to time restrictions.

Chemical oxidation is the most common method of removing organic matter, especially by using a solution of hydrogen peroxide (H_2O_2) (15 - 35%). The solution can be added in different volumes, depending on the organic content of the sample. The increase in temperature helps the digestion, as shown by an improvement in the results when the use of H_2O_2 was coupled with heating at 50°C (Avio et al., 2015b; Cole et al., 2014). H_2O_2 digestion has been shown to effectively remove organic matter without degrading or affecting the characterization process of most polymers (Tagg et al., 2015; Zhao et al., 2017). However, hydrogen peroxide has some drawbacks which advise its usage only when necessary. Zhao et al. (2017) showed that H_2O_2 can discolor some polymers, which can increase the complexity of the quan-

tification process, usually performed on a white glass fiber support (Nuelle et al., 2014). Hydrogen peroxide has also been linked to nylon degradation (Karami et al., 2017). In samples with high amounts of organic matter, H_2O_2 can form a dense foam that suspends lighter MPs and cause them to adhere to the container surface, reducing microplastics recovery (Zhao et al., 2017). Finally, the digestion protocol may require a long reaction time, depending on the initial organic content. Fenton's reagent, a solution of hydrogen peroxide and ferrous iron, can be used to fasten the process. Ferrous iron catalyzes the formation of hydroxyl radicals that act as strong oxidizers (Babuponnusami and Muthukumar, 2014). However, the reaction requires low pH (3 is the optimal value) (Babuponnusami and Muthukumar, 2014).

An emerging method to remove organic matter from collected samples is enzymatic degradation, which substitutes hydrogen peroxide with enzymes such as protease, cellulase and chitinase. These enzymes may be less hazardous and less likely to damage MPs (Löder et al., 2017; Prata et al., 2019a). Even though new protocols seem to address some of the drawbacks (von Friesen et al., 2019), enzymatic digestion is usually more complex, the reagents more expensive and the effectiveness could be dependent on the organic matter composition (Bretas Alvim et al., 2020; Prata et al., 2019a). Less frequently, organic matter has been removed with acid or alkali digestion. These techniques should be used with extreme caution since both can damage or destroy microplastics, which may lead to an underestimation of MPs concentration (Dehaut et al., 2016; Hurley et al., 2018).

Digested samples, depending on the origin, may still contain a high content of inorganic solids. Differences in density can be used to separate MPs from inorganic particles. In fact, polymer densities generally range from 0.8 to 1.6 kg/m^3 while typical sediment densities are around 2.7 kg/m^3 (Hidalgo-Ruz et al., 2012). The separation is performed by mixing the sample with a high-density salt solution, collecting the supernatant, and finally filtering it to recover the microplastics. NaCl is often used because it is cheap and environmentally friendly, but the relatively low density (1.2 kg/m^3) leads to low recovery rates and an underestimation of MPs concentration (Prata et al., 2019a). The use of NaI solutions (1.6 kg/m^3) is advised, even though it is more expensive and blackens cellulose filters, which may complicate visual identification (Prata et al., 2019a).

2.2.3 Characterization

Analyses of microplastics are divided into physical and chemical characterization. Physical characterization is used to estimate MPs concentration, to assess their size, shape and color distribution, and to obtain surface information such as the weathering state. Instead, chemical characterization can evaluate the composition of the analyzed particle.

In general, physical characterization is done through a microscope, counting the suspected MPs and characterizing their morphology. Even when chemical characterization is later performed, the use of a microscope as complementary tool is almost always required. Visual identification has two major drawbacks, which are its time-consuming nature and, above all, the subjectivity of the required evaluations. For example, deciding whether a particle is natural or synthetic is often difficult. Biological material can be confused for black plastic fragments, whereas natural fibers can be easily counted as synthetic fibers (Yang et al., 2019; Ziajahromi et al., 2017). Moreover, it can be challenging to notice particles similar in color to the background, and it is even likely to duplicate or miss counts in the presence of large amounts of MPs (Murphy et al., 2016; Sun et al., 2019). The inherent subjectivity of visual characterization may lead to an underestimation or an overestimation of MPs concentrations, with results varying greatly amongst operators. The inconsistencies in the results can be attributed to different levels of experience and fatigue of the operators. Actions have been taken to partially address some of these problems, like using sequentially numerated grids to divide the filter area into smaller portions (Carr et al., 2016). It has also been developed a criteria to help distinguishing larger microplastics: no cellular or organic structures must be visible, fibers must be equally thick throughout their entire length and particles must present clear and homogeneous colors (Hidalgo-Ruz et al., 2012; Norén, 2007). Still, up to 70% of the particles visually classified as MPs show a non-plastic composition after chemical characterization (Hidalgo-Ruz et al., 2012).

The application of dyes, like Rose bengal and Nile red, could help the visual identification of microplastics (Prata et al., 2019b; Ziajahromi et al., 2017). However, unsatisfactory results related to Rose bengal have been reported and a thorough digestion step is needed to avoid MPs staining due to biofilm residues (Bretas Alvim et al., 2020; Prata et al., 2019a). Nile red, on the contrary, is adsorbed on the surface of microplastics and it is visible with a fluorescence microscope. Nile red has been designated as the most promising staining protocol, thanks to its high recovery rates of MPs (Dowarah et al., 2020; Prata et al., 2019a). Nevertheless, Shim et al. (2016) encountered some stained particles that couldn't be classified by chemical characterization. Scanning electron microscopy, finally, can be used to study the surface characteristics of microplastic particles.

The chemical characterization can be performed with non-destructive spectroscopic techniques as well as destructive methods. Vibrational spectroscopic techniques, comprising Fourier transform infrared spectroscopy (FTIR) and Raman, are the most commonly used (Figure 2.2) (Prata et al., 2019a). Both operate by exciting the molecules of the sample, resulting in the recording of a characteristic spectrum that can be compared to a reference spectra library (Bretas Alvim et al., 2020). Due to the time requirements of chemical characterizations, it is normally used to assist the physical identification. Chemical

characterization is essential to ensure the quality of the physical characterization and to obtain information on the relative abundance of different polymer types (MSFD Technical Subgroup on Marine Litter, 2013; Sun et al., 2019). The MSFD Technical Subgroup on Marine Litter (2013) suggested to perform chemical characterization on 10% of the suspected MPs after physical characterization.

FTIR, the most adopted method (Figure 2.2), exposes the analyzed particle to infrared radiation and each peak of the obtained spectrum corresponds to a specific bond between atoms (Sun et al., 2019). FTIR measurements can be performed in transmittance or reflectance mode, which are best suited for samples with different characteristics (Shim et al., 2017). However, pretreated samples may still contain some residues of organic and inorganic material, and the microplastics can be weathered or can contain additives and fillers. All these conditions can cause the addition or disappearance of some peaks, influencing the measured spectra (Renner et al., 2019, 2017). Since most of the commercially available spectra libraries are based on pure, clean and non-degraded references, for some environmental samples the identification can be impeded (Murphy et al., 2016; Renner et al., 2019). Furthermore, FTIR characterization is labor-intensive as particles must be first selected with a microscope and then analyzed individually (Sun et al., 2019). Micro-FTIR coupled with focal plane array (FPA) could solve this last drawback by analyzing entire areas without requiring a preselection step (Harrison et al., 2012; Löder et al., 2015).

Raman spectroscopy, in contrast, records the inelastic component of the scattering produced by a sample when irradiated by light. The recorded scattering is characteristic of the internal structure and functional groups of the sample (Xu et al., 2020). Raman spectroscopy has the advantage of identifying particles as small as 20 μm (Bretas Alvim et al., 2020). Despite that, additives, oils or organic material attached to the sample can cause interference and considerably modify the spectrum of the polymer (Bretas Alvim et al., 2020; Rolsky et al., 2020). The use of Raman spectroscopy in WWTPs studies has been limited, mostly for the relatively high organic content in the samples (Sun et al., 2019).

Destructive techniques generally apply a thermal treatment to the pretreated sample, using differences in physical and chemical properties to identify polymers. Pyrolysis gas chromatography coupled to mass spectrometry (Py-GC-MS) is one of the most widely used method. The microplastics present in the sample are pyrolyzed and the gas is transferred to a GC-MS (Dümichen et al., 2017). This method, as well as other thermal analyses, can be applied to a single particle or a bulk sample, possibly improving the speed of the characterization process (Prata et al., 2019a; Shim et al., 2017). However, thermal analyses are destructive, preventing further examination of the sample (Shim et al., 2017). Also, if thermal analyses are used for bulk samples, they don't provide any information on the number, size, and shape of microplastics (Shim et al., 2017).

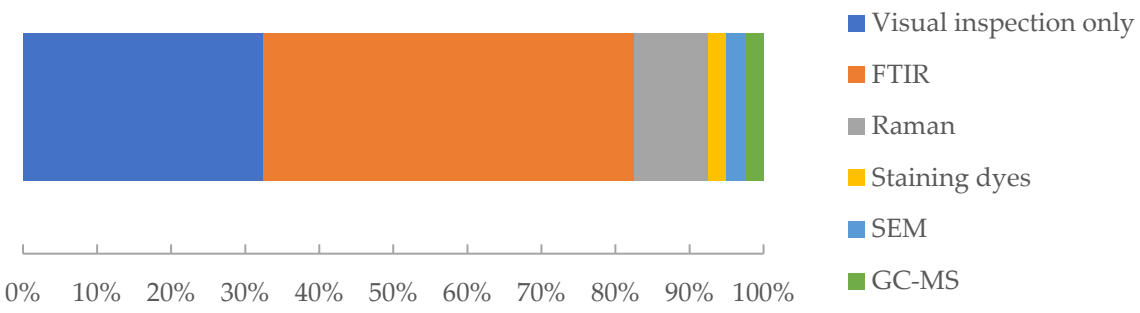

Figure 2.2 Techniques used for microplastics characterization in water and sediments (Prata et al., 2019a)

2.2.4 Quality assurance and quality control (QA/QC)

QA/QC procedures must be applied to the collection, pretreatment and characterization steps. The purpose of QA/QC is to guarantee reliable results by reducing and assessing sample contamination and sample losses throughout the detection process (Bretas Alvim et al., 2020). Microplastics contaminating the sample can originate from atmospheric deposition, the equipment used, and the clothing of workers (Sun et al., 2019). To reduce contamination of the samples, some guidelines must be followed. All equipment should be thoroughly rinsed and working surfaces should be cleaned with ethanol (Bretas Alvim et al., 2020; Sun et al., 2019). Glass and metal equipment should be preferred over plastic equipment (Prata et al., 2019a). The use of synthetic clothing, especially laboratory coats, should be avoided (Prata et al., 2019a). Samples should be sealed in Petri dishes or covered with aluminum foils as much as possible and preferentially handled in a fume hood (Prata et al., 2019a; Sun et al., 2019). It has also been suggested the setup of blanks throughout the detection process to evaluate sample contamination, as well as the placement of filters on the workspace to assess atmospheric deposition of MPs (Bretas Alvim et al., 2020; Sun et al., 2019). To evaluate potential sample loss during sample pretreatment, it has been recommended to test the recovery rate of microplastics (Löder et al., 2017). Finally, the characterization procedure used must be carefully studied to understand its technical limitations and to apply a reliable data-processing method (Bretas Alvim et al., 2020).

3 Materials and methods

3.1 Inoculum selection for the SBR

A laboratory-scale sequence batch reactor (SBR) was seeded with waste activated sludge from a local WWTP. The plant, located north of Valencia, serves 156,000 equivalent inhabitants from part of Valencia and other towns and villages north of the city. The WWTP treats approximately 36,600 m^3 of municipal and industrial wastewater daily. In 2018, this WWTP removed 97% of the suspended solids (SS), 97% of the biological oxygen demand (BOD_5), and 93% of the chemical oxygen demand (COD). The process outline of the WWTP involves preliminary, primary, secondary and tertiary treatments. In the pretreatment phase raw wastewater passes through coarse and fine screenings, then goes through a sand, grit and oil removal unit. After that, wastewater undergoes a primary settling step. As a secondary treatment, biodegradable matter and nitrogen are removed from wastewater with active sludge and secondary settling. In the tertiary treatment phase, wastewater goes through a coagulation and flocculation step, then gets filtered, and finally disinfected with UV light. The WWTP also treats the excess sludge from primary and secondary settling. First the sludge is thickened using gravity and flotation separation, then it is anaerobically digested producing biogas used for energy generation. Finally, the sludge is dewatered with centrifuges.

3.2 SBR design and operation

The secondary sludge of the WWTP was sampled on November 11th 2020 and transported to laboratory in a plastic container. 3 L of the sample were diluted with 3 L of tap water and poured into the SBR (Figure 3.1). The tap water was aerated before being used to remove any residual chlorine. The suspended solids of the diluted sludge were 2,46 g/L.

The reactor had a volume of 10 L (6 L working volume). The reactor was homogeneously mixed by the overhead stirrer Heidolph RZR 1 and aeration was supplied through a diffuser connected to an air pump. The reactor was connected to a 25 L tank through plastic tubes and a peristaltic pump Dinko D-21V. The peristaltic pump Dinko D-25VT, with another set of plastic tubes, drew off the effluent to the effluent sampling device. The effluent sampling device was constructed using PVC tube with a diameter of 6 cm and 50 cm tall. The effluent, arriving from the top of the tube, was filtered at the bottom of the device by a removable sieve with a mesh size of 150 μm. The filtered effluent was accumulated in a beaker

and removed with the peristaltic pump Millipore XX80EL04. The openings on the top of the reactor and of the feeding tank were sealed with aluminum foils to avoid environmental contamination.

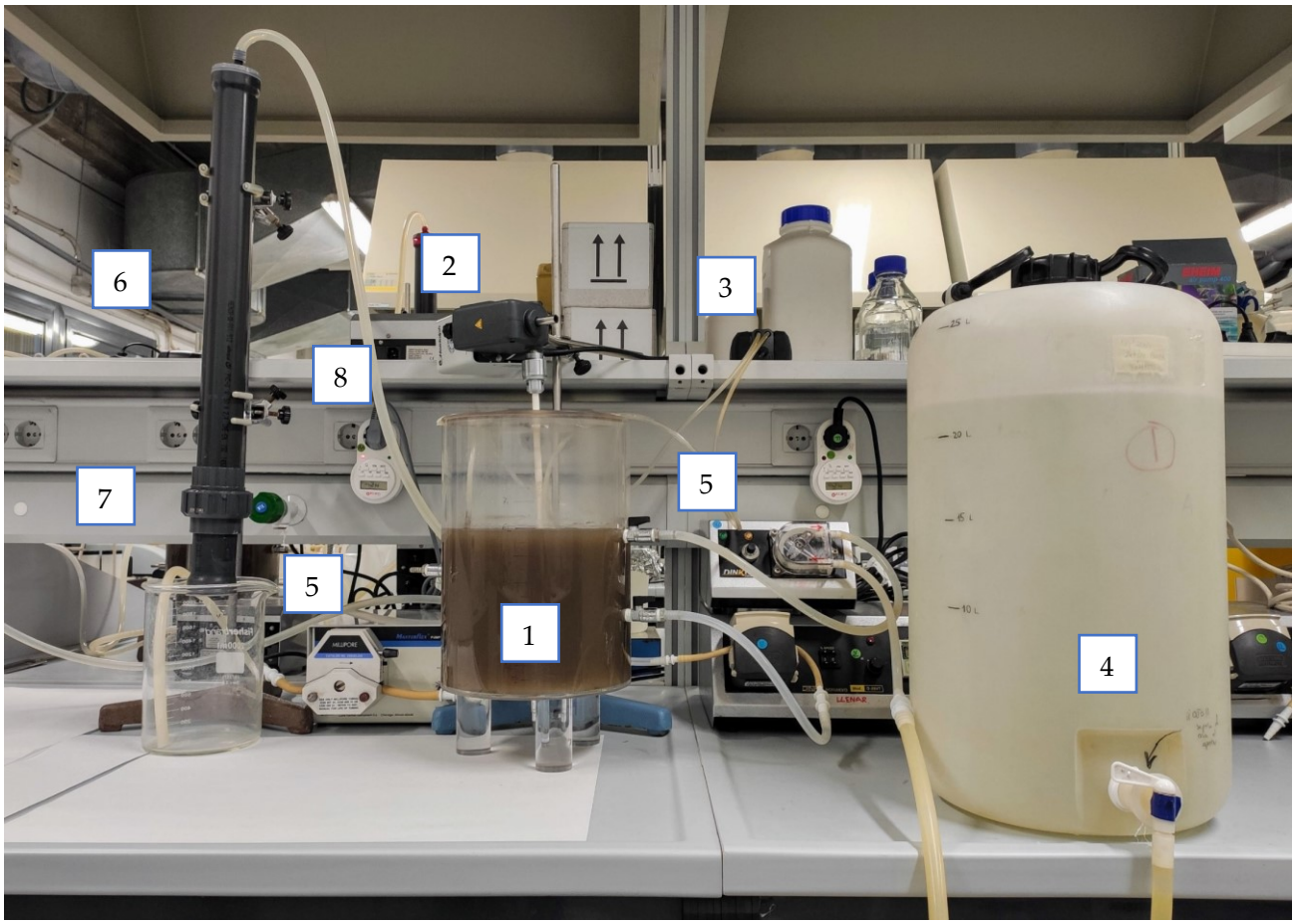

Figure 3.1 SBR design: (1) SBR; (2) overhead stirrer; (3) air pump; (4) feed tank; (5) peristaltic pumps; (6) effluent sampling device; (7) removable screen; (8) timer outlet

The SBR operated in an 8 h cycle for 93 days from the 11th of November 2019 to the 12th of February 2020. The SBR cycle was divided into four phases (Figure 3.2):

1. Feeding of 2 L of artificial wastewater (15 min);
2. Aeration and mixing (6 h);
3. Settling (1 h and 45 min);
4. Extraction of 2 L effluent (15 min).

The processing of 2 L in both the feeding phase and the extraction phase, resulted in an HRT of 1 day. The SBR cycle was automatically controlled by three programmable timer outlets Garza 400602.

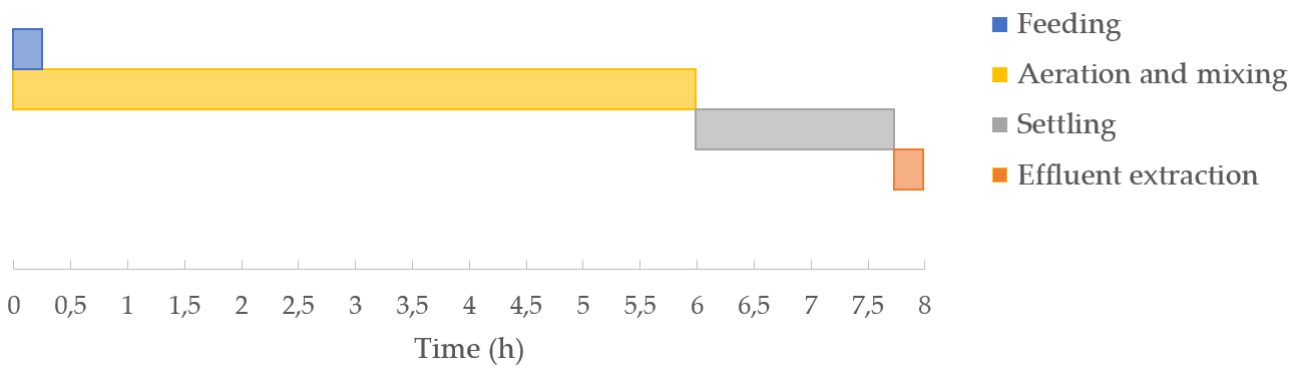

Figure 3.2 Visualization of the SBR 8-h cycle

The synthetic wastewater (SW) was prepared at need and stored in the feed tank. The SW was designed to provide the optimal substrate for the growth of the inoculated microorganisms. The selected COD of the SW was 500 mg/L with a proportion between carbon, nitrogen and phosphorus of 100:12:1. The C:N:P initial proportion was 100:12:4,5, but the phosphorus amount has been lowered after noticing high phosphorus concentrations in the effluent. To prepare the synthetic wastewater, the first step was to carefully clean the emptied feed tank and a beaker. Then 225 mg of peptone, 225 mg of meat extract and 28 mg of K_2HPO_4 were weighted and mixed with tap water in the beaker. Finally, the feed tank was filled with the prepared synthetic wastewater.

The mixed liquor suspended solids (MLSS) value was maintained between 2,5 g/L and 3,0 g/L. Whenever the MLSS value approached the 3,0 g/L mark, the excess sludge was substituted with an equivalent volume of tap water to restore a MLSS value of 2,5 g/L. Excess sludge removal was performed during the aeration and mixing phase.

3.3 Analytical procedures

3.3.1 Monitoring of the SBR performances

To verify the correct operation of the SBR, samples of the effluent and of the sludge were collected. Effluent samples were collected at the end of the settling phase, while sludge samples were collected during the aeration and mixing phase.

3.3.1.1 Effluent

The effluent analyses were conducted three times per week, on Monday, Wednesday and Friday (Table 3.1). The parameters analyzed were: pH, electric conductivity (EC), turbidity and COD. Once per week, on Wednesday, other parameters were analyzed: total nitrogen, NH_4^+, NO_2^-, NO_3^-, total phosphorus, PO_4^{3-}, total organic carbon (TOC), and soluble microbial products divided into carbohydrates (SMPc) and proteins (SMPp).

The effluent samples were collected from the glass beaker below the effluent sampling device. A volume of 150 ml was collected, and around 60 ml were filtered with a syringe filter with a pore size of 0,45 µm. Around 35 ml of the filtered sample were stored at -20 °C in the dark for future SMPc, SMPp and TOC analyses. The remaining 25 ml were used immediately to measure the concentration of COD, total nitrogen, NH_4^+, NO_2^-, NO_3^-, total phosphorus, and PO_4^{3-}. The measurements of pH, EC and turbidity were conducted using the remaining 90 ml of the unfiltered sample (Table 3.1).

Parameter	Instrument	Filtered sample	Mon	Wed	Fri
pH	pH meter		×	×	×
EC	EC meter		×	×	×
Turbidity	Turbidimeter		×	×	×
COD	COD cell test	√	×	×	×
N tot	Total N cell test	√		×	
NO_2^-	Nitrite cell test	√		×	
NO_3^-	Nitrate cell test	√		×	
NH_4^+	Ammonium cell test	√		×	
P tot	Phosphate cell test	√		×	
PO_4^{3-}	Phosphate cell test	√		×	
TOC	TOC analyzer	√		×	
SMPp	Micro BCA kit	√		×	
SMPc	Anthrone method	√		×	

Table 3.1 Summary of the effluent analyses

pH measurements were conducted on the unfiltered effluent sample with the pH meter 2 The electrode was carefully cleaned with distilled water and dried before use. Electric conductivity was measured on the unfiltered effluent sample with the EC meter Crison GLP 31+. The cell was carefully cleaned with distilled water and dried before use.

The turbidity was tested on the unfiltered effluent sample with the nephelometric turbidimeter Dinko D-112, expressing the result in nephelometric turbidity unit (NTU). The instrument was calibrated before every measurement with a set of turbidity standards. The sample cuvette was thoroughly washed with distilled water and with the effluent sample, then carefully dried to avoid interferences in the measurement. The effluent sample was mixed before the turbidity measurement.

The concentration of COD was measured with the Spectroquant COD cell tests 1.14540. The sediment at the bottom of a reaction cell was suspended by swirling, then 3,0 ml of the filtered effluent sample were carefully pipetted into the reaction cell. The screw cap was tightly attached to the cell and the content was vigorously mixed. The cell was heated in a preheated thermoreactor at 148 °C for 120 min, then it was transferred in a test-tube rack to cool. After 10 min the cell was swirled, and after 30 min the COD concentration was measured with the photometer Merck Nova 30 Spectroquant.

Total nitrogen concentration was measured with the Spectroquant total nitrogen cell tests 1.14763. Following the digestion procedure, 1,0 ml of the filtered effluent sample was pipetted into a cleaned and dried empty cell. 9,0 ml of distilled water were added to the cell and the content was mixed. 1 level microspoon of the reagent N-1K was added and the content of the cell was mixed. Finally, 6 drops of the reagent N-2K were added to the cell, the cell was tightly closed, and the content was mixed. The cell was heated in a preheated thermoreactor at 120 °C for 60 min, then it was transferred in a test-tube rack to cool. After 10 min the cell was shaken. After 30 min 1,0 ml of the digested content was pipetted into a reaction cell, without mixing the contents. Then, 1,0 ml of the reagent N-3K was pipetted into the reaction cell, the cell was tightly closed, and the content was mixed. After a reaction time of 10 minutes, the total nitrogen concentration was measured with the photometer Merck Nova 30 Spectroquant.

The concentration of NO_2^- was measured with the Spectroquant nitrite cell tests 1.14540. 5,0 ml of the filtered effluent sample were pipetted into a reaction cell. The reaction cell was tightly closed and shaken vigorously until the reagent was completely dissolved. After a reaction time of 10 minutes, the NO_2^- concentration was measured with the photometer Merck Nova 30 Spectroquant.

NO_3^- concentration was tested with the Spectroquant nitrate cell tests 1.14764. 0,5 ml of the filtered effluent sample were pipetted into a reaction cell, without mixing the content. Then, 1,0 ml of the reagent NO_3-1K was pipetted into the reaction cell. The reaction cell was tightly closed, and the content was

mixed. After a reaction time of 10 minutes, the NO_3^- concentration was measured with the photometer Merck Nova 30 Spectroquant.

The concentration of NH_4^+ was measured with the Spectroquant ammonium cell tests 1.14559. 0,1 ml of the filtered effluent sample were pipetted into a reaction cell. 1 dose of the reagent NH_4-1K was added to the cell, which was then tightly closed and shaken vigorously until the reagent was completely dissolved. After a reaction time of 15 minutes, the NH_4^+ concentration was measured with the photometer Merck Nova 30 Spectroquant.

Total phosphorus concentration was assessed with the Spectroquant phosphate cell tests 1.14729. Following the digestion procedure, 1,0 ml of the filtered effluent sample was pipetted into a reaction cell. 1 dose of the reagent P-1K was added, the cell was tightly closed, and the content was mixed. The cell was heated in a preheated thermoreactor at 120 °C for 30 min, then it was transferred in a test-tube rack to cool. After 30 min, the cell was vigorously shaken. 5 drops of the reagent P-2K were added, the cell was tightly closed, and the content was mixed. Finally, 1 dose of the reagent P-3K was added into the reaction cell, the cell was tightly closed and shaken vigorously until the reagent was completely dissolved. After a reaction time of 5 minutes, the total phosphorus concentration was measured with the photometer Merck Nova 30 Spectroquant.

The concentration of PO_4^{3-} was measured with the Spectroquant phosphate cell tests 1.14729. 1,0 ml of the filtered effluent sample was pipetted into a reaction cell and the content was mixed. 5 drops of the reagent P-2K were added, the cell was tightly closed, and the content was mixed. Then, 1 dose of the reagent P-3K was added, the cell was tightly closed and shaken vigorously until the reagent was completely dissolved. After a reaction time of 5 minutes, the PO_4^{3-} concentration was measured with the photometer Merck Nova 30 Spectroquant.

One day before the concentrations of TOC, SMPc and SMPp were tested, the filtered samples stored at -20 °C in the dark were transferred in a storage area where they were kept at 5 °C in the dark. The TOC concentration was measured with the Shimadzu TOC analyzer TOC-LCPH/CPN. 5,0 ml of the samples were pipetted in clean numbered vials, which were inserted in the Shimadzu ASI-L autosampler. The measurements were performed alongside 2 background blanks.

The SMPp content was measured with a micro BCA protein assay kit. The required amount of working reagent was prepared mixing the reagents A, B and C in the ratio of 24:24:1. Then, 0,5 ml of the sample were pipetted into an appropriately labeled microcentrifuge tube. 1,0 ml of the working reagent was added and the tube was mixed. The process was repeated three times per sample and three background blanks were also performed. The tubes were incubated at 60°C in a water bath for 60 min, then cooled to room temperature with iced water. The spectrophotometer Hach DR6000 was set to 562 nm, then it was

zeroed on a cuvette filled with distilled water. Subsequently, each sample was transferred into a clean cuvette to measure the SMPp concentration. The results were calculated by subtracting to each measurement the average of the three background blanks measurements.

The SMPc content was measured with the anthrone method. Anthrone reagent was prepared 2 hours before use dissolving 1 g of anthrone in 500 ml of H_2SO_4. Then, 2 ml of the anthrone reagent were pipetted into an appropriately labeled microcentrifuge tube. 1,0 ml of the effluent sample was added and the tube was mixed by vortexing. The process was repeated three times per sample and three background blanks were also performed. The tubes were incubated at 100°C in a water bath for 15 min, then cooled to room temperature with iced water. The spectrophotometer Hach DR6000 was set to 620 nm, then it was zeroed on a cuvette filled with distilled water. Subsequently, each sample was transferred into a clean cuvette to measure the SMPc concentration. The results were calculated by subtracting to each measurement the average of the three background blanks measurements.

3.3.1.2 Sludge

The SBR sludge was analyzed three times per week, on Monday, Wednesday and Friday, measuring the MLSS (Table 3.2). Once per week, on Wednesday, the mixed liquor volatile suspended solids (MLVSS) and the zeta potential were also analyzed.

The sludge samples were collected in a glass beaker opening a sludge outlet on the side of the reactor. 60 ml of sludge were collected for the assessment of the solids. On Wednesday, for the zeta potential analysis, 5 ml of sludge were collected in a glass beaker at the end of the aeration (A) and mixing (M) phase (Table 3.2).

Parameter	Method	End of A&M phase	Mon	Wed	Fri
MLSS	Oven 105 °C		×	×	×
MLVSS	Oven 550 °C			×	
Zeta potential	Zeta potential analyzer	√		×	

Table 3.2 Summary of the sludge analyses

The MLSS content was determined by heating the samples in an oven at 105 °C. Two fiberglass filters with a pore size of 1 μm were placed on two watch glasses, then both watch glasses were weighted. 25 ml of the collected sludge were measured in a graduated cylinder immediately after mixing the sludge

sample in the glass beaker. The 25 ml of sludge were filtered through one of the fiberglass filters, using a vacuum filtration system. The graduated cylinder used to measure the sludge volume was carefully rinsed with distilled water to ensure all material was transferred properly. The same procedure was repeated filtering 25 ml of sludge through the second filter. The fiberglass filters were placed on the respective watch glass and heated at 105 °C in the oven for 120 min. Then, the samples were cooled to room temperature for 30 min in a desiccator. Finally, both samples were weighted and the MLSS content was determined using the formula:

$$\mathrm{MLSS} = \frac{\mathrm{M_{150out}} - \mathrm{M_{in}}}{\mathrm{V}}$$

where $\mathrm{M_{150out}}$ is the mass of the sample after the thermal treatment at 105 °C, $\mathrm{M_{in}}$ is the initial mass of the sample, V is the volume of sludge analyzed. The MLSS content was calculated as the average of the two results.

The MLSS content was determined by heating the same fiberglass filters used for the MLSS assessment in a muffle furnace at 550 °C. The two fiberglass filters were transferred on two porcelain bowls, then both porcelain bowls were weighted and stored in a desiccator. The samples were subsequently heated at 550 °C in a muffle furnace for 60 min and cooled for 60 min in a desiccator. Finally, both samples were weighted and the MLSS content was determined using the formula:

$$\mathrm{MLVSS} = \frac{\mathrm{M_{550out}} - \mathrm{M_{in}}}{\mathrm{V}}$$

where $\mathrm{M_{550out}}$ is the mass of the sample after the thermal treatment at 550 °C, $\mathrm{M_{in}}$ is the initial mass of the sample, V is the volume of sludge analyzed. The MLVSS content was calculated as the average of the two results.

The zeta potential was measured with the zeta potential analyzer Malvern Zetasizer Zeta Nano ZS. The capillary cell was cleaned by flushing it with distilled water, ethanol, and distilled water again using two syringes. The collected sludge was inserted in the capillary cell with a clean syringe, ensuring that no bubbles were present in the capillary. Finally, the zeta potential was measured inserting the capillary cell in the analyzer. The measurement was repeated three times and the zeta potential was calculated as the average of the three results.

3.3.2 Microplastics assessment

The concentrations of microplastics in the effluent and in the sludge were monitored throughout the whole operation of the SBR. MPs concentration in the effluent was assessed once per week, on Monday. For the sludge, MPs concentration was measured when excess sludge removal was needed, roughly once per week.

3.3.2.1 Collection

MPs were collected from the effluent of the SBR with the effluent sampling device previously described. The effluent was filtered through a removable screen made of steel with 150 μm openings. The screen was removed from the casing and the retained material was transferred into a cleaned glass beaker washing the sieve thoroughly with distilled water. The beaker was immediately sealed with aluminum foil to avoid any contamination. The screen was analyzed under the stereomicroscope Leica MZ APO to verify that no microplastics were trapped in the structure of the sieve. The screen was cleaned and placed back into the casing.

For the sludge, when excess sludge had to be extracted from the sludge outlet of the SBR, 100 ml were collected in a cleaned glass beaker. Initially, the collected volume was 50 ml, but after the 4th of December 2019 the collected volume was doubled to increase sample representativeness. The beaker was immediately sealed with aluminum foil to avoid any contamination. If the pretreatments were not performed immediately, the samples were stored at 5°C in the dark before further process.

3.3.2.2 Pretreatments

Both effluent and sludge samples were subjected to pretreatments to reduce their organic matter content. After an in-depth analysis of the available options described in bibliography, chemical oxidation with a hydrogen peroxide solution (35%) was selected. H_2O_2 has shown to effectively remove organic matter without degrading or affecting the characterization process of most polymers (Tagg et al., 2015; Zhao et al., 2017). Hydrogen peroxide use has been associated with some problems, such as the possibilities of nylon degradation and polymer discoloration (Karami et al., 2017; Zhao et al., 2017). These drawbacks were considered during the selection process, but the reliable effectiveness of H_2O_2 outweighed its known limitations.

To establish the protocol for the organic matter digestion, a series of tests were performed. Several secondary sludge samples, collected from the WWTP, were digested varying the amount of H_2O_2 used and the reaction time. To evaluate the efficiency of the digestion, for every sludge sample the solids content (SST_{tot}) was measured, following the procedure described for the MLSS assessment. The same procedure was repeated for the digested sludge, obtaining a new value (SST_{dig}). The efficiency was determined using the formula:

$$\text{Efficiency} = \frac{SST_{tot} - SST_{dig}}{SST_{tot}}$$

The results of the digestion tests allowed for an adjustment of the protocol parameters. The selected sludge to H_2O_2 solution ratio was 2:1 For the effluent samples, a 100:1 ratio was enough, due to the low organic content of the recovered material. The selected reaction time was 120 min for both effluent and sludge samples.

For the effluent samples, firstly the beaker with the recovered material was heated at 45 °C mixing its content with a magnetic stirrer. The glass beaker was sealed with aluminum foils to avoid contamination of the sample. Then, the digestion was performed by pipetting 1 ml of H_2O_2 (35%) per 100 ml of material in the glass beaker. The beaker was sealed again and was heated at 60 °C for 120 min, mixing its content with a magnetic stirrer. The sample was heated to help the digestion of the organic matter (Avio et al., 2015b; Cole et al., 2014). Then, the digested sample was filtered through a fiberglass filter with 1 μm pore size to recover the microplastics. A vacuum filtration system was employed, which improved performances over gravity filtration. The beaker was rinsed with distilled water multiple times to ensure that all particles were transferred properly. The filter was put in an open Petri dish, cleaned with distilled water and ethanol. The filter was heated at 55 °C in an oven for 120 min and cooled in a desiccator overnight. Then the Petri dish was closed and stored in the dark.

For the sludge samples, 100 ml were measured in a cleaned graduated cylinder and poured into a cleaned glass beaker. The graduated cylinder was rinsed with distilled water to ensure that all particles were transferred properly. The beaker was heated at 45 °C mixing its content with a magnetic stirrer. The glass beaker was sealed with aluminum foils to avoid contamination of the sample. 50 ml of hydrogen peroxide (35%) were measured in a cleaned graduated cylinder and slowly poured into the beaker to reduce foam formation. The rapid addition of H_2O_2 can form a dense foam that suspends lighter MPs and cause them to adhere to the beaker surface, reducing microplastics recovery (Zhao et al., 2017). The beaker was sealed again and heated at 60 °C for 120 min, mixing its content with a magnetic stirrer and manually, if part of the material was suspended. After the digestion, the content of the beaker was filtered through a sieve made of steel with 150 μm openings. This step was necessary for future comparisons of MPs concentrations in sludge samples and effluent samples, which were collected with different methods. Then, the retained material was transferred into a cleaned glass beaker washing the filter thoroughly with distilled water. The recovered material was filtered through a fiberglass filter with 1 μm pore size to separate the microplastics from the distilled water. A vacuum filtration system was employed to improve the performance of the process. The beaker was rinsed with distilled water multiple times to ensure that all particles and eventual foam residues were transferred properly. The filter was put in an open Petri dish, previously cleaned with distilled water and ethanol. The filter was heated at 55 °C in an oven for 120 min and cooled in a desiccator overnight. Finally, the Petri dish was closed and stored in the dark.

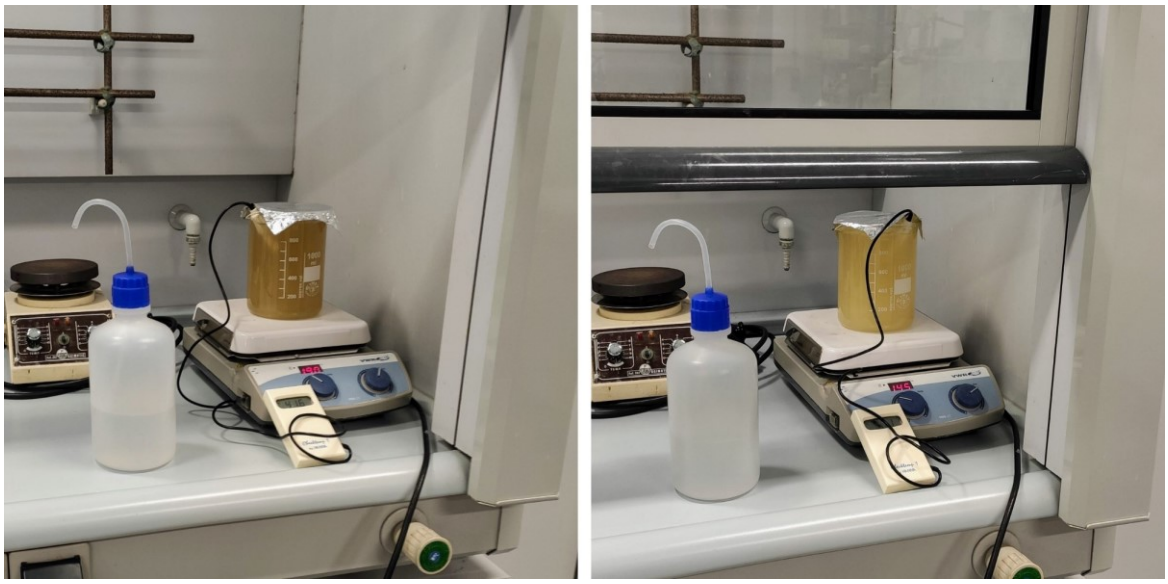

Figure 3.3 Digestion of a sludge sample, at the start of the process (left) and 15 min into the digestion (right)

Even though the samples are subjected to pretreatment steps, up to 70% of the particles that are visually classified as MPs show a non-plastic composition after chemical characterization (Hidalgo-Ruz et al., 2012). The distinction between plastic microfibers and natural fibers, especially cotton fibers, is particularly difficult. To solve this problem, a digestion protocol using H_2SO_4 (70%) (AATCC, 2018) was applied on two pretreated sludge samples. The procedure aims to digest most natural fibers such as cotton, hemp and linen without altering most of plastic materials (AATCC, 2018). However, the method doesn't eliminate wool fibers and digests some synthetic or semi-synthetic polymers such as spandex and rayon (AATCC, 2018). The two analyzed samples, collected on the 13th of November 2019 and on the 27th of January 2020, were characterized as described in the next section before applying the digestion protocol. The protocol described by the AATCC (2018) was adapted to the characteristics of our samples, specifically to the fact that the recovered microfibers were on the surface of a filter.

The digestion protocol was performed under a fume hood. The filter with the recovered particles was removed from the petri dish, folded and inserted in a cleaned glass funnel. The funnel was placed over a Buchner flask connected to a vacuum pump. The pump was needed to help the filtration process through the filter. Batches of small quantities of H_2SO_4 (70%) were poured into the funnel until 100 ml were filtered overall. The acid was poured taking care that it didn't overflow over the filter's edges, which could cause the loss of some MPFs. After 15 min the vacuum pump was turned on to drain the excess liquor. The filter was washed applying suction, first with 50 ml of a solution of H_2SO_4 (5%), then with distilled water. Both liquids were poured in batches of small quantities taking care that the liquid didn't

overflow over the filter's edges. The pH of the filtrate was measured with a pH indicator and distilled water was added until its neutrality. The pump was turned off and 25 ml of NH_4OH solution (8%) were poured into the funnel, again in small quantities. The filter was let to soak the NH_4OH solution for 10 min before applying suction to drain the excess liquor. Then, the filter was washed one final time with 150 ml of distilled water, poured in batches of small quantities again. The filter was let to soak the distilled water for 10 min before applying suction to drain the distilled water left. Then, the filter was removed from the funnel, carefully unfolded, and placed in a Petri dish, previously cleaned with distilled water and ethanol. The Petri dish was left open in a desiccator overnight. Finally, the Petri dish was sealed and the sample was stored at room temperature in the dark. The 27th of January 2020 filter was treated with a first and different adaptation of the protocol. The filter was placed in a Buchner funnel instead of being folded in a glass funnel. Also, the reagents were carefully pipetted on the unfolded filter, taking extreme care that the liquid didn't fall from the filter's edges. For this reason, in the first adaptation of the protocol the reagents were used in lower volumes than the ones prescribed by the AATCC protocol. Also, in the first adaptation of the protocol the filter was never completely covered by the reagents, which is one of the indications of the AATCC protocol.

3.3.2.3 Characterization

Physical characterization was performed on each of the pretreated effluent and sludge samples. The filters were visually analyzed with the stereomicroscope Leica MZ APO connected to a computer with the imaging software Leica LAS EZ. The filters were divided in 8 sequentially numerated portions using a grid (Carr et al., 2016), to lower the probabilities of duplicated or missed counts (Sun et al., 2019). The first analyzed parameter was the number of MPFs recovered, to calculate the concentration in each sample. MPFs were selected as the focus of the research because some difficulties estimating the concentration of microplastics with other shapes were encountered. Specifically, it has been challenging to reliably distinguish MPs fragments or sheets from residual organic structures. Due to the utilization of sieves with 150 µm openings during the collection or pretreatment phases, the recovery rate of microfibers smaller than 150 µm was lower than the recovery rate of larger microfibers. For this reason, only the MPFs longer than 150 µm were counted. To help distinguishing plastic microfibers from natural fibers, the following criteria was applied: no cellular or organic structures must be visible, fibers must be equally thick throughout their entire length and must present clear and homogeneous colors (Hidalgo-Ruz et al., 2012; Norén, 2007).The second analyzed parameter was the dimension of the microfibers. The dimension of each fiber was calculated with the help of the imaging software Leica LAS EZ. The same functionality

was helpful during the counting process to evaluate the exact size of MPFs close to 150 μm in length. The third parameter visually analyzed was the color of the microfibers, determined with the help of the imaging software Leica LAS EZ. Due to the time-consuming nature of the visual analysis, for samples with a high number of microfibers the determination of the dimension and color of the MPFs was limited to a subgroup of the portions delimited by the grid. The number and location of the chosen portions were selected to obtain color and dimension distributions representative of the entire sample.

Chemical characterization was employed to assist the visual identification of the microfibers. Its use was essential to ensure the quality of the physical characterization and to obtain information on the relative abundance of different polymer types (MSFD Technical Subgroup on Marine Litter, 2013; Sun et al., 2019). In our study, microfibers were identified by the FTIR spectrometer Bruker Vertex 80. Due to the thinness of the fibers (around 20 μm thick), the FTIR spectrometer was coupled with the FTIR microscope Bruker Hyperion 1000 operated in ATR mode. The FTIR microscope was equipped with the dedicated germanium ATR head and the measurements were performed with the Bruker Opus software. Due to the time-consuming nature of the FTIR analysis, it was performed on part of the visually identified microfibers, as suggested by the MSFD Technical Subgroup on Marine Litter (2013). The first analyzed sample was the initial SBR sludge sample, collected on the 13th of November 2019. The spectra of 25 of the recovered suspected MPFs were measured. The second analyzed sample was the sludge sample collected on the 27th of January 2020, from which 7 of the recovered microfibers were analyzed. The microfibers were analyzed after the execution of the H_2SO_4digestion protocol. Finally, the initial SBR sludge sample, collected on the 13th of November 2019, was analyzed again after the execution of the H_2SO_4 digestion protocol.

The first step of the FTIR analysis was the measurement of the background spectrum. This spectrum was automatically subtracted from the collected spectra of the sample by the Bruker Opus software, achieving the best signal to noise ratio possible. Then, the Petri dish containing the filter with the recovered MPs was opened and examined under a stereomicroscope. One of the suspected MPFs was transferred from the filter to a metallic plate with apposite tweezers. The metallic plate was placed under the FTIR microscope Bruker Hyperion 1000 and the dedicated germanium ATR head was carefully lowered to apply pressure on the microfiber. Finally, the spectrum of the suspected MPF was collected.

Then, the collected spectrum was analyzed with the KnowItAll software. To preprocess the spectrum, a manual baseline correction was applied first. The spectral baseline can be distorted as a result of scattering, absorption by the supporting substrate, changing conditions during data collection, or the variableness due to instrumental factors (Lasch and Lasch, 2012). Then, a spectral subtraction was performed in the spectral regions of 650-700 cm^{-1} and 2250-2450 cm^{-1}. Contamination of the samples, for example

by CO_2 or water vapor, often results in additional bands or spectral distortions (Lasch and Lasch, 2012). Spectral subtraction automatically corrects the parts of the spectrum where the signal was originated from interactions between the contaminants and IR radiation. The last preprocessing procedure was the normalization of the spectrum, to allow an effective comparison across heterogeneous sets of samples (Lasch and Lasch, 2012). The preprocessed spectrum was compared to the built-in reference spectra library to identify the composition of the analyzed microfiber. The spectrum was also compared with the spectra library of textile fibers developed by the Institute of Chemistry University of Tartu (Institute of Chemistry University of Tartu, 2018).

3.3.2.4 Quality assurance and quality control (QA/QC)

To limit any contamination of the samples, specific guidelines were followed. All equipment was thoroughly rinsed and working surfaces were cleaned with ethanol (Bretas Alvim et al., 2020; Sun et al., 2019). Plastic equipment was replaced by glass and metal counterparts, when possible (Prata et al., 2019a). The use of synthetic clothing was avoided, using laboratory coats made of cotton (Prata et al., 2019a). All samples were sealed in cleaned Petri dishes or covered with aluminum foils as much as possible (Prata et al., 2019a; Sun et al., 2019).

The concentration of MPFs in the tap water, used to prepare the simulated wastewater, was measured in two different ways. In the first method, 5 L of tap water were filtered through a fiberglass filter with a pore size of 1 μm, with the help of a vacuum filtration system. The filter was put in an open Petri dish, cleaned with distilled water and ethanol. The filter was heated at 55 °C in an oven for 120 min and cooled in a desiccator overnight. The Petri dish was sealed and stored in the dark and, finally, the concentration of MPFs in the tap water was assessed by counting the recovered microfibers under the stereomicroscope Leica MZ APO. The second method measured the MPFs concentration using the effluent sampling device. Thanks to this second measurement, the MPFs recovery rate of the effluent collection phase was assessed. After the end of the operation of the SBR, the components were thoroughly cleaned and the reactor was filled with tap water. The effluent pump was turned on transferring the tap water to the effluent sampling device, where the tap water was filtered through the removable screen. The screen was then removed from the casing and the retained material was transferred into a cleaned glass beaker washing the sieve thoroughly with distilled water. Then, the content of the beaker was filtered through a fiberglass filter with 1 μm pore size using a vacuum filtration system. The beaker was rinsed with distilled water to ensure that all particles were transferred properly. The filter was put in an open Petri dish, cleaned with distilled water and ethanol. The filter was heated at 55 °C in an oven for 120 min and

cooled in a desiccator overnight. Then, the Petri dish was closed and stored in the dark. This procedure was repeated 2 times, the first one filtering 40 L of tap water and the second time filtering 10 L of tap water. Both filters were analyzed under the stereomicroscope Leica MZ APO, counting the recovered microfibers to calculate the concentration of MFPs in the tap water.

Atmospheric deposition was assessed by placing a fiberglass filter with a pore size of 1 μm on the workspace in an open Petri dish for 1 week. The Petri dish was sealed and stored in the dark before assessing the concentration of MPFs in the tap water by counting the recovered microfibers under the stereomicroscope Leica MZ APO. The result was compared to the number of MPFs present in a new fiberglass filter.

4 Results and discussion

4.1 Monitoring of the SBR performances

4.1.1 Effluent analyses

Figures 4.1-4.12 show the results of the monitoring analyses on the SBR effluent.

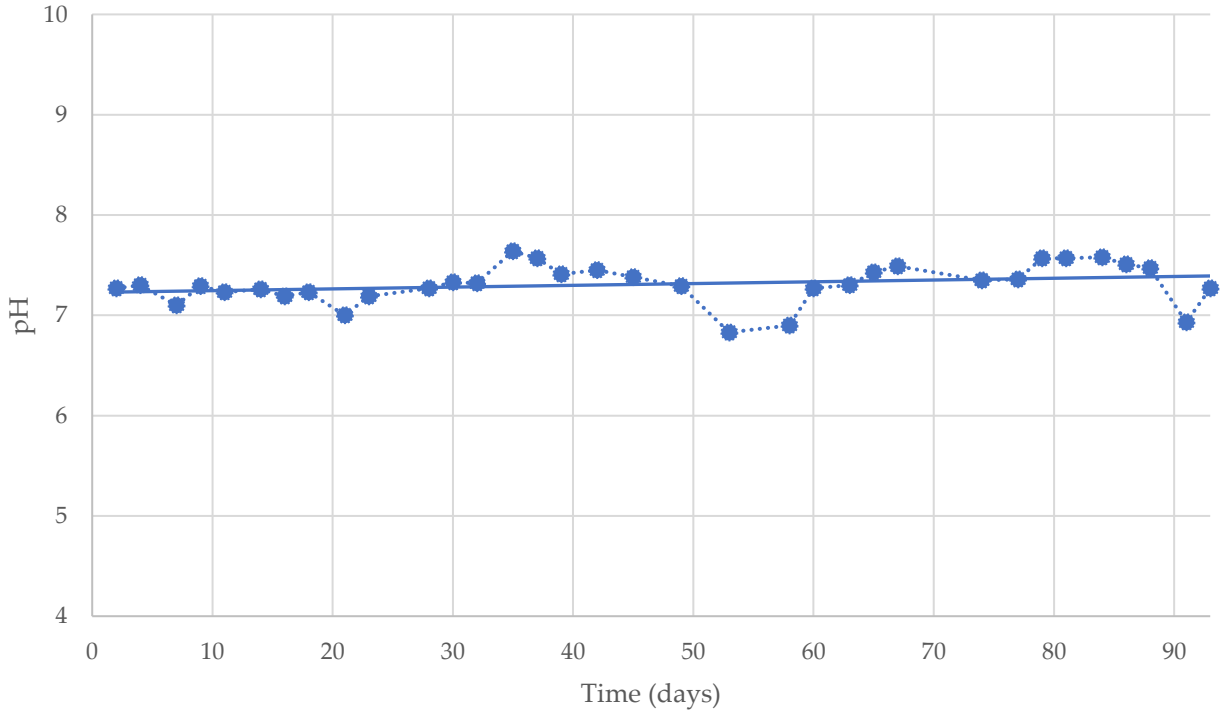

Figure 4.1 pH of the SBR effluent throughout the operation of the SBR

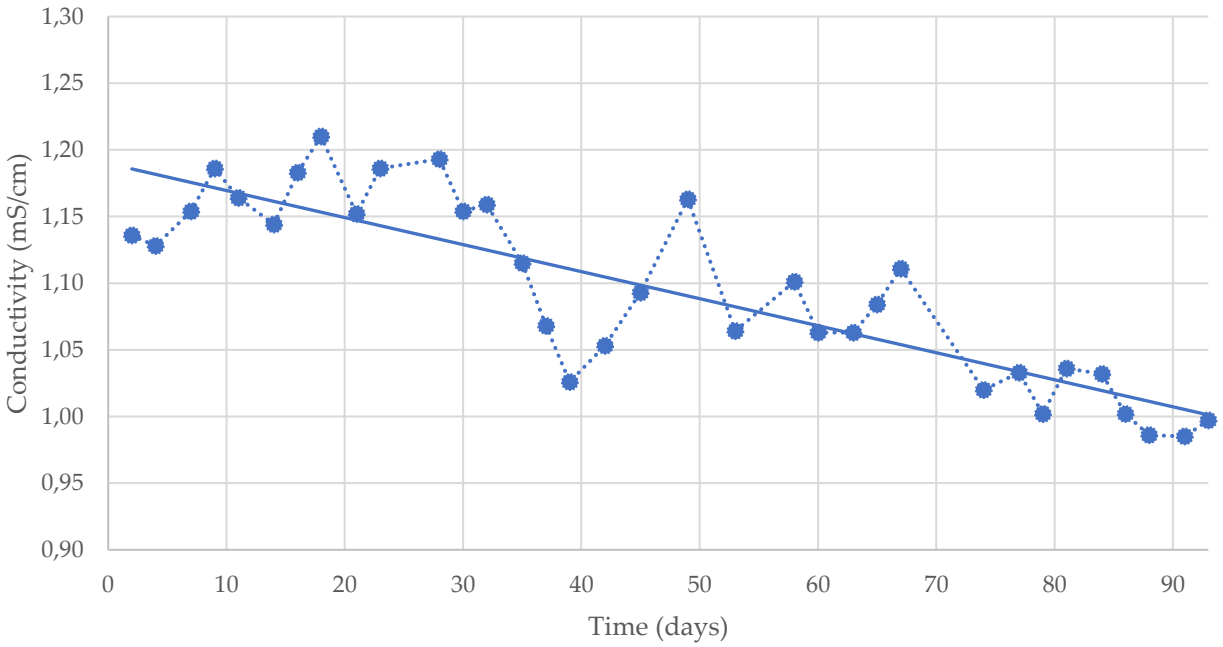

Figure 4.2 Conductivity of the SBR effluent throughout the operation of the SBR

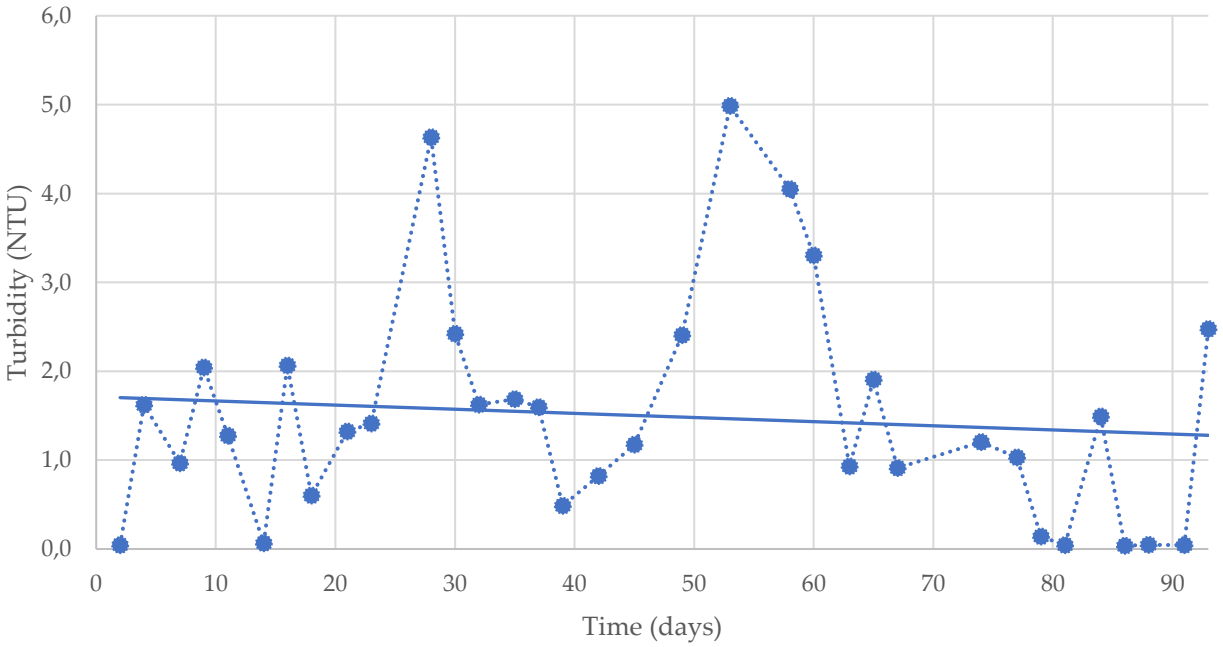

Figure 4.3 Turbidity of the SBR effluent throughout the operation of the SBR

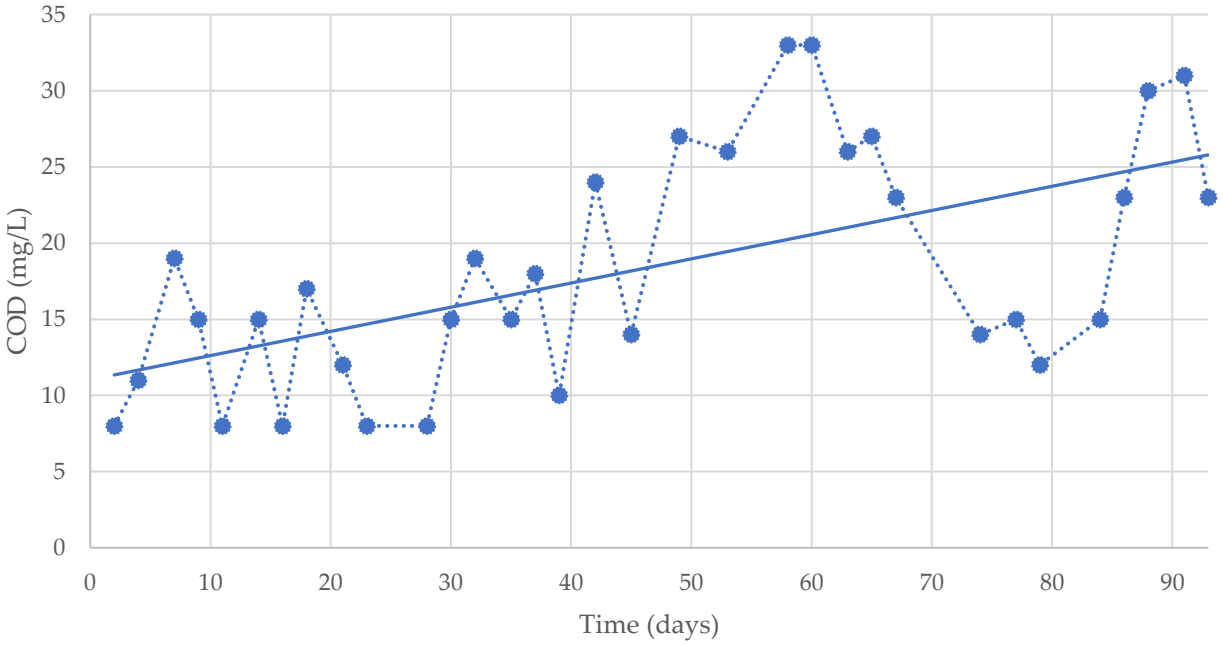

Figure 4.4 COD concentration of the SBR effluent throughout the operation of the SBR

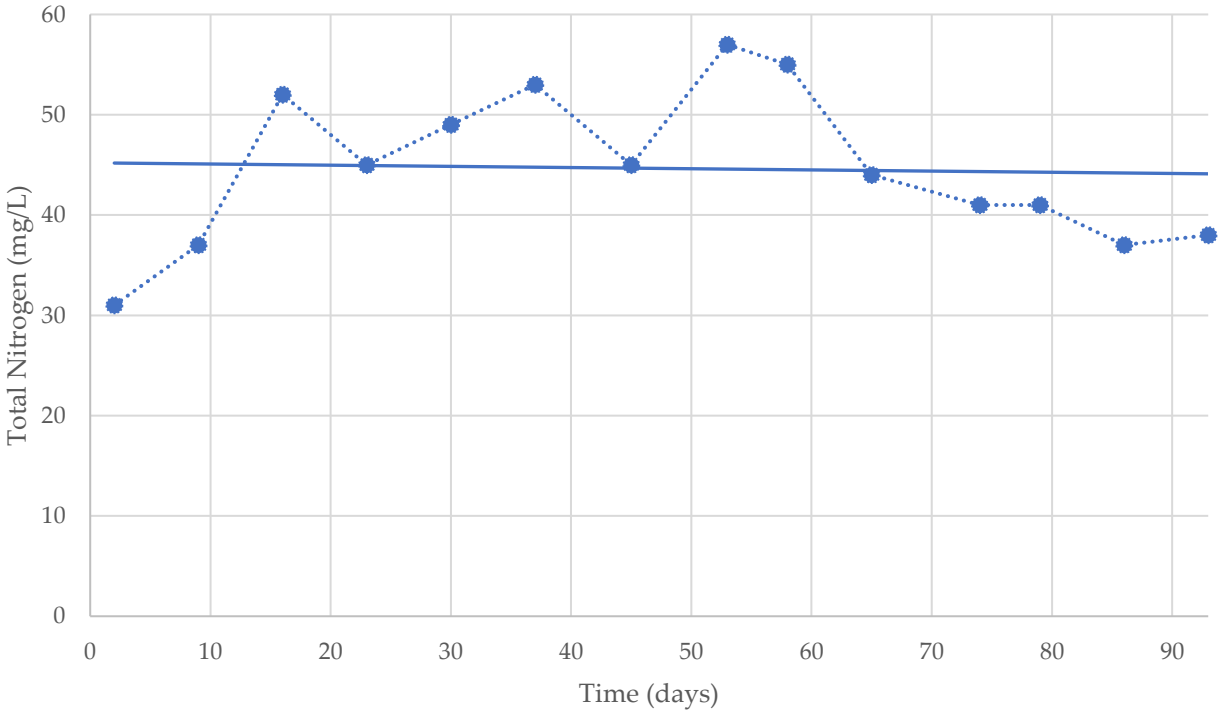

Figure 4.5 Total nitrogen concentration of the SBR effluent throughout the operation of the SBR

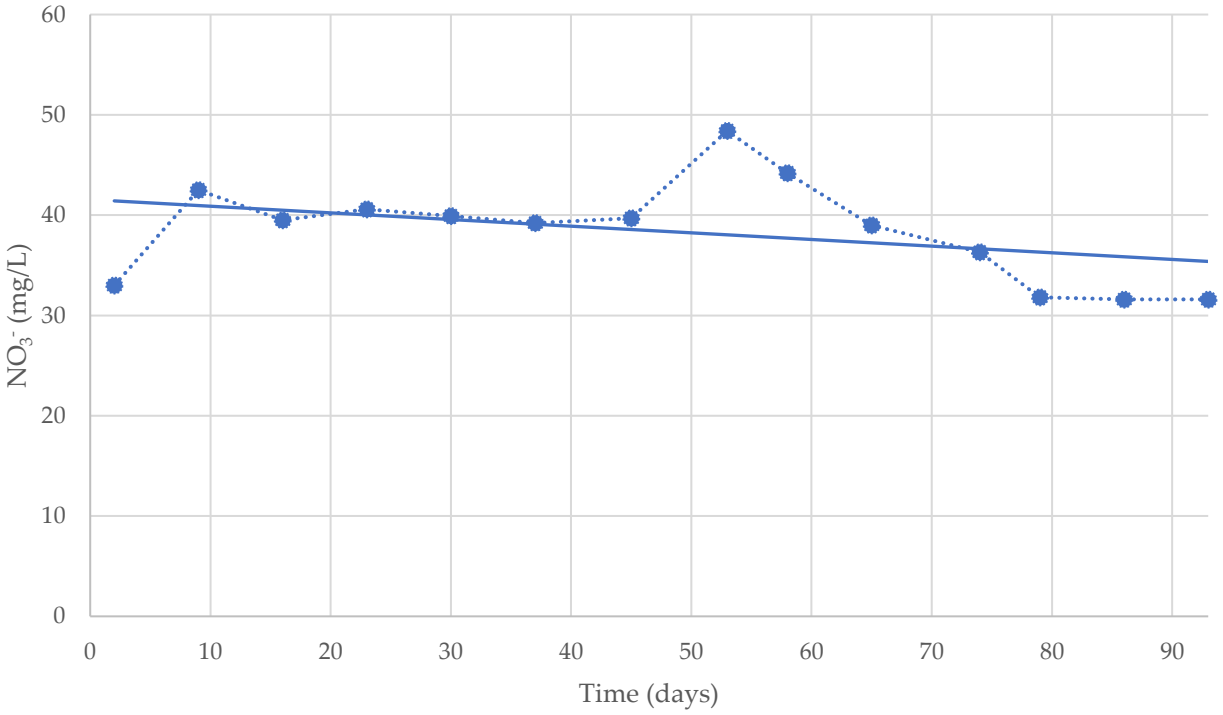

Figure 4.6 NO_3^- concentration of the SBR effluent throughout the operation of the SBR

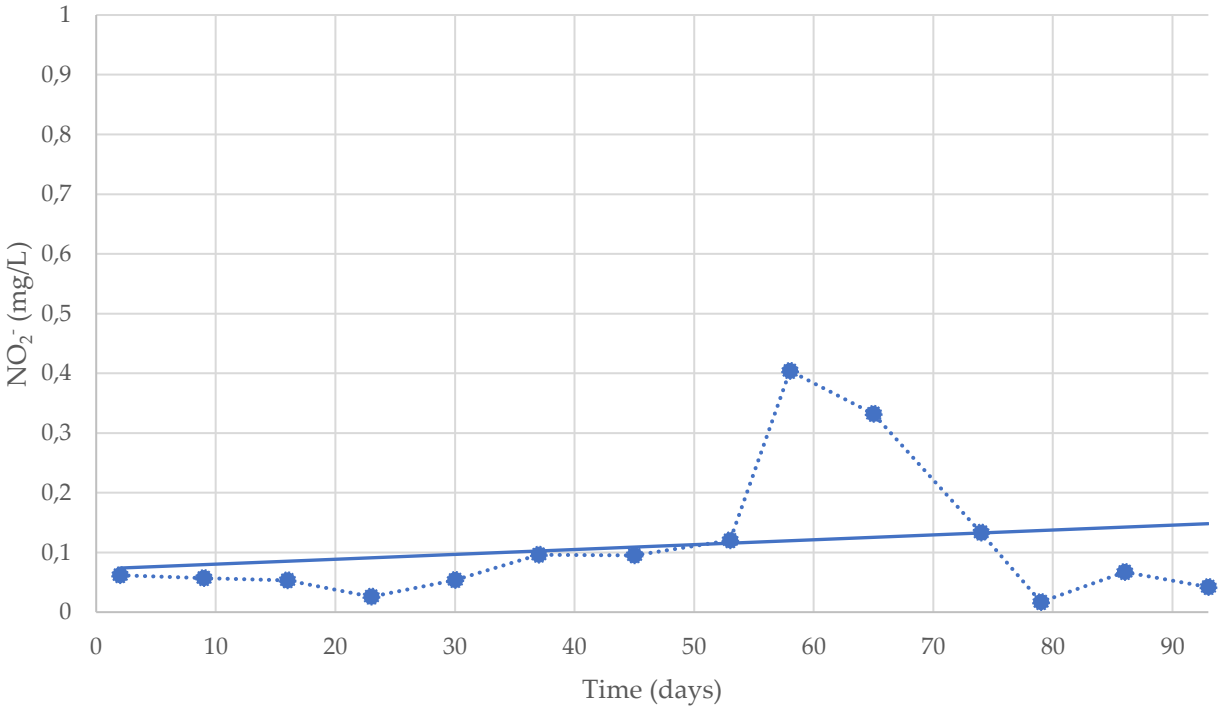

Figure 4.7 NO_2^- concentration of the SBR effluent throughout the operation of the SBR

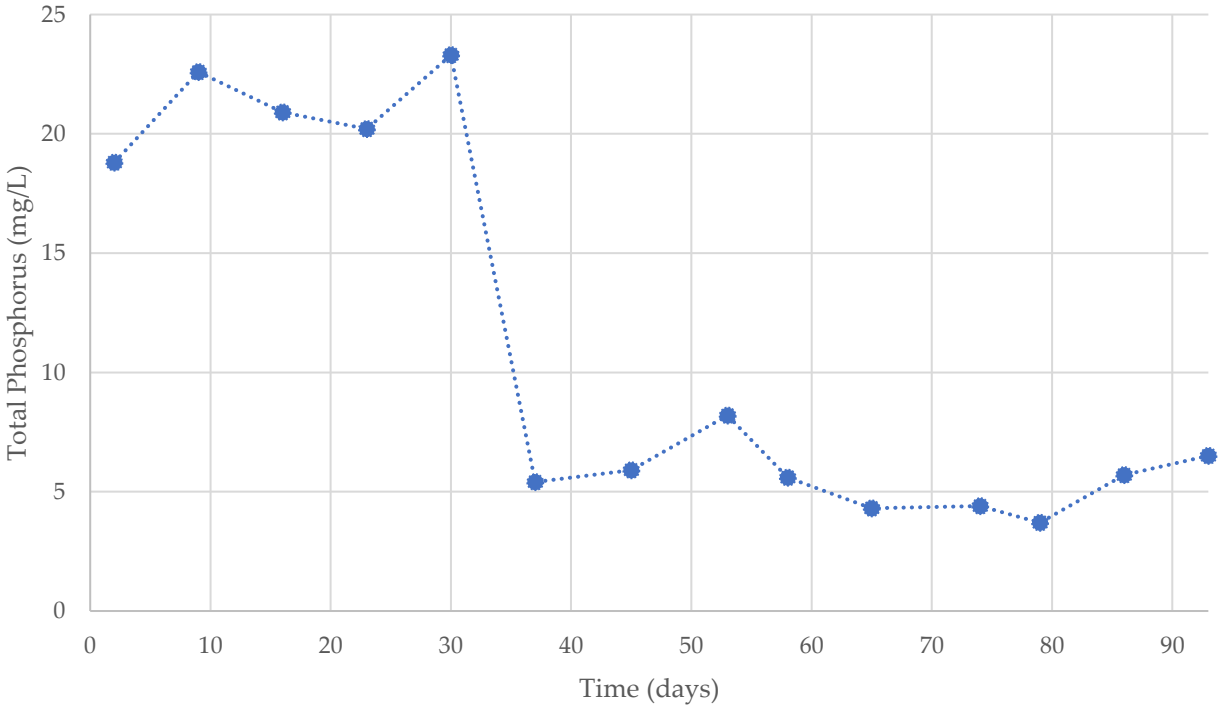

Figure 4.8 Total phosphorus concentration of the SBR effluent throughout the operation of the SBR

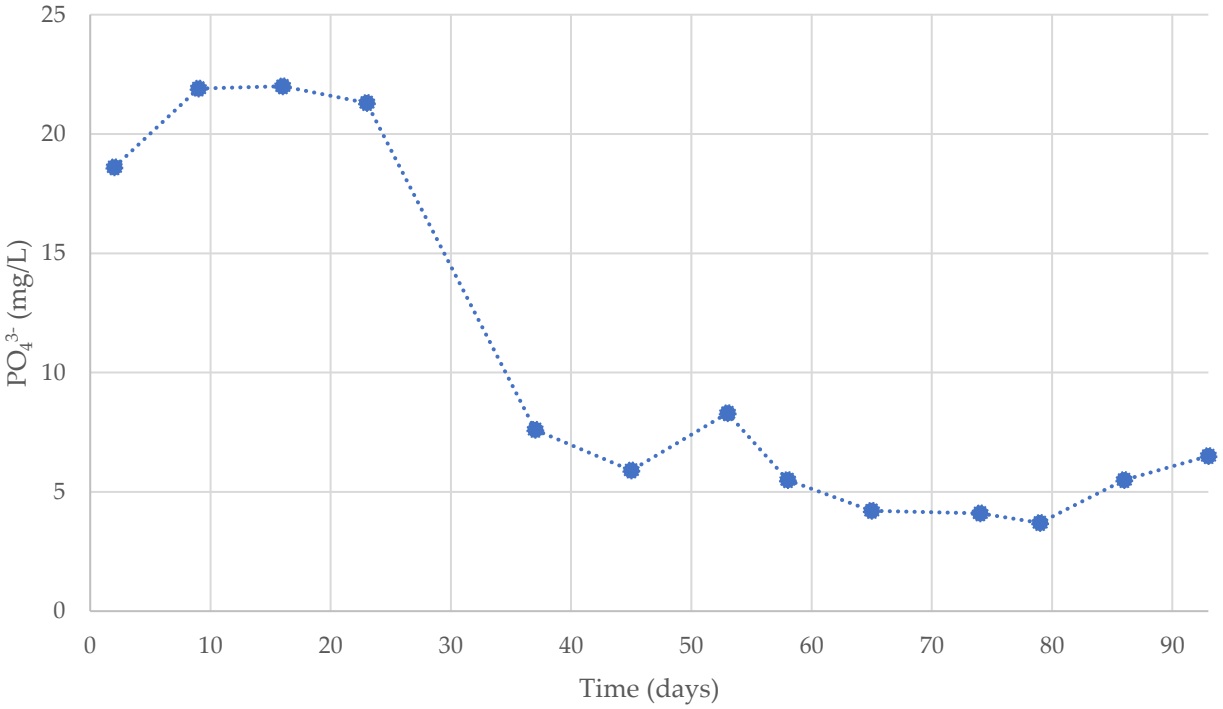

Figure 4.9 PO_4^{3-} concentration of the SBR effluent throughout the operation of the SBR

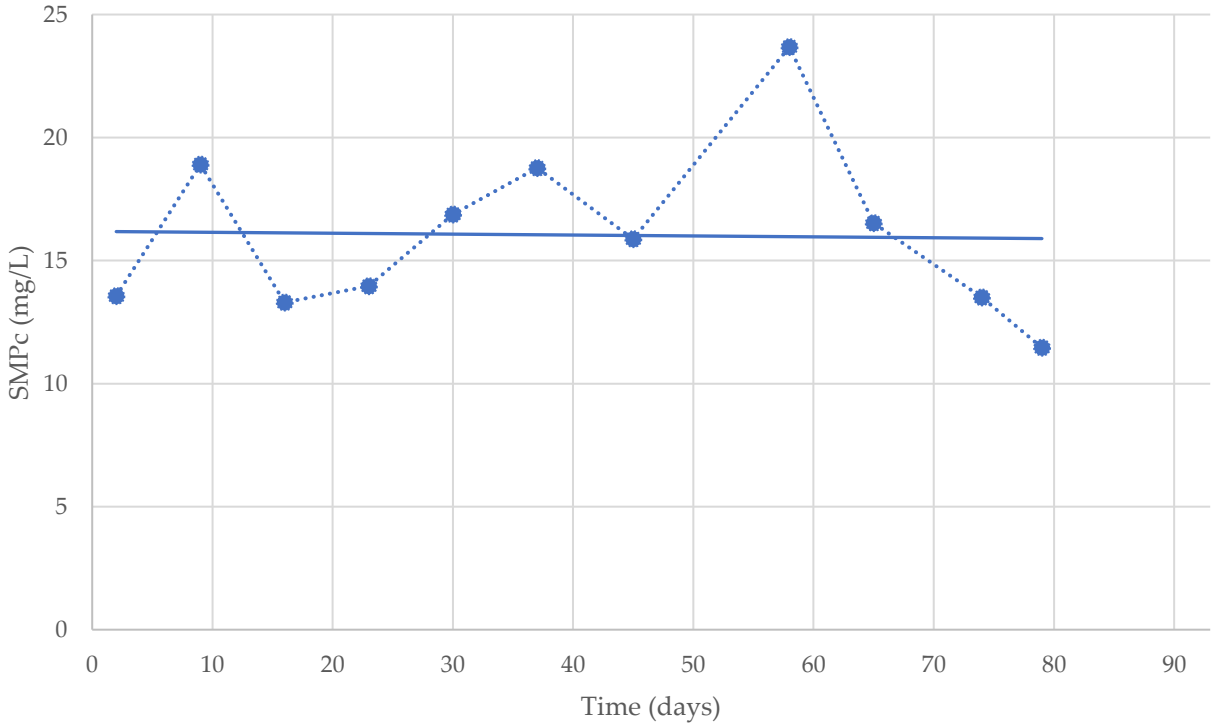

Figure 4.10 SMPc concentration of the SBR effluent throughout the operation of the SBR

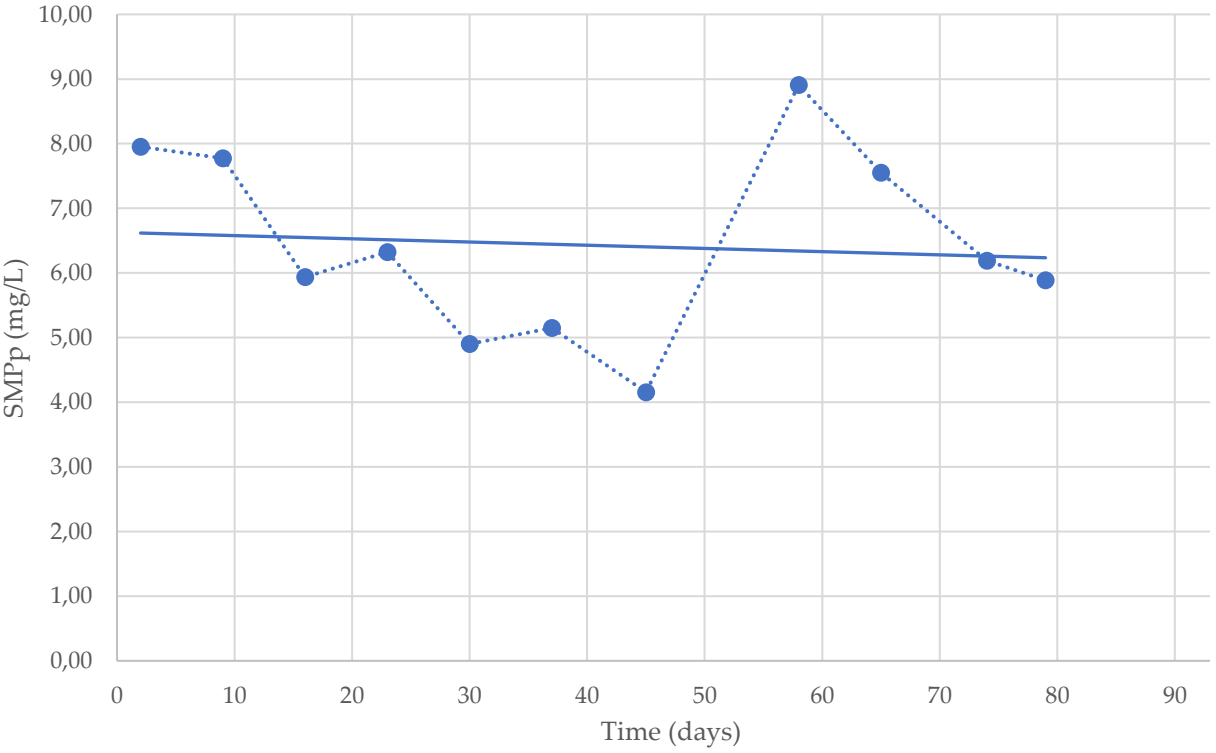

Figure 4.11 SMPp concentration of the SBR effluent throughout the operation of the SBR

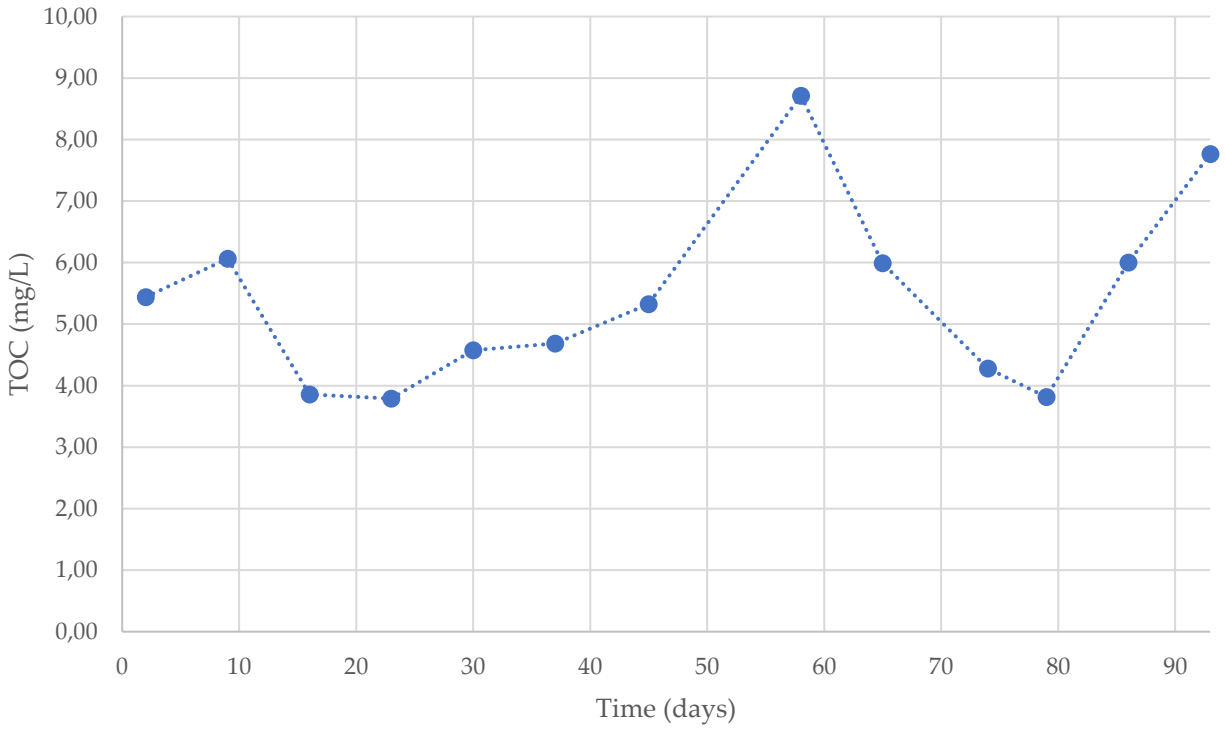

Figure 4.12 TOC concentration of the SBR effluent throughout the operation of the SBR

The results show a relatively stable behavior for the pH (Figure 4.1), the total nitrogen concentration (Figure 4.5), the NO_3^- concentration (Figure 4.6), and the NH_4^+ concentration. The average of total nitrogen concentration, NO_3^- concentration and pH were respectively 45 mg/L and 38,4 mg/L and 7,31. The concentration of NH_4^+ was under the detection limit of the test (4,0 mg/L) for the entire operation of the SBR. The average turbidity, 1,50 NTU, remained stable throughout the SBR operation (Figure 4.3), but the variance of the results is higher compared to the other parameters. A possible factor contributing to the higher variance could have been the nature of the detected particles. For most parameters, the analysis was performed on filtered effluent samples (Table 3.1). Instead, a turbidimeter measures the scattering effect of suspended particles on the absorption or transmittance of light (Chahal et al., 2016). Suspended particles could sediment both prior to the collection phase, at the bottom of the glass beaker, and during the measuring process, at the bottom of the cuvette. To limit the effect of sedimentation, the effluent in the glass beaker was mixed before collection, and the content of the cuvette was mixed prior to the measurement. However, the mixing energy was limited to avoid the formation of bubbles which would have interfered with the turbidity measurement (Joannis et al., 2008).

As expected, after the phosphorus amount added to the simulated wastewater was lowered, the average concentrations of total phosphorus (Figure 4.8) and PO_4^{3-} (Figure 4.9) decreased, respectively from 21,2 mg/L to 5,5 mg/L and from 21,0 mg/L to 5,7 mg/L. However, the results of the total phosphorus

concentration and PO_4^{3-} concentration were stable both before and after the modification. The electric conductivity followed a similar trend, but less evidently (Figure 4.13). This behavior can be explicated knowing that the concentration of PO_4^{3-} ions is one of the contributors of the EC value, along with HCO_3^-, NO_3^-, NH_4^+, K^+, Mg^{2+}, Ca^{2+} and so on (Kim et al., 2007). The average EC was 1,095 mS/cm.

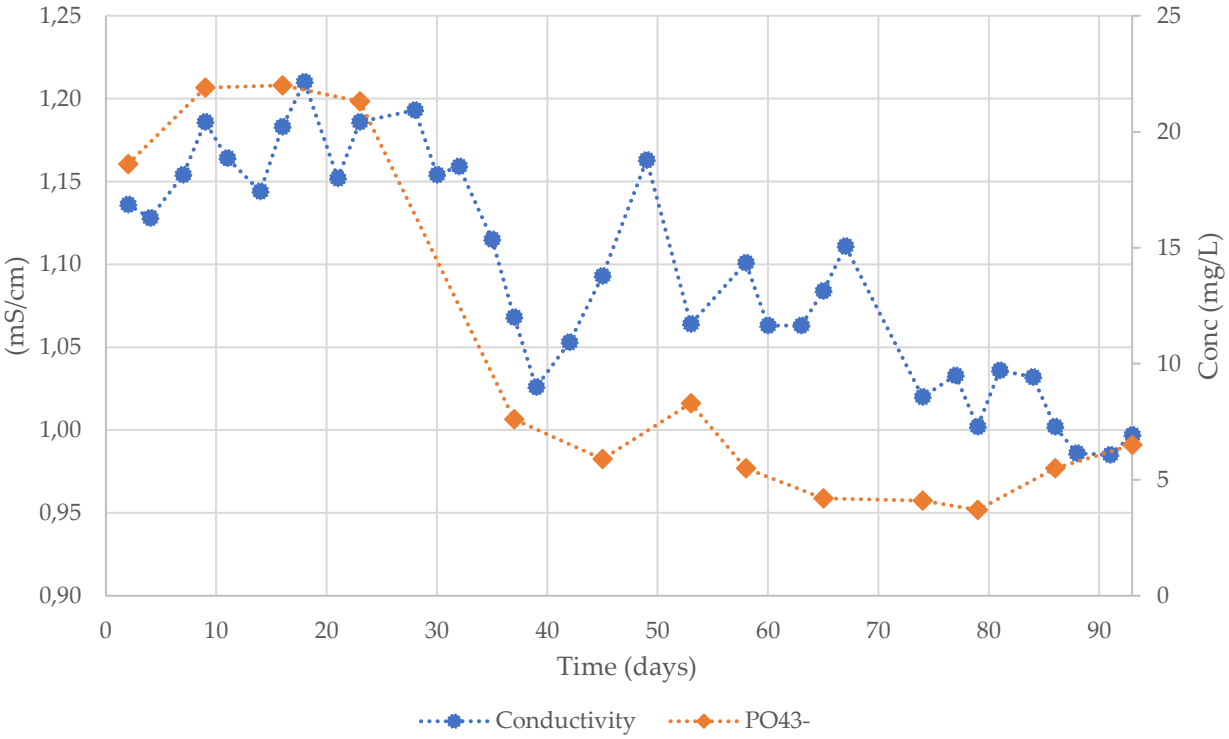

Figure 4.13 Comparison between conductivity and PO_4^{3-} trends

The COD concentration (Figure 4.4), the NO_2^- concentration (Figure 4.7), the SMPc content (Figure 4.10), the SMPp content (Figure 4.11) and the TOC concentration (Figure 4.12) were relatively stable throughout the SBR operation. However, between 45 and 60 days after the start of the experiment for all these parameters one or multiple anomalously high measurements were recorded. These anomalies, registered from the 30th of December to the 15th of January, have been partly addressed to the winter holidays. During that period, the excess sludge removal was performed less frequently. Also, the simulated wastewater was prepared and stored in the feed tank in larger volumes, always assuring the safe and correct operation of the SBR. The COD concentration was generally under 20 mg/L, with peaks just above 30 mg/L. The average COD concentration was 18,2 mg/L. These values were much lower than the designed COD concentration of the simulated wastewater, 500 mg/L, as a proof of the steady activity of the microorganisms in the SBR. The average NO_2^- and TOC concentration were respectively 0,111 mg/L and 5,41 mg/L. The average SMPc and SMPp content were respectively 16,04 mg/L and 6,43 mg/L. For most

samples, the sum of the SMPc and SMPp contents was higher than the COD concentration (Figure 4.14). This result was unexpected because SMP are just one of the contributors to the COD concentration in the effluent. The SMPp/SMPc ratio can vary depending on design parameters, such as the sludge retention time, the temperature and the organic load rate (Duan et al., 2013; Ferrer-Polonio et al., 2018; Ni, 2013). The calculated average SMPp/SMPc ratio was 0,41, which is lower than values observed in previous studies with similar operational designs (Ferrer-Polonio et al., 2018). This consideration suggested an overestimation of the SMPc content during the analysis. However, similar results were obtained when the SMPc, SMPp and COD analyses were repeated on the filtered effluent samples stored at -20 °C in the dark (Figure 4.15).

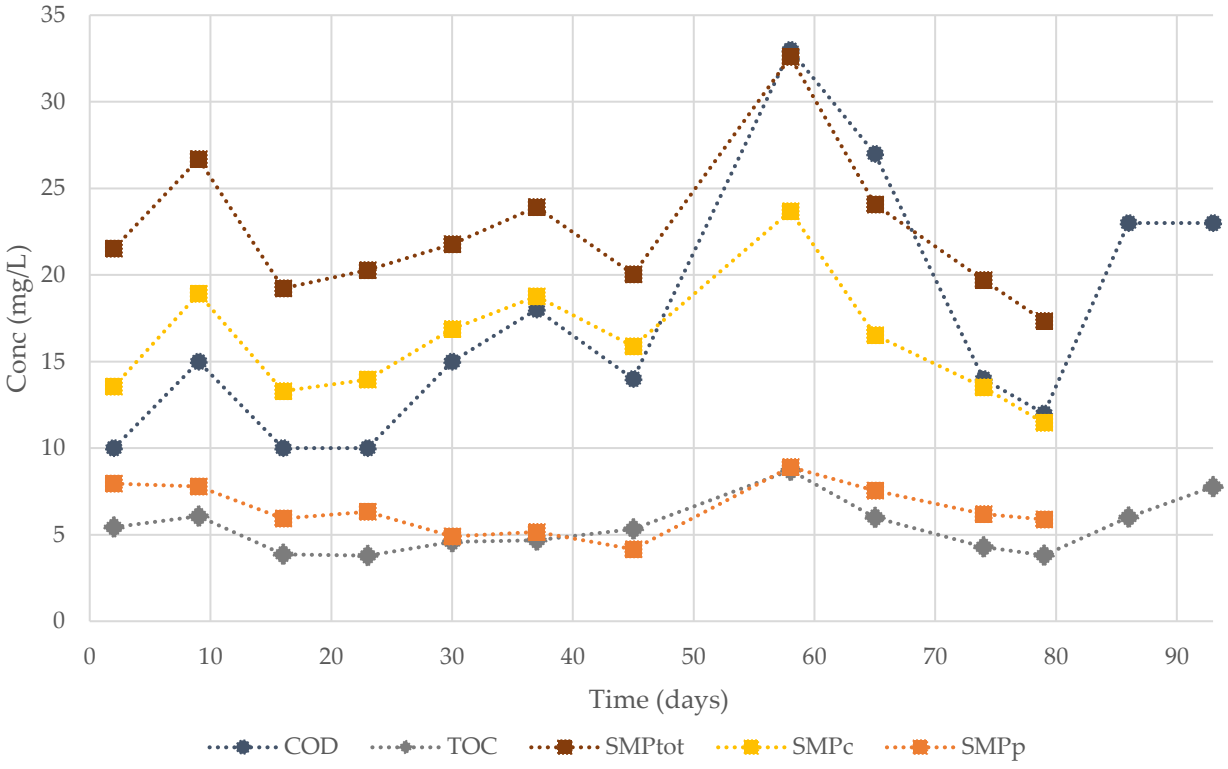

Figure 4.14 Comparison of effluent analyses: COD, TOC, SMPtot (SMPc +SMPp), SMPc, and SMPp concentration

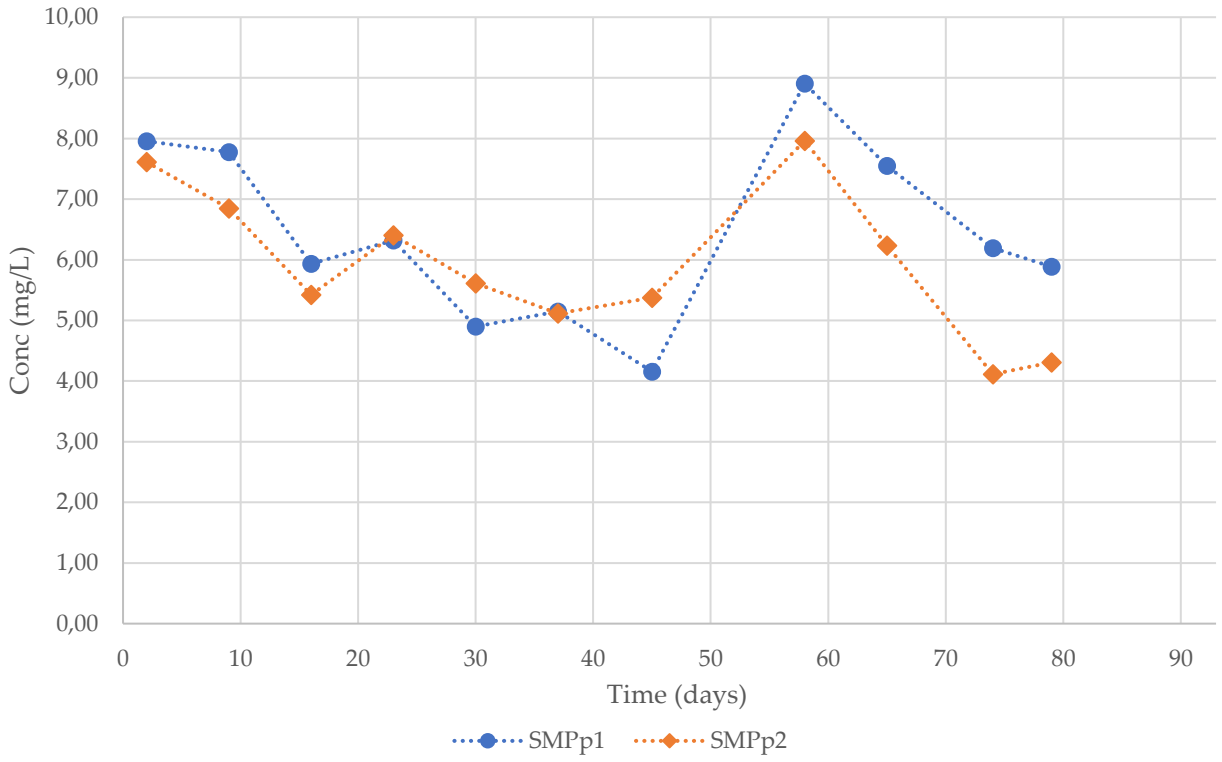

Figure 4.15 Comparison of repeated SMPp tests: initial results (SMPp1) and repeated results (SMPp2)

Between 45 and 60 days after the start of the experiment, a less evident deviation in the results can be noticed in other parameters as well. In that period, some of the turbidity, total nitrogen, NO_3^-, total phosphorus, and PO_4^{3-} results were slightly higher than the average (Figure 4.3; Figure 4.5; Figure 4.6; Figure 4.8; Figure 4.9), whereas pH results were slightly lower than the average (Figure 4.1).

4.1.2 Sludge analyses

The results of the MLSS analyses on the SBR sludge are resumed in Figure 4.16.

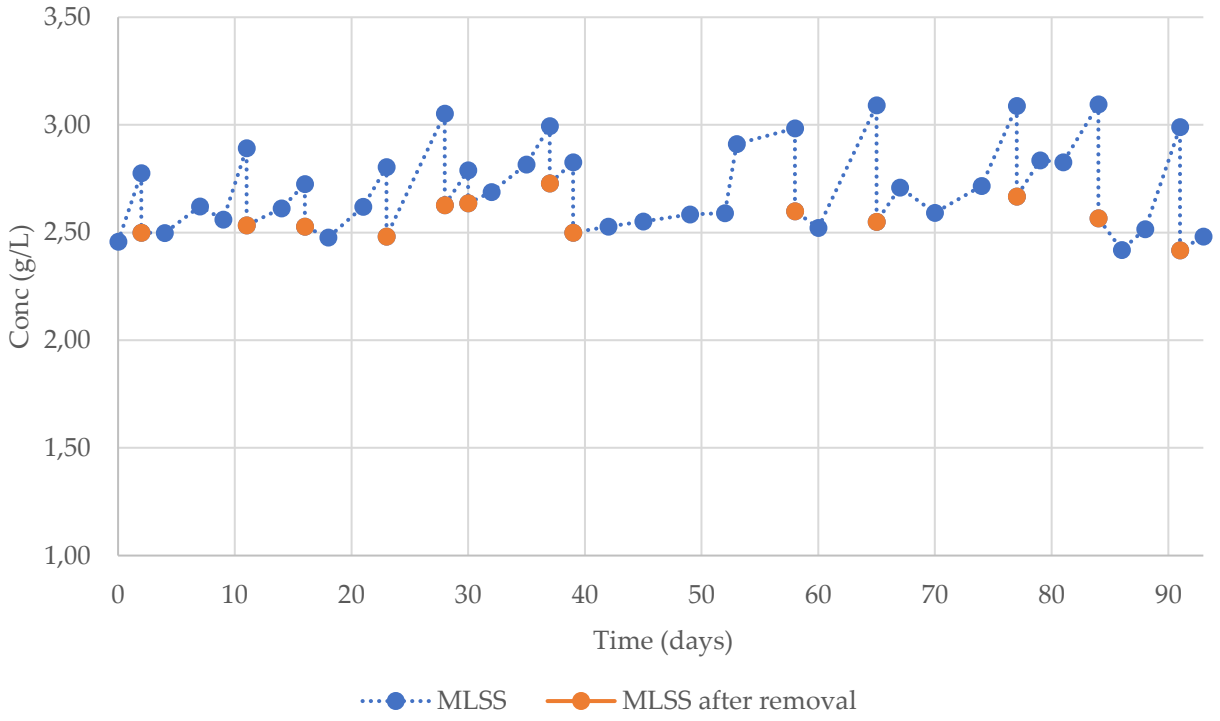

Figure 4.16 MLSS of the SBR sludge. In orange are highlighted the MLSS values measured after the excess sludge removal

To better evaluate the growth of the microorganisms in the SBR sludge, the cumulative MLSS (MLSSc) trend was analyzed. The MLSSc was calculated with the following formula:

$$MLSSc(d) = MLSS(d) + \sum_{i=0}^{d} MLSSr_i$$

where d refers to a specific day, $MLSSr_i$ is the difference between the MLSS concentration before and after an excess sludge removal event, and $\sum_{i=0}^{d} MLSSr_i$ is the sum of the decreases in MLSS concentration due to excess sludge withdrawal from the beginning of the SBR operation to the day d. The growth of the microorganisms (EGM) was estimated normalizing the cumulative MLSS with the initial MLSSc value:

$$EGM\ (d) = \frac{MLSSc(d)}{MLSSc(0)}$$

Analyzing the MLSS and the EGM trends (Figure 4.16; Figure 4.17), it was verified that the growth of the microorganisms in the SBR sludge matched the expectations and was generally steady throughout the SBR operation.

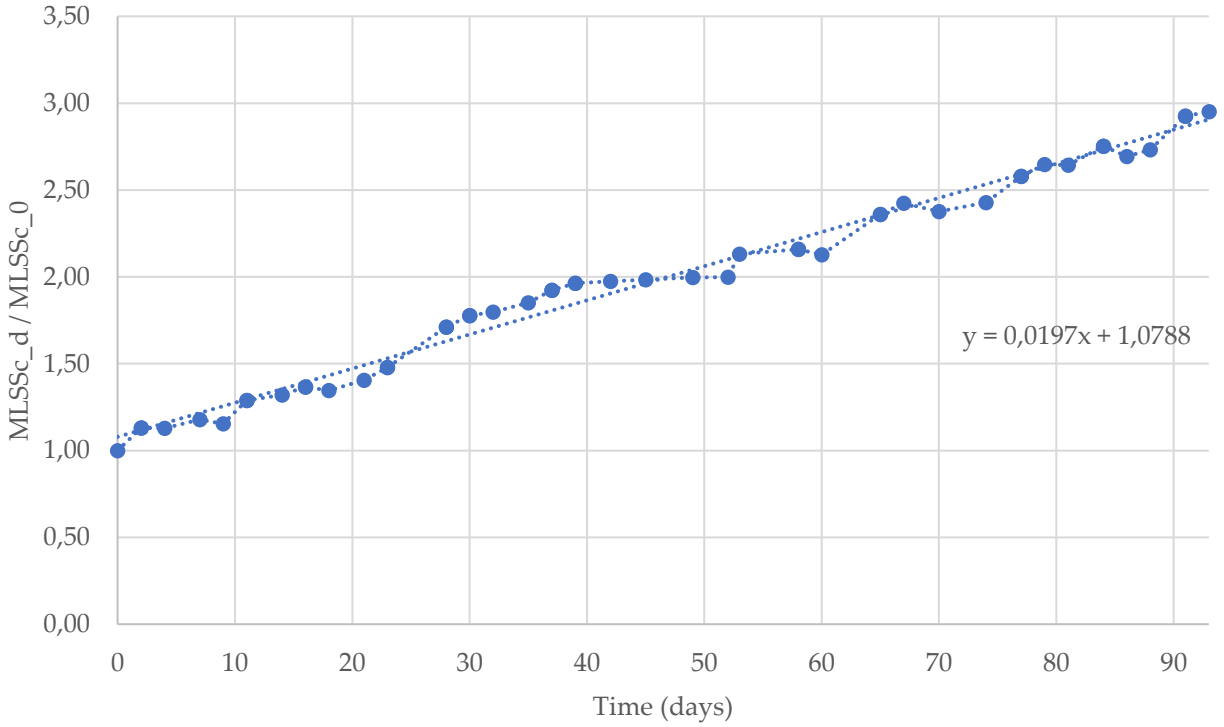

Figure 4.17 Estimated growth of the microorganisms of the SBR sludge

The rate of the EGM (EGMwr) was calculated on a weekly basis, using the formula:

$$EGMwr = \frac{EGM_1 - EGM_2}{d_1 - d_2} \cdot 7 \cdot 100$$

EGM_1 and EGM_2 are referred to EGM values separated by approximatively 7 days, EGM_1 being the more recent value. d_1 and d_2 are the times, expressed in days, between the start of the SBR operation and the MLSS measurements used to calculate respectively EGM_1 and EGM_2. The average EGMwr was 14,7%. Analyzing the graph where the EGMwr was plotted against time (Figure 4.18), a significant drop in the EGMwr was noticeable between 45 and 60 days after the start of the experiment. This drop in the EGMwr was confirmed by a coincident lower gradient in both the EGM and MLSS curves (Figure 4.16; Figure 4.17). The lower growth rate of the microorganisms during that period coincided with the anomalies in the measurements of most of the parameters monitored for the SBR effluent. These anomalies have been partly attributed, once again, to the winter holidays. During that period, the excess sludge removal was performed less frequently. Also, the simulated wastewater was prepared and stored in the feed tank in larger volumes, always assuring the safe and correct operation of the SBR. The correlation between the EGMwr and the pH (Figure 4.19) was particularly interesting. The pH is an important parameter that

affects the properties of the sludge and the metabolism of microorganisms (Jiang et al., 2019). Variations in pH can affect the thermodynamics of microbial redox reactions, determining whether microbial respiration reactions are thermodynamically favorable or not (Jin and Kirk, 2018). Looking at Figure 4.19 it was noticed that a decrease in pH below 7,20 was associated to a decrease in EGMwr. A similar decrease in the EGM weekly rate was observed around 35 and 85 days after the start of the experiment, when the pH increased over 7,50. These findings could suggested that the optimal pH value for the growth of the microbial populations (pHopt) present in the SBR sludge was comprised between 7,20 and 7,60. Even though pHopt is usually around neutrality for aerobic bacteria (Najafpour, 2015), different geochemical conditions of the environment are able to modify the microbial respiration response to pH variations (Jin and Kirk, 2018). It should be noted that the definition of pHopt for the microbial populations present in the SBR sludge was not the focus of the research. For this reason, more rigorous and focused studies should be performed to confirm the hypotheses of the correlation between pH variations and microbial growth, and the suggested pHopt range.

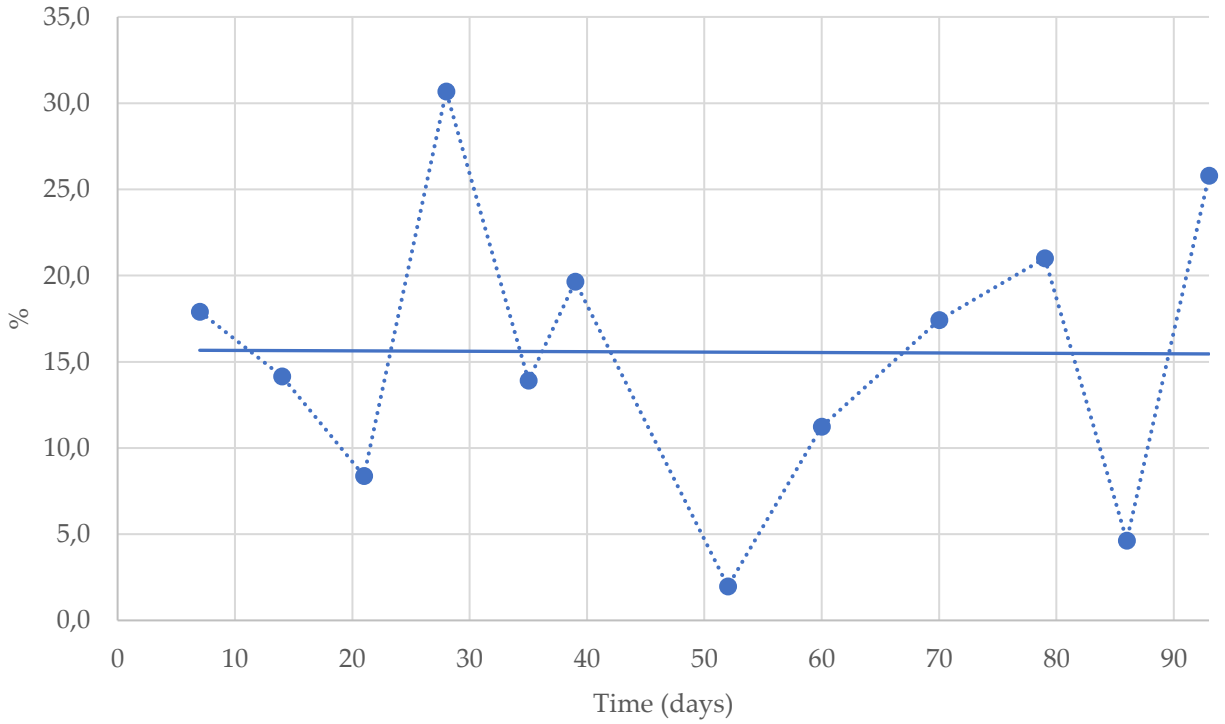

Figure 4.18 EGMwr of the SBR sludge

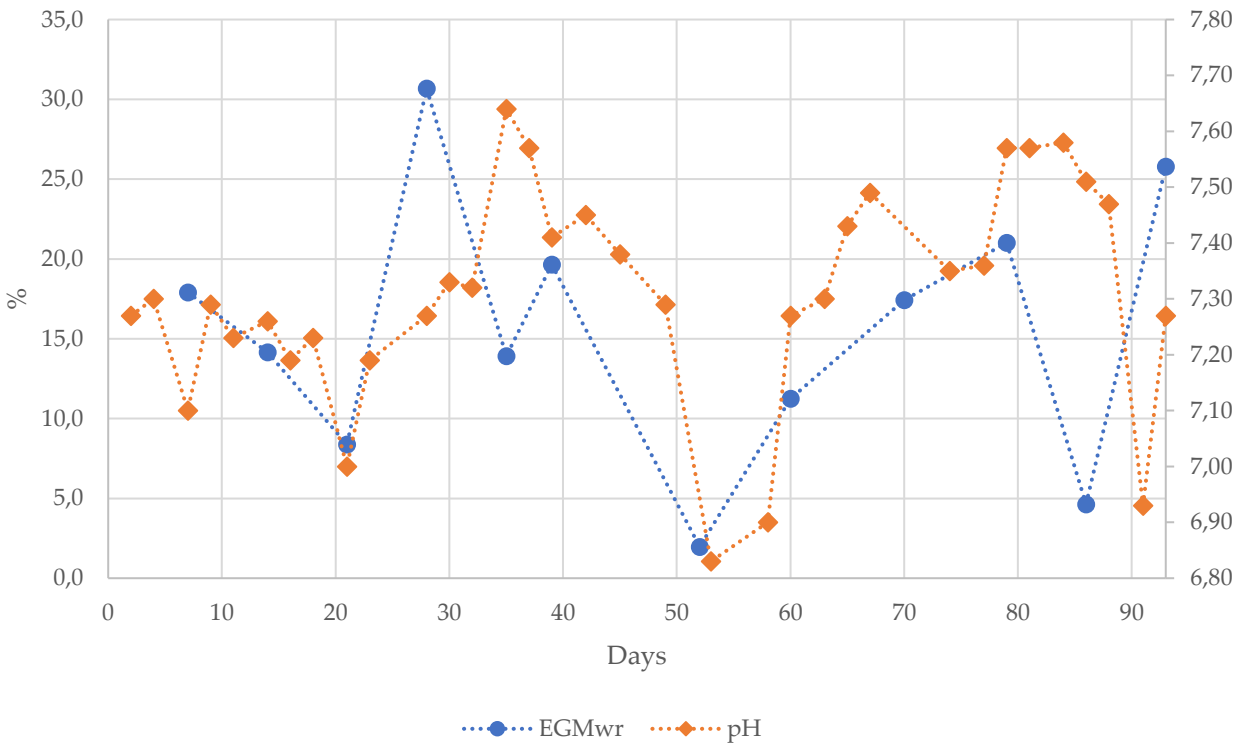

Figure 4.19 Evolution of EGMwr and pH over time

The results of the MLVSS analyses are shown in Figure 4.20, where MLVSS and MLSS data are compared.

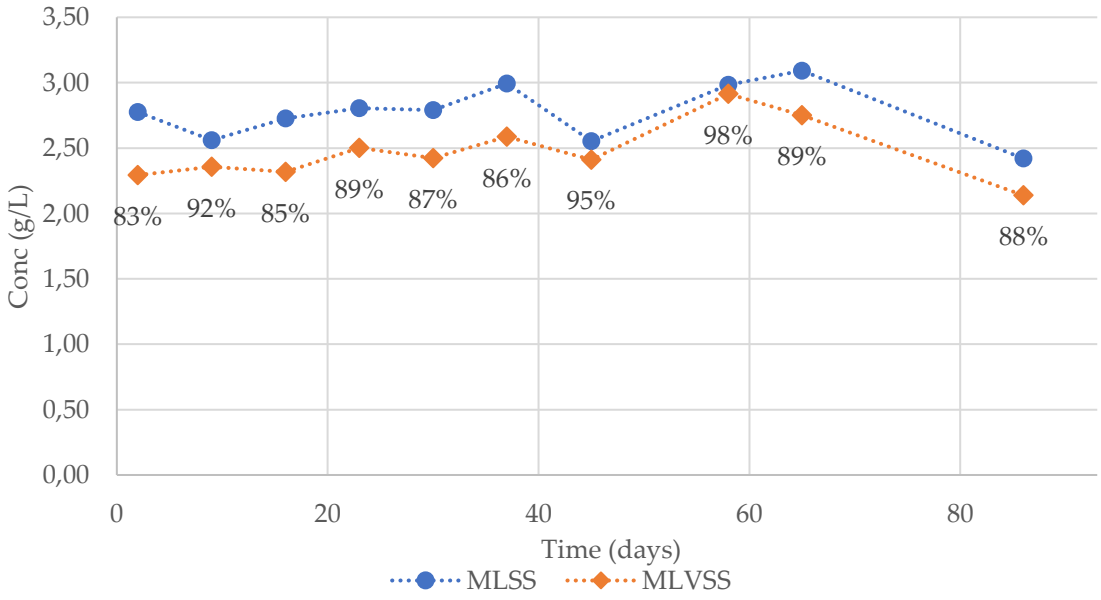

Figure 4.20 MLSS and MLVSS concentrations of the SBR sludge, with indication of the contribution of volatile solids due to the MLSS measurements

The results displayed in Figure 4.20 show that volatile solids contribution to the MLSS concentration was stable throughout the SBR operation, ranging from 83% to 92%. For the sludge samples analyzed between 45 and 60 days after the start of the experiment, however, the volatile solids contribution to the MLSS concentration increased to 95 % and 98%.

The z potential results showed the stability of the parameter throughout the SBR operation, with an average z potential of -10,8 mV.

4.2 Microplastics assessment

4.2.1 Physical characterization

The physical characterization process allowed the assessment of the MPFs concentration in the SBR sludge and in the effluent, the MPFs size distribution, and the MPFs color distribution. The concentration of MPFs in the simulated wastewater was also assessed, as well as the atmospheric contamination.

4.2.2 MPFs concentration

The analysis of the MPFs concentration in the SBR sludge showed a clear decrease in the first 40 days of the experiment, from 5 525 MPFs/L to 800 MPFs/L (Figure 4.21). The rate of the decrease diminished with time and after 40 days the concentration of MPFs in the SBR sludge remained quite stable ranging from 800 MPFs/L to 1410 MPFs/L.

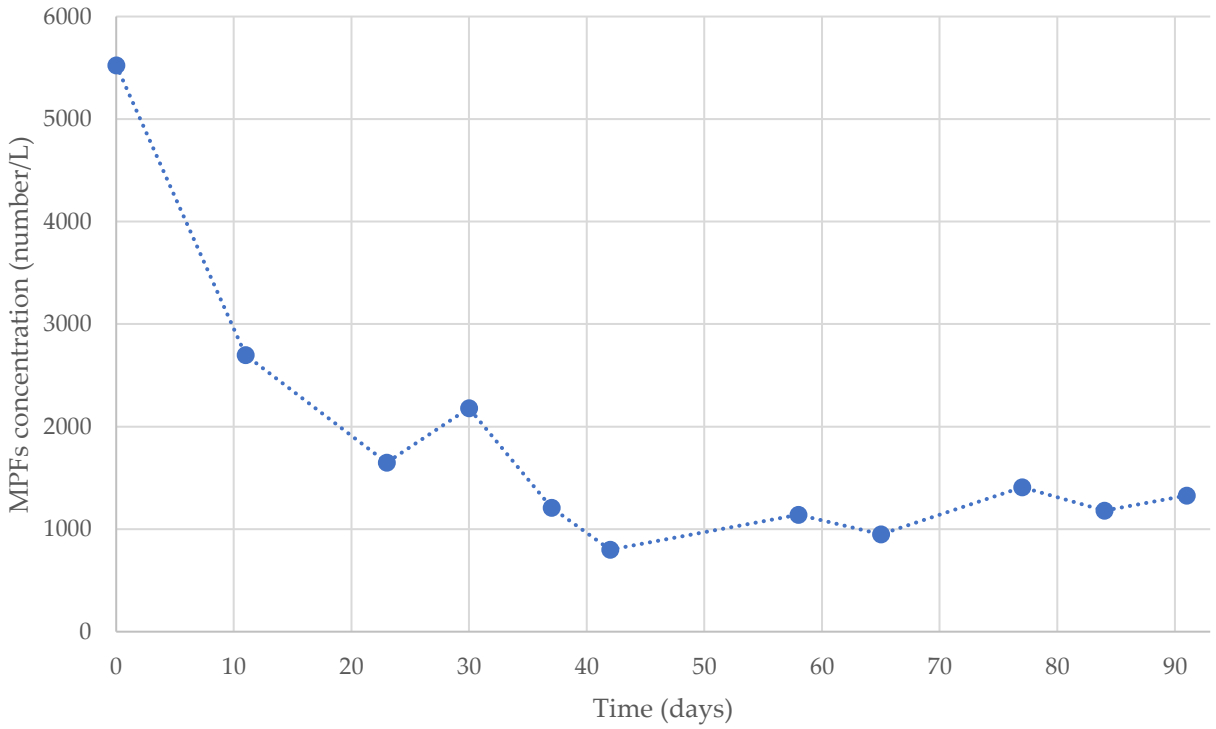

Figure 4.21 Variation in the concentration of MPFs in the SBR sludge

The analysis of the MPFs concentration in the SBR effluent showed a rapid decrease of the MPFs concentration in the first 10 days of the experiment, from 14,99 MPFs/L to 0,96 MPFs/L (Figure 4.22). Throughout the remaining of the SBR operation time the concentration of MPFs in the effluent was relatively stable, ranging from 0,55 MPFs/L to 2,28 MPFs/L. However, for the effluent filtered between 64 and 70 days after the start of the experiment, a concentration of 5,81 MPFs/L was measured. Various factors could have caused this anomalous spike in MPFs concentration. The first reason could be an error occurred during the collection or pretreatment processes. Also, a spike in the MPFs concentration in the tap water, used to prepare the simulated wastewater, could have caused a subsequent increase in the MPFs concentration in the SBR effluent. This hypothesis was suggested by the slight increase in MPFs concentration after the anomaly in the data, both in the effluent and in the sludge samples. Finally, it must be noted that the amount of water filtered through the effluent sampling device during that period was relatively low (Figure 4.22), which led to a lower representativeness of that specific sample. The previously described factors are not mutually exclusive and could have contributed to the observed result.

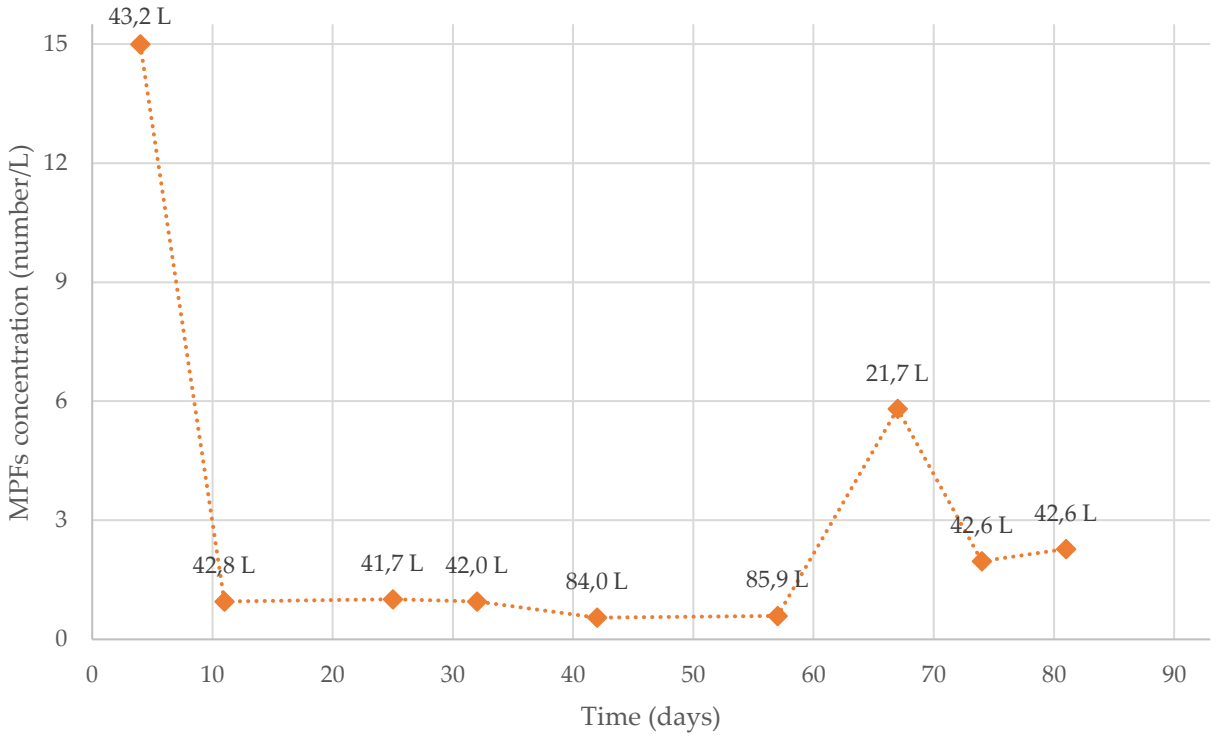

Figure 4.22 Concentration of MPFs in the SBR effluent, with indication of the amount of effluent filtered for each sample

Comparing the variation of the MPFs concentration in the SBR sludge and effluent with time (Figure 4.23), some similarities can be noticed. The first similarity is the trend: both concentrations decrease with time, as expected. In fact, before the start of the experiment the sludge was in the WWTP, where it was treating influents with a much higher concentration of microplastics compared to the simulated wastewater. The activated sludge have the capacity of removing and storing part of the MPs in the influent (Carr et al., 2016; Lares et al., 2018). The results showed in Figure 4.23 demonstrate that the sludge can also release microplastics when the influent has a low MPs concentration. The second feature noticeable in Figure 4.23 that is common between the two series of data is the presence of a horizontal asymptote. This finding shows that, when the later stage of the experiment was approached, an equilibrium between the MPFs entering in the SBR and exiting from the SBR was reached.

The relatively slow decrease in MPFs concentration in the SBR sludge suggests that during the settling phase microplastic fibers have a strong tendency to settle with the sludge. This consideration is supported by the persistence of the difference in MPFs concentration at the later stages of the experiment and by previous studies (Carr et al., 2016; Liu et al., 2019; Mahon et al., 2016).

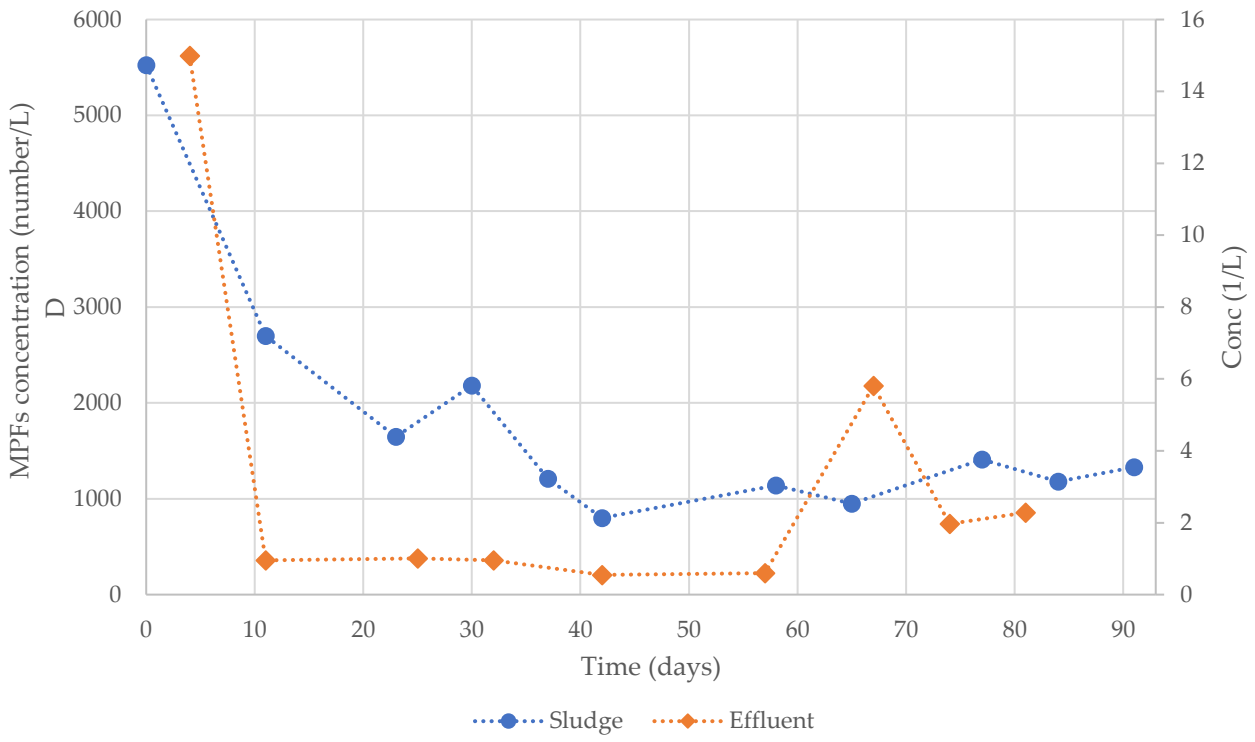

Figure 4.23 Variation of the MPFs concentration in the SBR sludge and effluent with time

The concentration of MPFs in the tap water, used to prepare the simulated wastewater, was measured in two different ways. In the first method, 5 L of tap water were directly filtered through a fiberglass filter with a pore size of 1 µm. The measured MPFs concentration was 11,4 MPFs/L. The second method measured the MPFs concentration filtering the tap water through the effluent sampling device and analyzing the removable screen. This procedure was repeated 2 times, the first one filtering 40 L of tap water and the second time filtering 10 L of tap water. The average of the measured MPFs concentrations was 2,3MPFs/L. Thanks to this second measurement, the MPFs recovery rate of the effluent sampling device was estimated at 20%. The recovery rate is relatively low because fibers longer then the mesh size can pass longitudinally through the sieve (Bretas Alvim et al., 2020; Sun et al., 2019)

Atmospheric deposition was assessed by analyzing a fiberglass filter with a pore size of 1 µm that was placed on the workspace in an open Petri dish for 1 week. A new fiberglass filter was also analyzed and the number of identified MPFs was subtracted to the previous result. 13 MPFs were identified in the fiberglass filter placed on the workspace and 1 MPF was identified on the new fiberglass filter. Dividing the result for the filtering area and for the duration of the test, it was calculated that the daily flux of deposited MPFs is 247 MPFs/m^2·day.

To describe the evolution over time of the concentration of MPFs larger than 150 µm in the sludge, a model was created. The model is based on a balance of the MPFs in the SBR system. The initial number

of MPFs is calculated multiplying the initial MPFs concentration of the SBR sludge by the sludge volume. For each day, the MPFs entering the system were added and the MPFs removed from the system were subtracted. Then, the modelled sludge concentration was calculated dividing the estimated total number of MPFs by the sludge volume. The same process was repeated for every day of the experiment obtaining a curve that models the MPFs concentration of the SBR sludge. The MPFs entering in the SBR were divided into two contributions: the MPFs present in the simulated wastewater and the MPs entering from a circular opening on top of the SBR for atmospheric deposition. The two contributions were calculated with the following formulas:

$$FEED_{in} = C_{tw} \cdot V_{feed}$$

where $FEED_{in}$ is the number of MPFs entering in the system with the simulated wastewater, C_{tw} is the concentration of MPFs in the tap water, measured using the effluent sampling device, and V_{feed} is the volume of simulated wastewater entering the system.

$$ATMD_{in} = F_{dep} \cdot A_{op}$$

Where $ATMD_{in}$ is the number of MPFs entering in the system for atmospheric deposition, F_{dep} is the daily flux of deposited MPFs, and A_{op} is the area of the circular opening on top of the SBR. The MPFs leaving the system were divided into two contributions: the MPFs present in the SBR effluent and the MPFs contained in the excess sludge removed. The two contributions were calculated with the following formulas:

$$EFFL_{out} = C_{effl} \cdot V_{effl}$$

Where $EFFL_{out}$ is the number of MPFs leaving the system with the effluent, C_{effl} is the concentration of MPFs in the effluent, and V_{effl} is the volume of effluent leaving the system.

$$EXCS_{out} = C_{slud} \cdot V_{slud}$$

Where $EXCS_{out}$ is the number of MPFs leaving the system with the excess sludge removed, C_{slud} is the concentration of MPFs in the SBR sludge, and V_{slud} is the volume of excess sludge removed from the system. In Figure 4.24 the curve that models the MPFs concentration of the SBR sludge is plotted against the measured MPFs concentration of the SBR sludge. The trend of the two series is decreasing, but the curve that models the MPFs concentration of the SBR sludge decreases at a slower rate initially. Also, the modelled curve does not have a horizontal asymptote approaching the later stage of the experiment. Both differences can be partly addressed to the low recovery rate of MPFs recovery rate of the effluent collection. The low recovery rate underestimates the actual concentration of MPFs $EFFL_{out}$ leaving the SBR with the effluent, which could explicate the initial slow decrease rate in the modelled sludge MPFs concentration. The effluent concentration was not corrected accounting for the recovery rate of the effluent

sampling device, because that value is not representative of the whole collection process of the SBR effluent. The recovery rate of the effluent sampling device has been measured filtering continuously tap water through the device. On the contrary, the effluent was sampled discontinuously for a period of 1 week. The discontinuity of the process may favor the rearrangement of the fibers captured by the removable sieve, which could increase the portion of MPFs that pass longitudinally through the sieve. To maintain uniformity between the protocols used for the measurements, the MPFs concentration of the tap water used in the model is the value measured with the effluent sampling device. This choice, although improving the uniformity between the measuring protocols, underestimates the number of MPFs $FEED_{in}$ entering in the system with the simulated wastewater. The underestimation of $FEED_{in}$ could explain why in the model, at the later stage of the experiment, the positive and negative contributions are not balanced and the modelled curve does not have a horizontal asymptote, shown by the measured data. To improve the fit of the model, further refinements would be needed. Firstly, the quantification of the exact recovery rate of the effluent collection phase, as well as the recovery rate of the sludge collection phase, would be needed. Then, it would be advised to monitor eventual variations of MPFs concentration in the tap water.

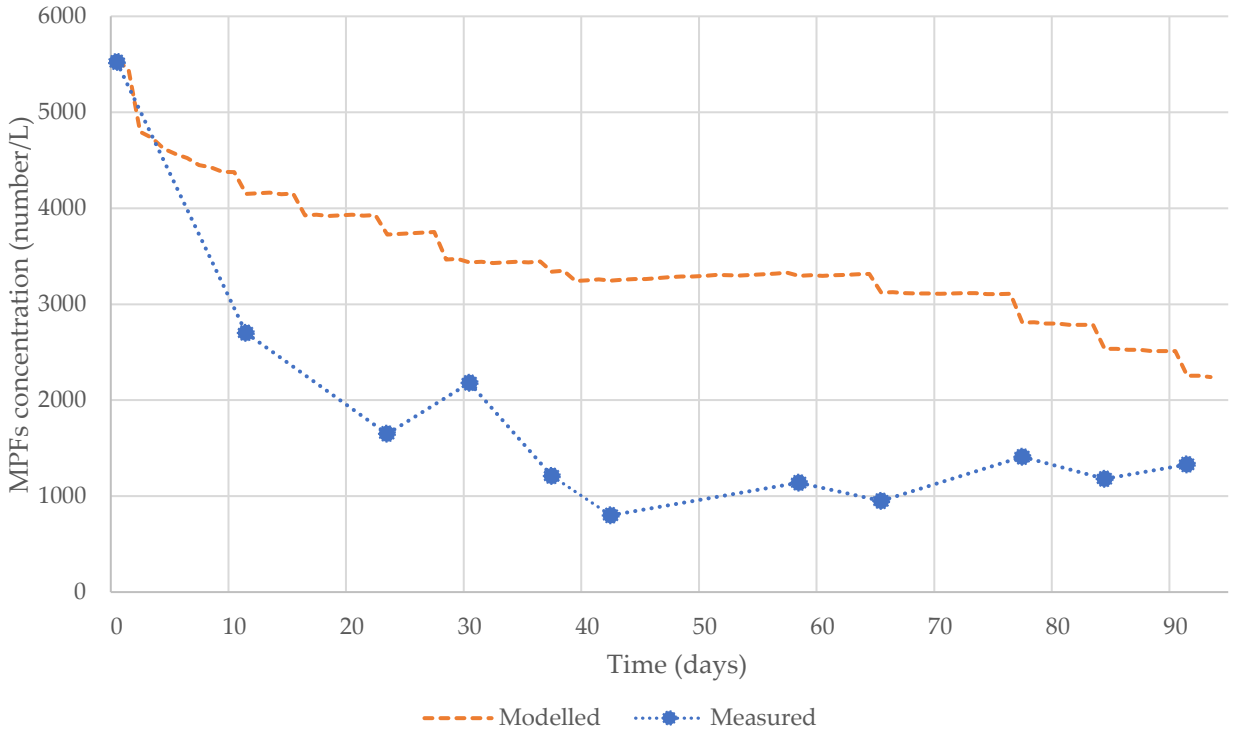

Figure 4.24 Measured and modelled MPFs concentration of the SBR sludge.

4.2.3 MPFs size distribution

The size distribution of the MPFs in the SBR sludge was estimated using the data obtained from all the sludge samples. The 150 μm – 5 000 μm range was divided in 50 μm intervals and for each interval the number of recovered MPFs was counted. The size distribution of the MPFs recovered from the SBR sludge samples was characterized by the probability mass function (PMF) (Figure 4.25) and by the cumulative distribution function (CDF) (Figure 4.26). It is noticeable that the majority of MPFs recovered from the SBR sludge were relatively small. The 64,9% of the recovered MPFs were smaller than 1 000 μm and the average size of the MPFs was 968 μm.

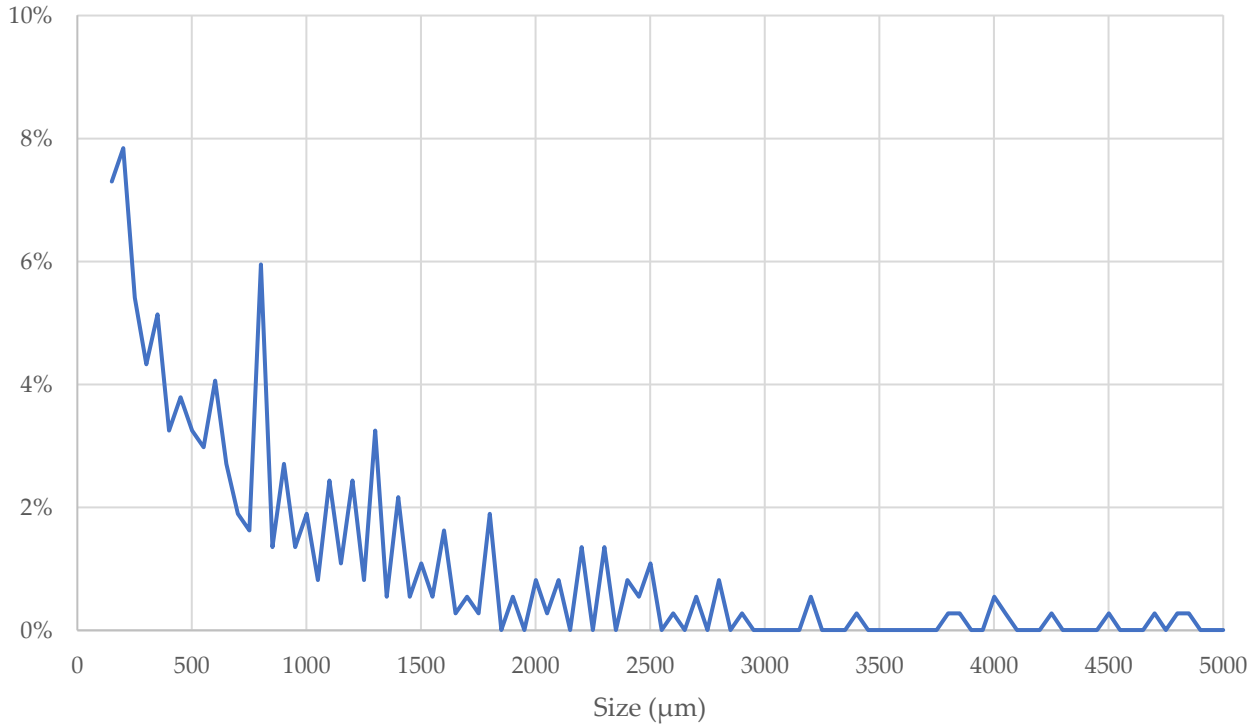

Figure 4.25 PMF of the sizes of the MPFs recovered from the sludge samples

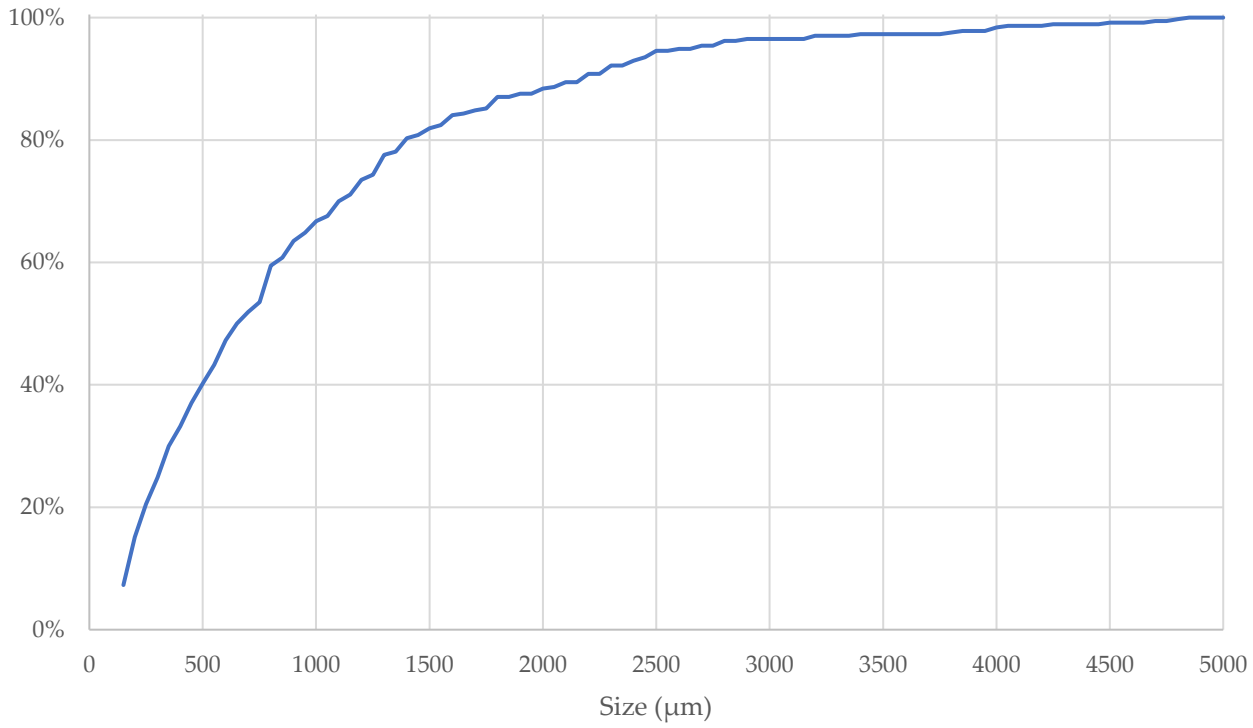

Figure 4.26 CDF of the sizes of the MPFs recovered from the sludge samples

The PMF and CDF of the MPFs recovered from the SBR sludge were also calculated using only the initial samples and only the final samples, to investigate eventual modifications (Figure 4.27, Figure 4.28). The samples collected from the 11th of October to the 18th of December were defined as initial samples, whereas the samples collected from the 8th of January to the 10th of February were defined as final samples. The comparison highlighted a higher percentage of small MPFs in the sludge in the later stage of the SBR operation. The percentage of recovered MPFs smaller than 500 µm was 27,7% for the initial sludge samples and 46,4% for the final sludge samples. In a similar way, the average size of the recovered MPFs decreases towards the end of the SBR operation. The average size of the MPFs was 1 124 µm for the initial sludge samples and 818 µm for the final sludge samples. The first value was in line with the results of Murphy et al. (2016), which found that MPs recovered from the sludge of a secondary sludge were on average 1 342 µm in size, whereas the second value was significantly lower. These differences can be attributed to the origin of the AS sample used to seed the SBR. The WWTPs influents have high abundance of larger MPs, as the number of microplastics over 500 µm could sometimes reach over 70% (Sun et al., 2019). On the contrary, the effluents of WWTPs generally have a higher proportion of small MPs. In their review, Sun et al. (2019) found that, on average, in WWTPs effluents over 90% of microplastics were smaller than 500 µm. It is safe to assume that the simulated wastewater used to feed the SBR, which was prepared with tap water, had a higher proportion of small MPFs compared to the WWTP

influent. The change in the size distributions of the influents could have resulted in a shift in the MPFs size distribution in the SBR sludge, ultimately leading to an increase of the percentage of small MPFs.

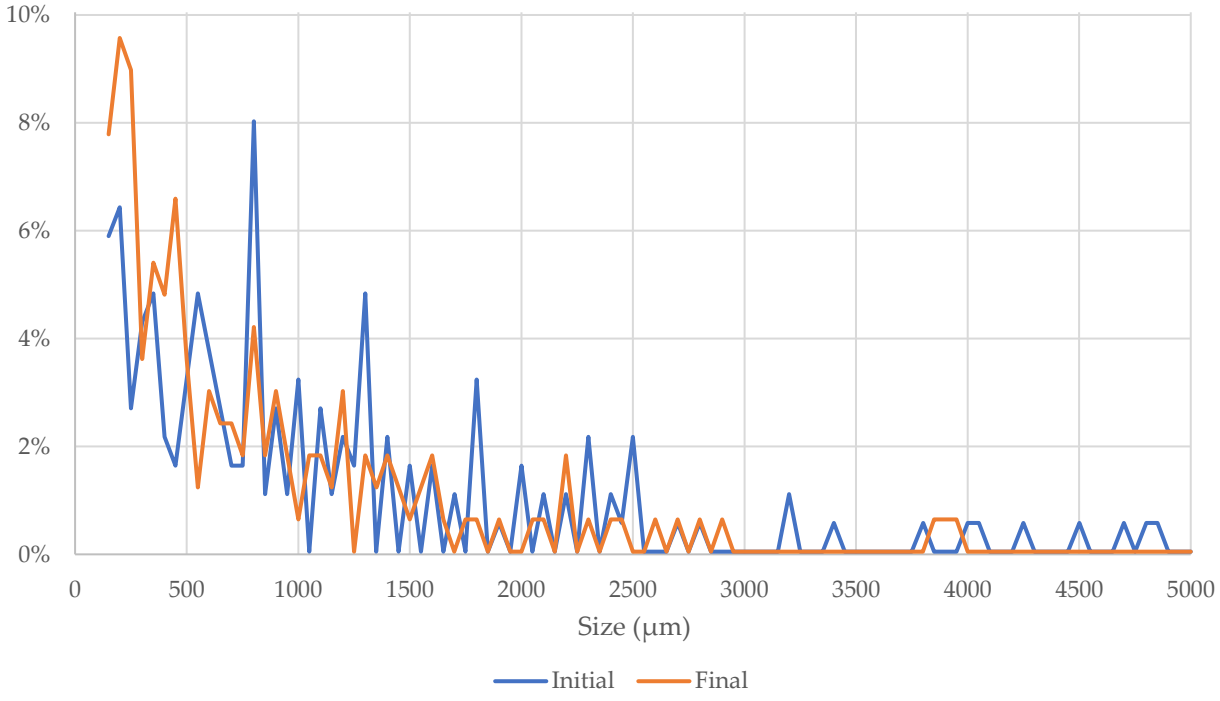

Figure 4.27 PMFs of the MPFs recovered from initial and final sludge samples

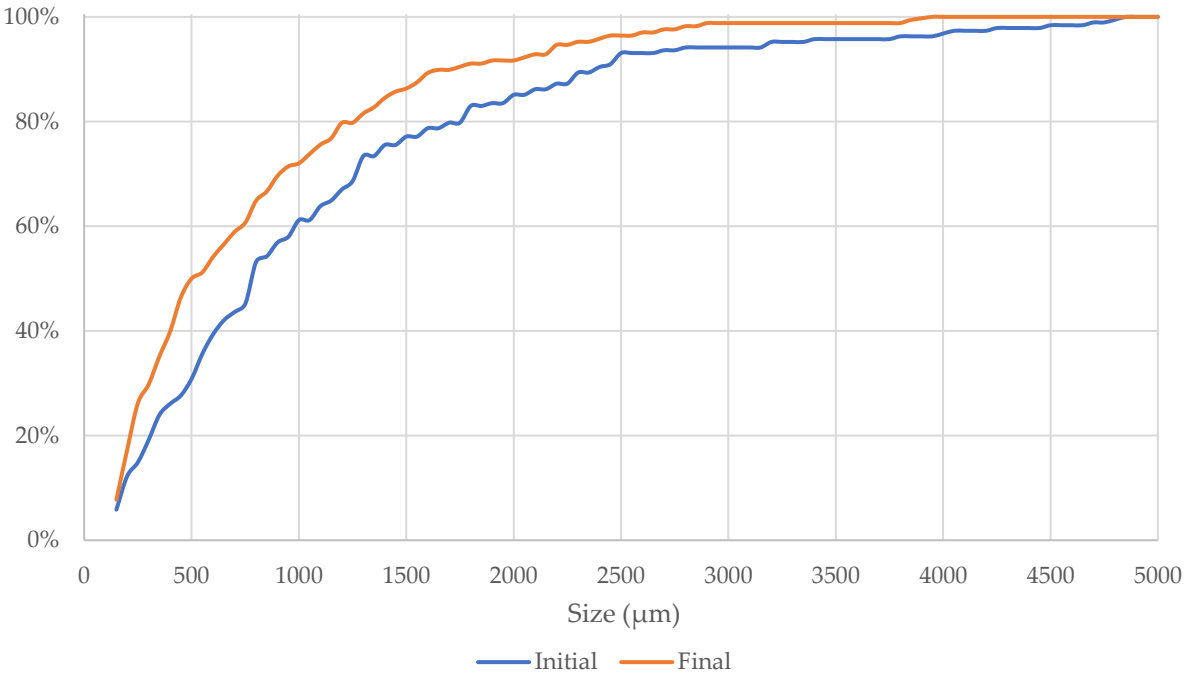

Figure 4.28 CDF of the MPFs recovered from initial and final sludge samples

The size distribution of the MPFs in the SBR effluent was estimated following the procedure previously described for the SBR sludge, using the data obtained from all the effluent samples (Figure 4.29, Figure 4.30).

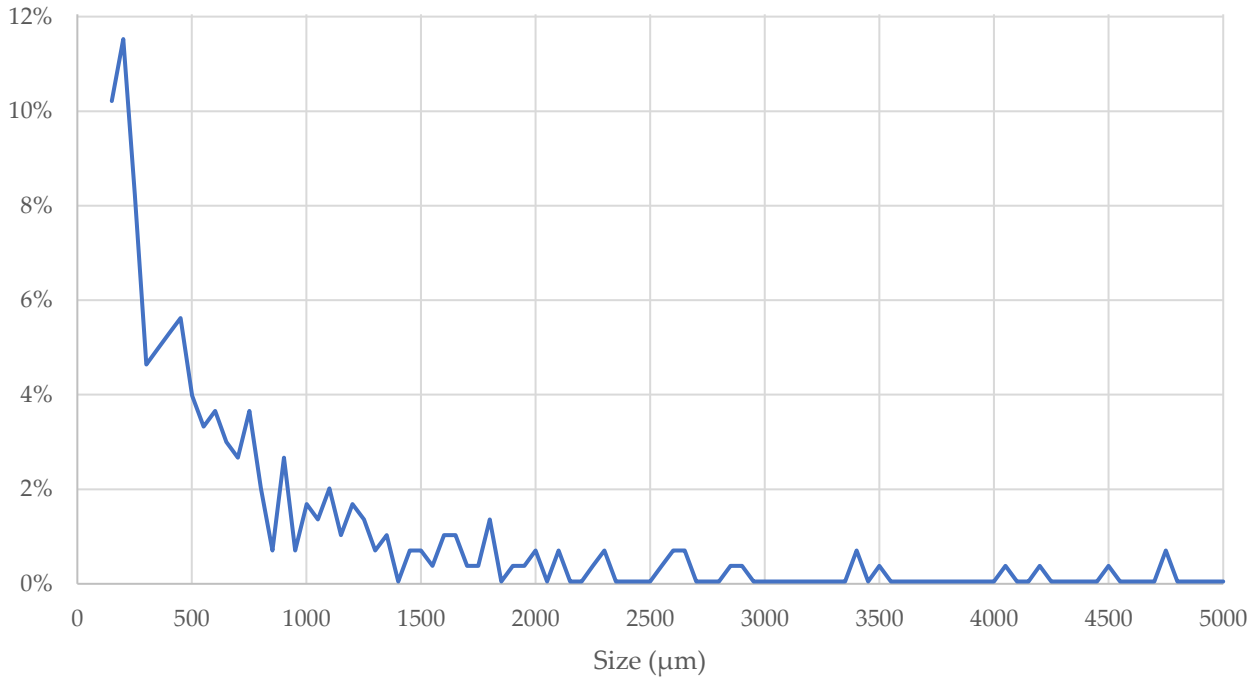

Figure 4.29 PMF of the sizes of the MPFs recovered from the effluent samples

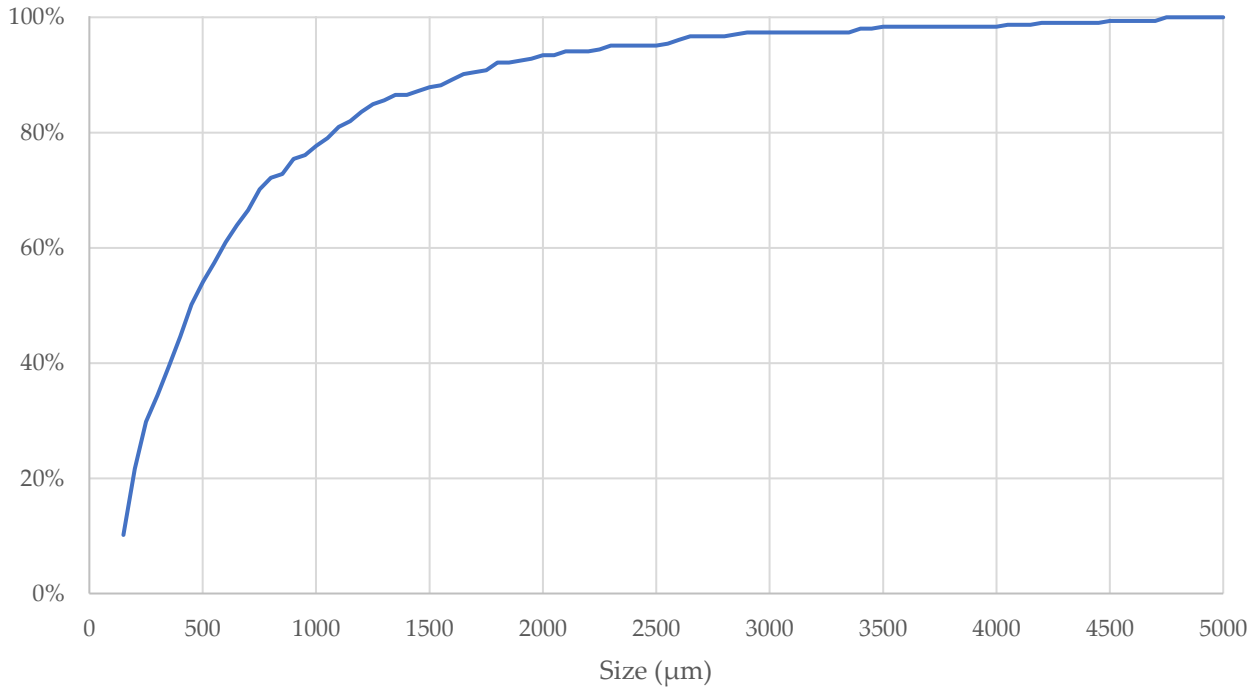

Figure 4.30 CDF of the sizes of the MPFs recovered from the effluent samples

The 76,1% of the recovered MPFs were smaller than 1 000 μm and the average size of the MPFs was 772 μm. It was noticeable a higher proportion of small fiber compared to the sludge samples. This finding confirmed the results of previous studies (Murphy et al., 2016) and supported the evidence that larger MPFs are more likely to be removed during the sedimentation phase (Murphy et al., 2016).

4.2.4 MPFs color distribution

The results of the color characterization of the MPFs recovered from the sludge and the effluent samples are shown respectively in Figure 4.31 and in Figure 4.32. The color distributions of the MPFs recovered from the sludge and the effluent samples are similar. In the effluent samples a slight decrease in the proportion of brightly colored (black, red) and transparent MPFs is accompanied by an increase in the proportion of gray MPFs. However, these small differences must be examined with caution due to the various factors affecting the color distribution analysis. Firstly, even after performing balance procedure indicated by the stereomicroscope manufacturer, a slight shift in the color displayed in the imaging software can be present. Moreover, the boundaries between different colors are not sharp and the adopted discretization of the color spectrum implied the loss of part of the color distribution information. However, the biggest challenge was noticing particles similar in color to the background (Murphy et al., 2016), which was white in our specific case. That could explain why most studies showed a higher proportion of white MPFs, which often accounted for the majority of the recovered MPFs (Hidalgo-Ruz et al., 2012; Li et al., 2018). The problem may be worsen by hydrogen peroxide usage during the pretreatment phase, which may cause discoloration in MPFs (Prata et al., 2019a).

Particles with eye-catching colors have a higher probability of being isolated for subsequent chemical identification whereas those with dull colors are easily overlooked, thus potentially introducing bias (Hidalgo-Ruz et al., 2012; Nuelle et al., 2014). However, MPFs color has been found to be unlikely associated with a polymer type (Hidalgo-Ruz et al., 2012), which lowered the probabilities of bias during the chemical identification. Still, the difficulty in noticing particles similar in color to the background could be a problem for MPFs counts, suggesting that the analysis of variations in concentration is more reliable than single measurements.

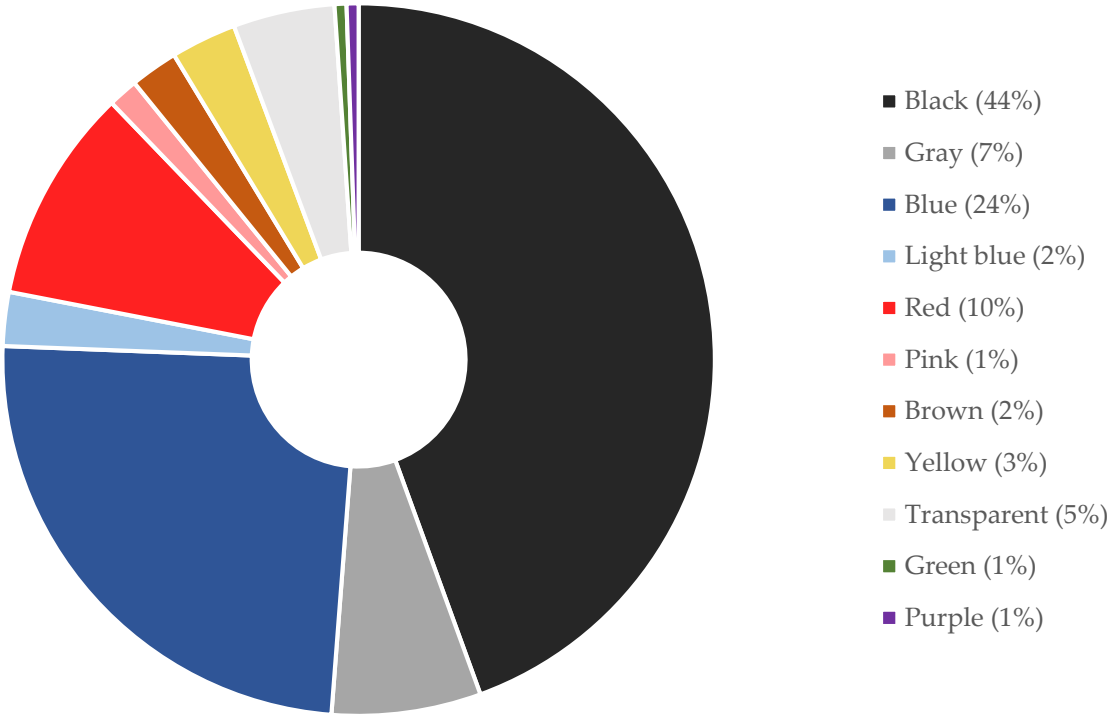

Figure 4.31 Color distribution of the MPFs recovered from the sludge samples

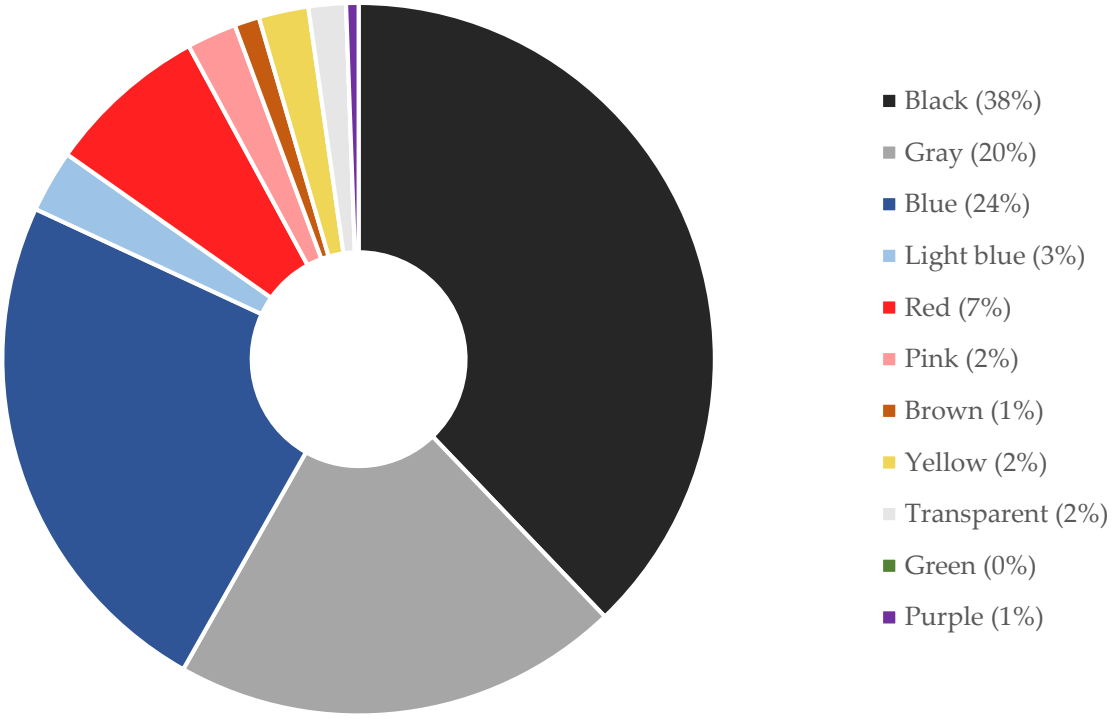

Figure 4.32 Color distribution of the MPFs recovered from the effluent samples

4.3 Chemical characterization

Chemical characterization was essential to ensure the quality of the physical characterization and to obtain information on the relative abundance of different polymer types (MSFD Technical Subgroup on Marine Litter, 2013; Sun et al., 2019). Due to the time-consuming nature of the FTIR analysis, in our study part of the visually identified microfibers were analyzed by the FTIR spectrometer as suggested by the MSFD Technical Subgroup on Marine Litter (2013). The first analyzed sample was the initial SBR sludge sample, collected on the 13th of November 2019. The spectra of 25 of the recovered suspected MPFs were measured and the collected spectra were analyzed with the KnowItAll software. The preprocessed spectrum was compared to the built-in reference spectra library and to the spectra library of textile fibers developed by the Institute of Chemistry University of Tartu (Institute of Chemistry University of Tartu, 2018). Of the analyzed fibers, 18 were identified as cotton fibers, 2 as PET fibers, 1 as rayon fiber and 4 fibers were unidentified (Figure 4.33). Two examples of chemical characterization by FTIR analysis are shown in Figure 4.34 and Figure 4.35. The 4 unidentified fibers had similar spectra, and the closest match was the spectrum of wool fibers (Figure 4.36). However, the differences between the characteristic wavelengths of the wool fibers' spectrum and the peaks of the 4 unidentified spectra are significative, which impeded the identification of the fibers' material.

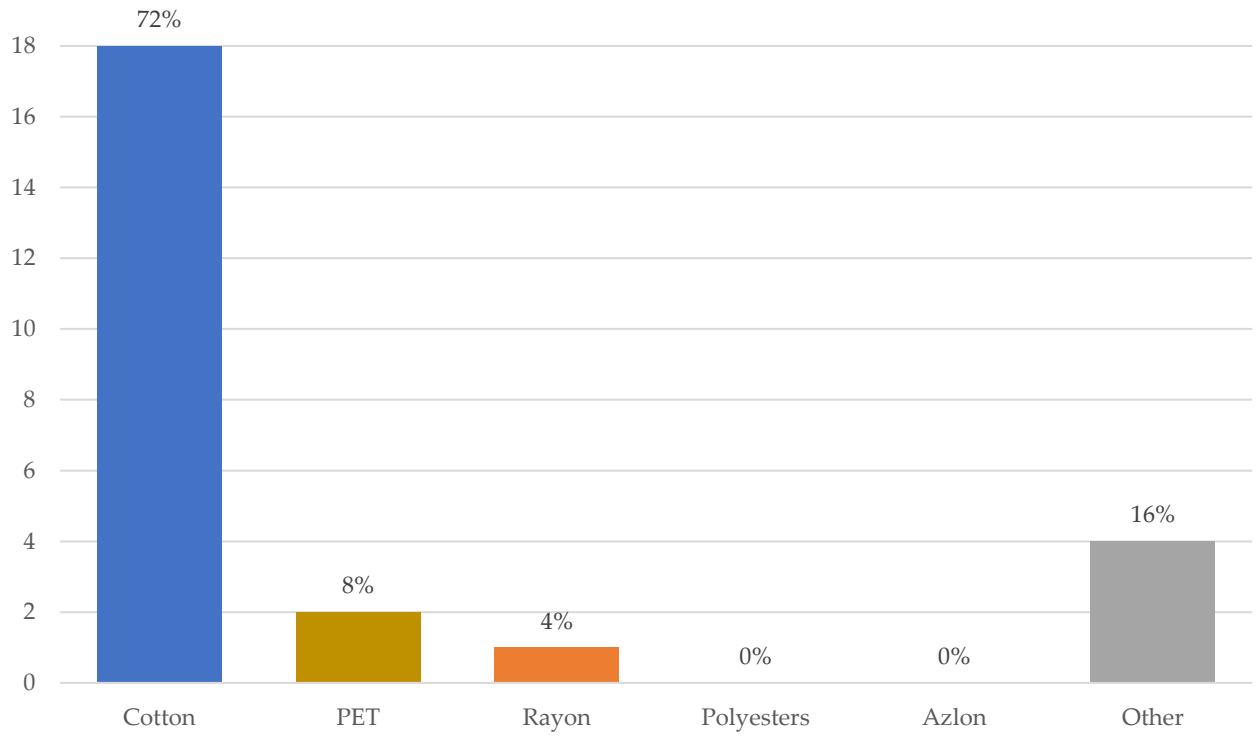

Figure 4.33 MPFs composition of the 13/11/2019 sludge sample

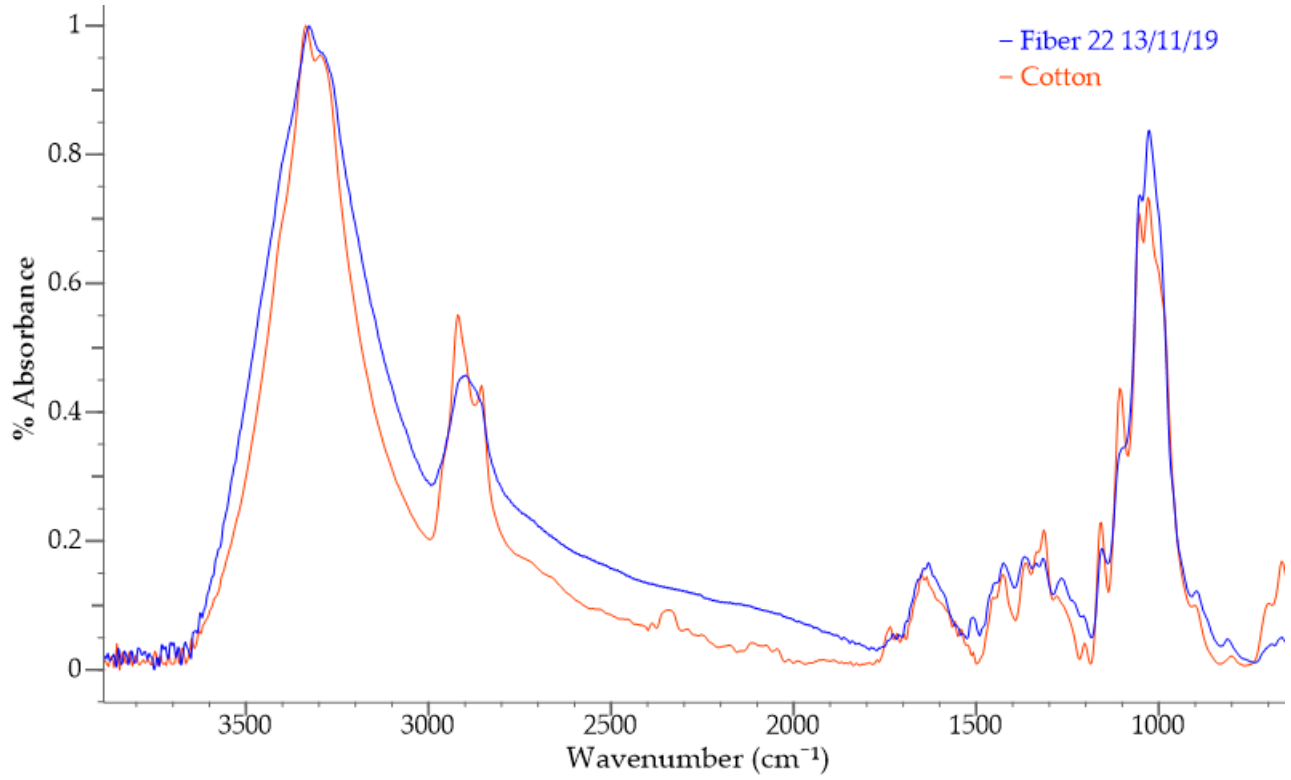

Figure 4.34 FTIR spectrum of a Cotton fiber from the 13/11/2019 sludge sample compared to the reference spectrum

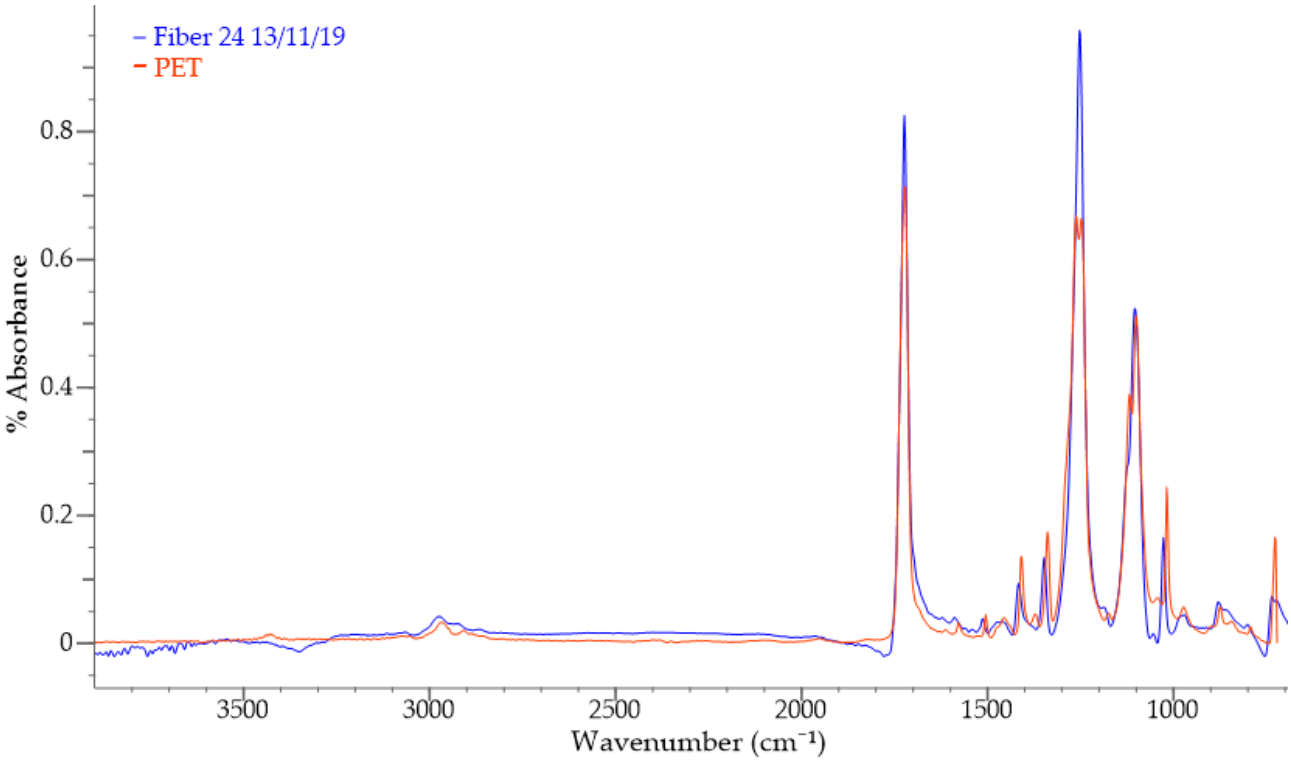

Figure 4.35 FTIR spectrum of a PET fiber from the 13/11/2019 sludge sample compared to the reference spectrum

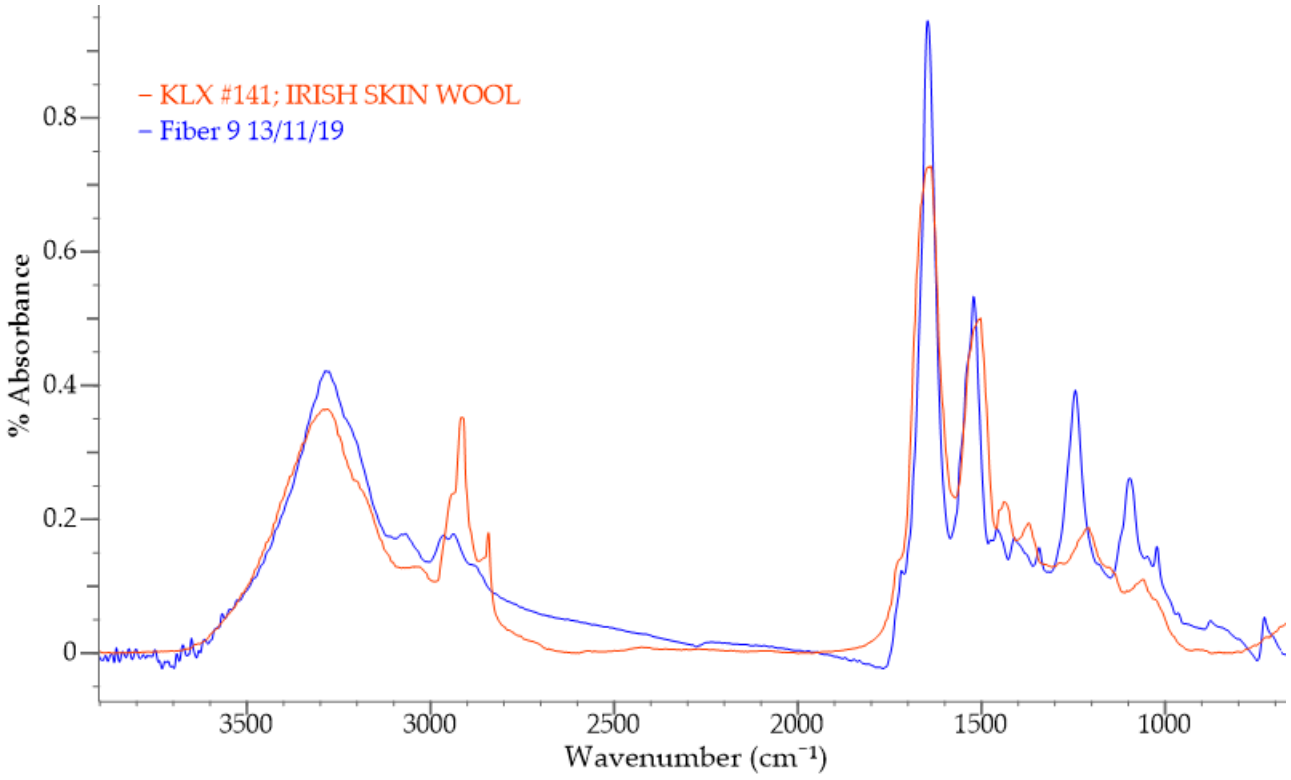

Figure 4.36 FTIR spectrum of a Fiber 9 from the 13/11/2019 sludge sample compared to the wool reference spectrum

The comparison of the suspected MPFs with reference libraries was performed considering the drawbacks of the method. The presence of residues of organic and inorganic material, the weathering of the fiber, or the presence of additives and fillers can cause the addition or disappearance of some peaks (Renner et al., 2019, 2017). These modifications influence the measured spectra and the comparison with the reference libraries, most of which are based on non-degraded pure and often synthetic reference materials(Renner et al., 2019, 2017). That problem is exacerbated when the analyzed fiber has a natural origin, as even the spectra of pure and non-degraded samples acquired from different reference libraries can vary slightly.

Figure 4.33 highlights that 88% of the suspected MPFs recovered from the initial sludge sample were natural fibers. which confirmed the findings of previous studies (Gies et al., 2018; Hidalgo-Ruz et al., 2012; Yang et al., 2019; Ziajahromi et al., 2017). The high proportion of natural fibers amongst suspected MPFs underlined the urge for the definition of a more reliable procedure to visually distinguish natural and plastic microfibers. For this reason, the other samples were chemically characterized after the execution of the digestion protocol with H_2SO_4 (70%) (AATCC, 2018). The second analyzed sample was the sludge sample collected on the 27th of January 2020, from which 7 of the recovered microfibers were analyzed. The protocol described by the AATCC (2018) was performed on the sludge sample collected

on the 27th of January 2020 in its first adaptation, in which the filter was placed in a Buchner funnel instead of being folded in a glass funnel. The reagents were carefully pipetted on the unfolded filter, which was never completely covered by the reagents. Also, the reagents were used in lower volumes than the ones prescribed by the AATCC protocol. Of the 7 analyzed microplastics, 5 were identified as cotton fibers, 1 as PET fiber and 1 was unidentified (Figure 4.37). Two examples of chemical characterization by FTIR analysis are shown in Figure 4.34 and Figure 4.39.

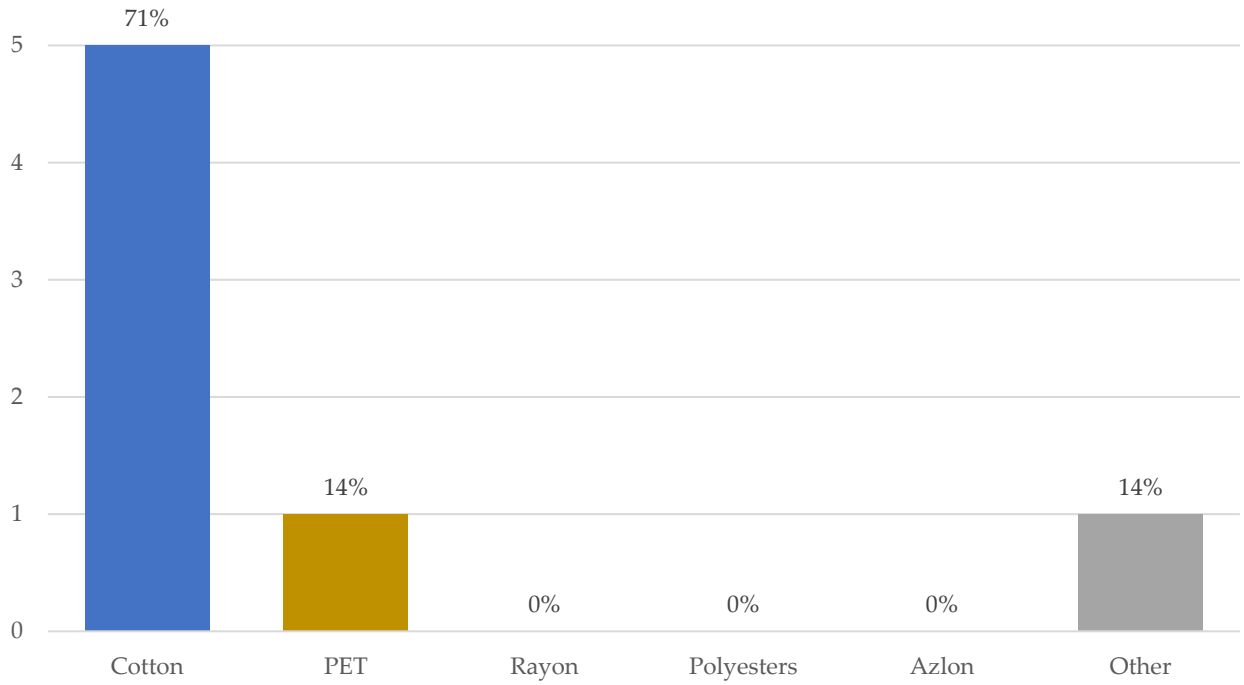

Figure 4.37 MPFs composition of the 27/01/2020 sludge sample, after the digestion protocol

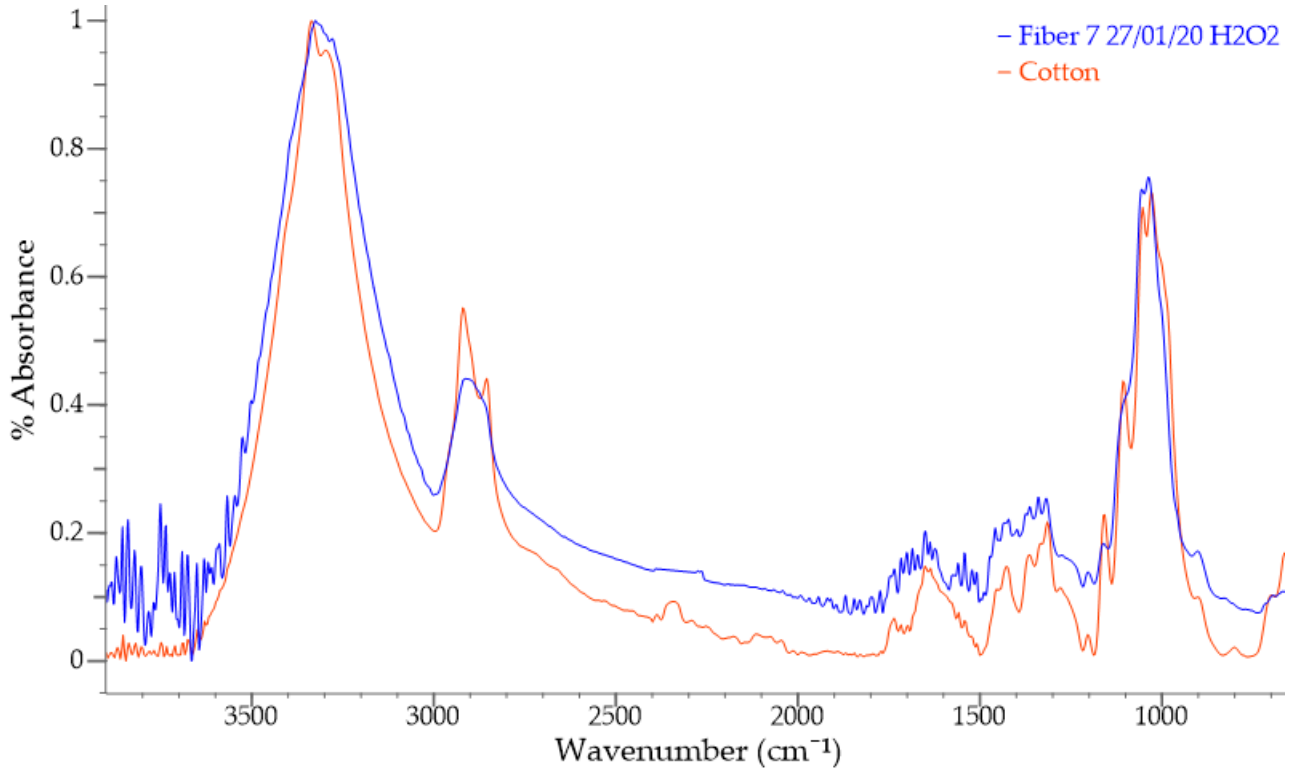

Figure 4.38 FTIR spectrum of a Cotton fiber from the 27/01/2020 sludge sample digested with H_2O_2, compared to the reference spectrum

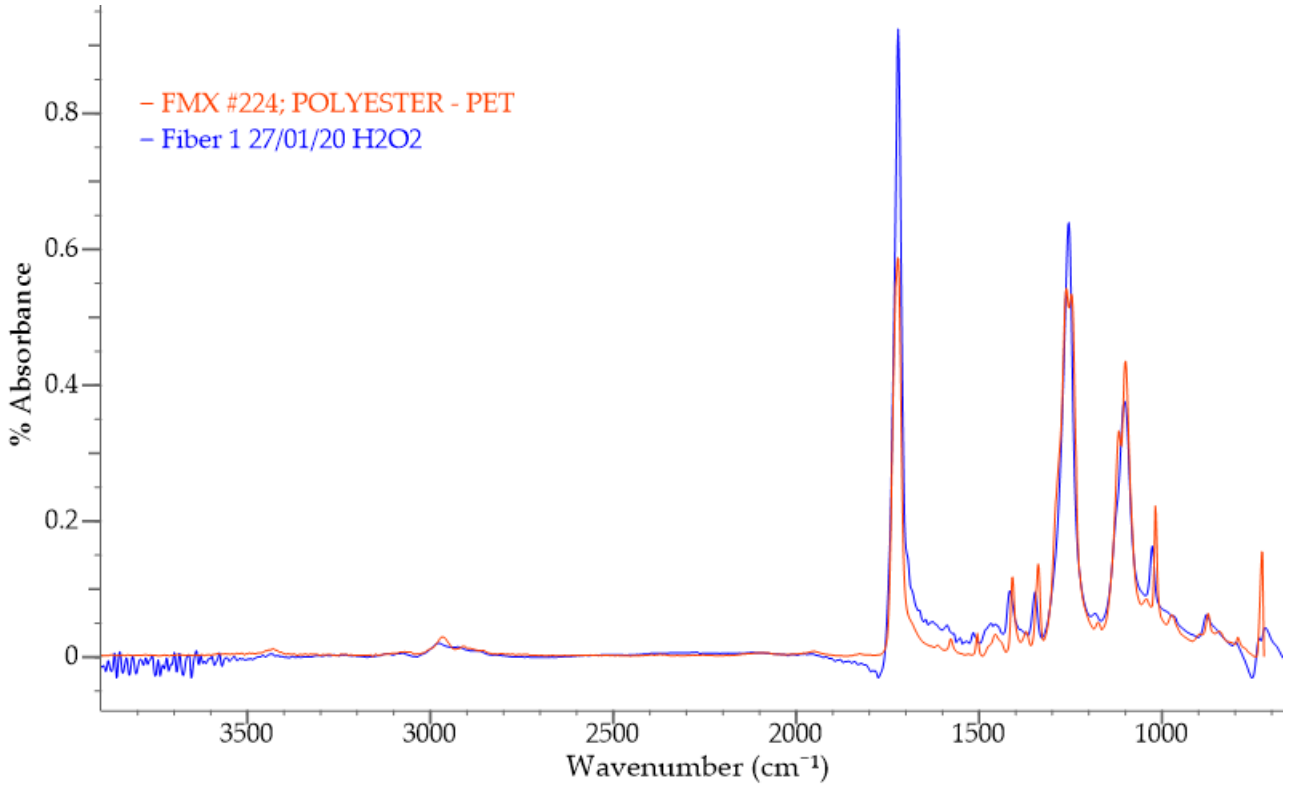

Figure 4.39 FTIR spectrum of a PET fiber from the 27/01/2020 sludge sample digested with H_2O_2, compared to the reference spectrum

The FTIR analysis demonstrated that the first iteration of the adaptation of the AATCC (2018) digestion protocol was unsuccessful, as cotton fibers still accounted for the majority of the suspected MPs. To improve the effectiveness, the second iteration of the adaptation increased the volume of the used reagents to match the prescriptions of the protocol. The biggest improvement, however, was the implementation of a funnel where the filter with the recovered MPFs was folded. This modification allowed the surface of the filter to be completely covered by the reagents throughout the procedure, representing more accurately the prescription of the AATCC digestion protocol. The last analyzed sample was the initial SBR sludge sample, which was characterized for the second time after the execution of the final adaptation of the H_2SO_4 digestion protocol. Of the analyzed fibers, 9 were identified as polyester fibers, 2 as PET fibers, 2 as Azlon fibers and 1 fiber was unidentified (Figure 4.40). Three examples of chemical characterization by FTIR analysis are shown in Figure 4.41Figure 4.34, Figure 4.42, Figure 4.43. The application of the protocol was successful in eliminating natural fibers, as the proportion of natural fibers in the 13/11/2019 sludge sample decreased from 88% to non-detected after the digestion. Even though the results of the test were very promising, further studies are needed to better understand the effect of the adapted digestion protocol to the MPFs, with particular attention to nylon, rayon and spandex, which are soluble or partially soluble in H_2SO_4 (70%) (AATCC, 2018).

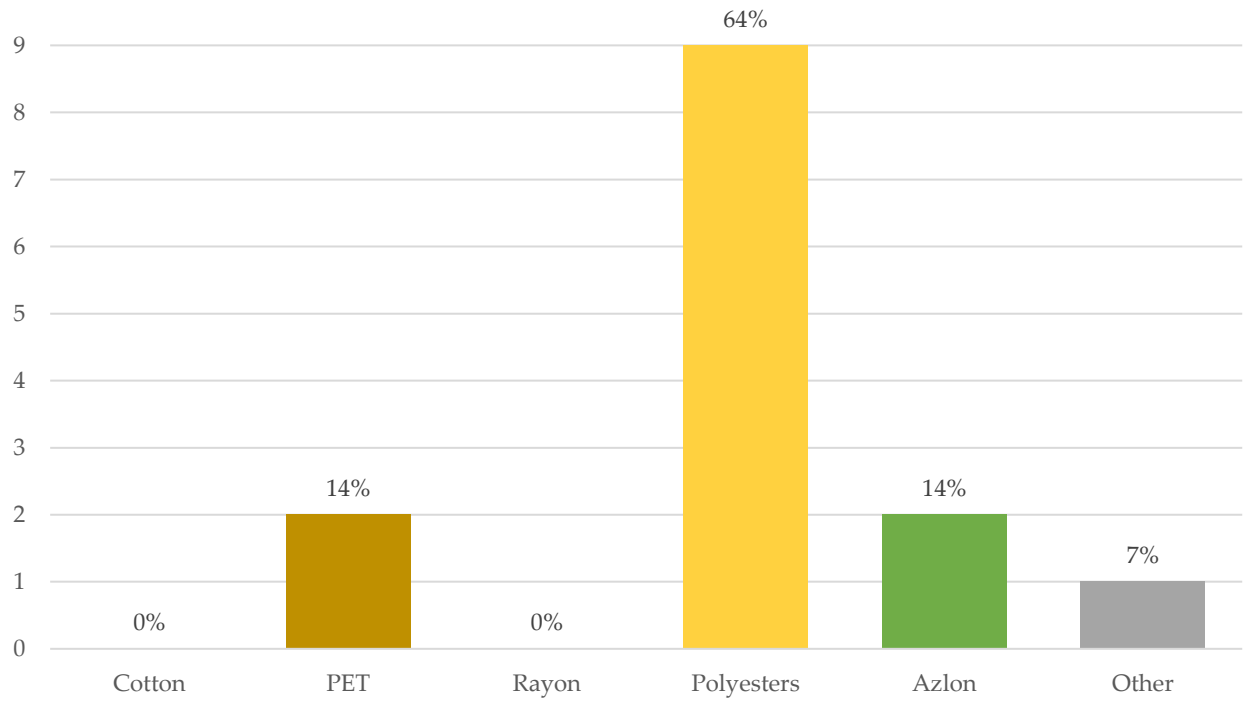

Figure 4.40 MPFs composition of the 13/11/2019 sludge sample, after the digestion protocol

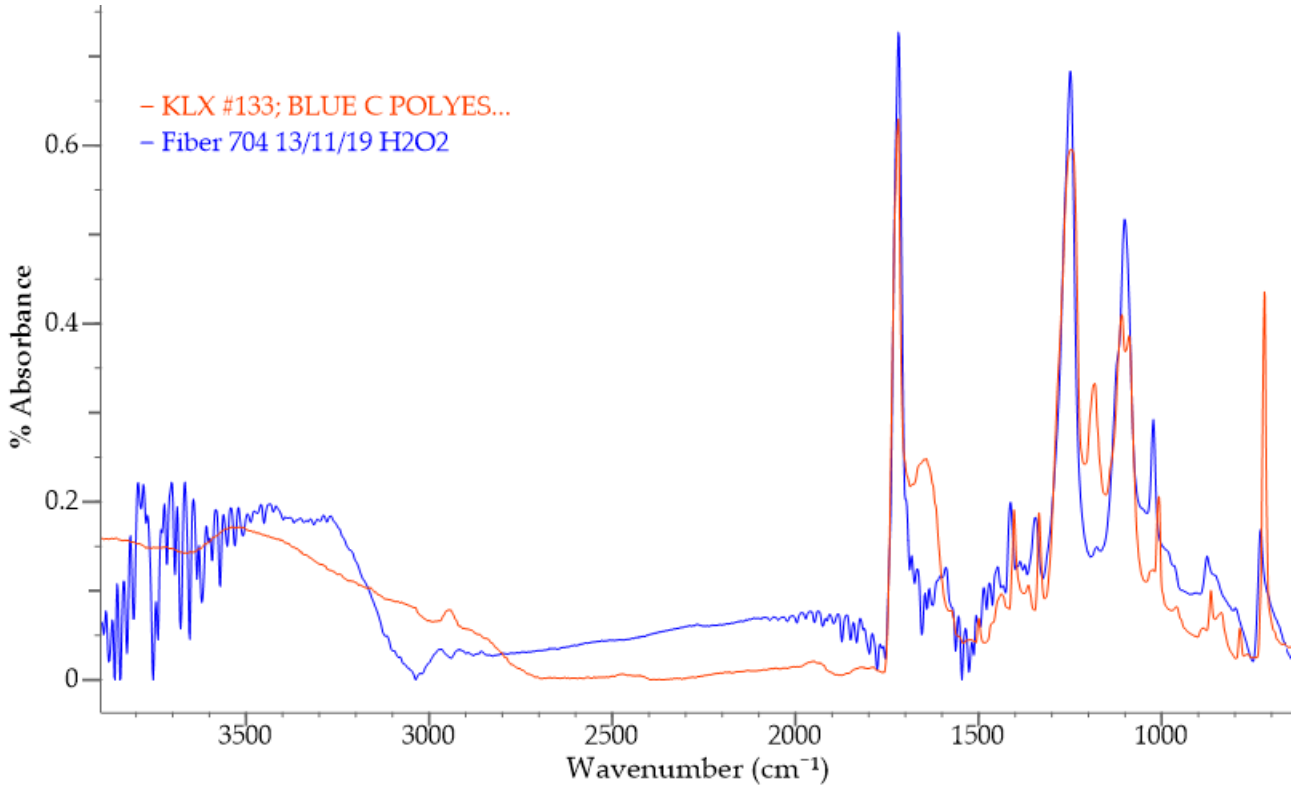

Figure 4.41 FTIR spectrum of a Polyester fiber from the 13/11/2019 sludge sample digested with H_2O_2, compared to the reference spectrum

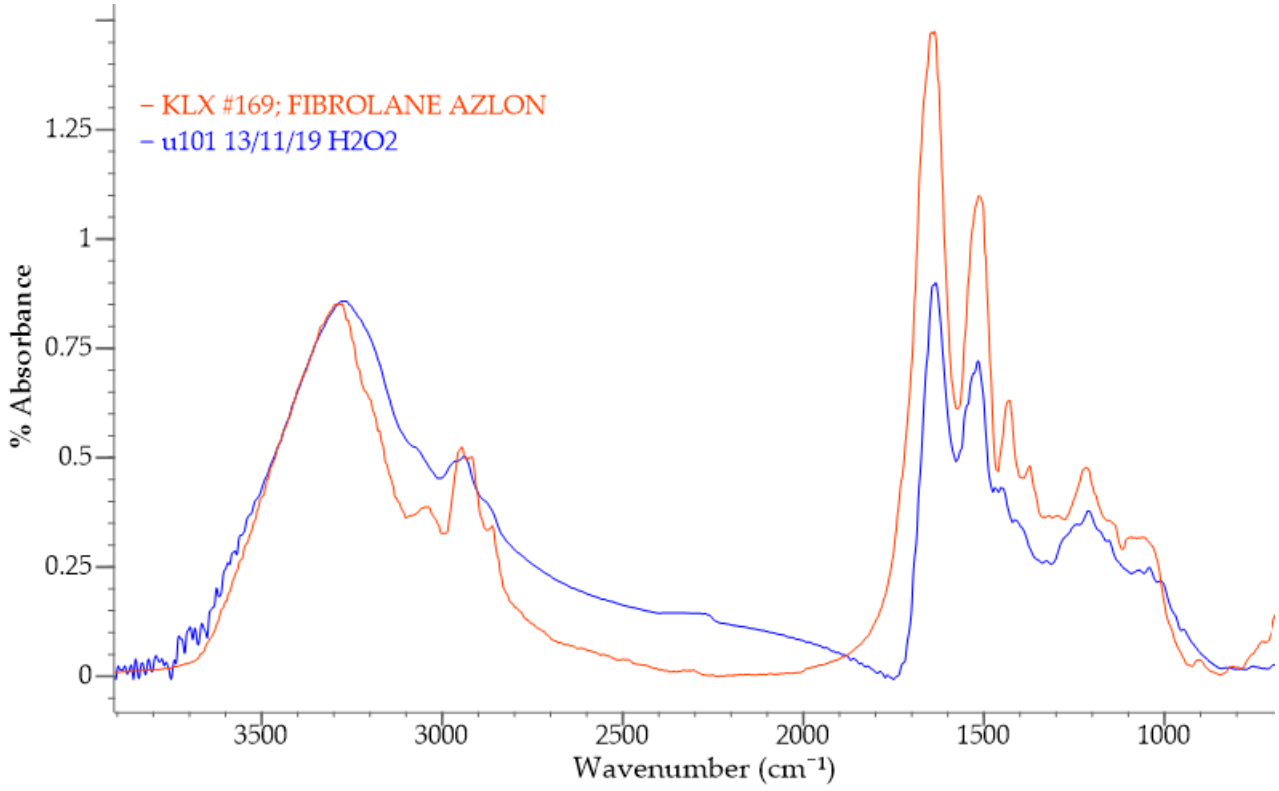

Figure 4.42 FTIR spectrum of a Azlon fiber from the 13/11/2019 sludge sample digested with H_2O_2, compared to the reference spectrum

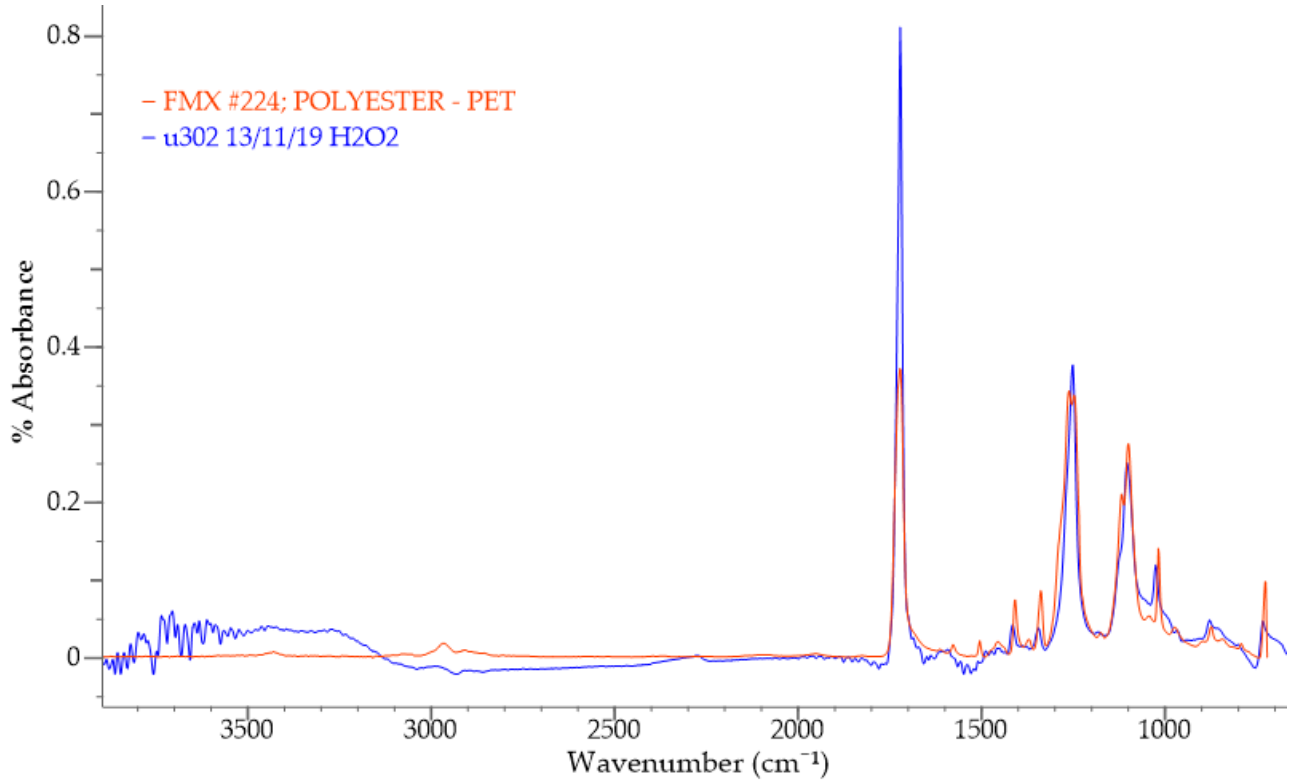

Figure 4.43 FTIR spectrum of a PET fiber from the 13/11/2019 sludge sample digested with H_2O_2, compared to the reference spectrum

5 Conclusions

MPs are an emerging pollutant that can be found worldwide, raising concerns especially in aquatic ecosystems. WWTPs are the ultimate barrier preventing MPs from being discharged into natural waters. For this reason, the MPFs behavior in secondary treatment was evaluated.

The analysis of the MPFs concentration in the SBR sludge showed a clear decrease in the first 40 days of the experiment, from 5 525 MPFs/L to 800 MPFs/L, after which remained quite stable. The analysis of the MPFs concentration in the SBR effluent showed a similar trend characterized by a faster decrease developed in the first 10 days. The decreasing trends were expected, as before the start of the experiment the sludge was treating influents with a much higher concentration of MPs compared to the simulated wastewater. The shift of the influent, with the feeding of the simulated wastewater, can also explain the decrease in the average MPFs size over time. The two series of data approached a horizontal at the later stage of the experiment, showing that an equilibrium between the MPFs entering in the SBR and exiting from the SBR was reached. The relatively slow decrease in MPFs concentration in the SBR sludge suggested that during the settling phase microplastic fibers have a strong tendency to settle with the sludge. This consideration is supported by the persistence of the difference in MPFs concentration at the later stages of the experiment and by previous studies. The results also showed that, when the influent has a low MPs concentration, the WWTPs sludge can release MPs, which confirms the concerns over the land usage of the WWTPs sludge. Finally, the effluent had a higher proportion of small fibers, confirming the results of previous studies and supporting the evidence that larger MPFs are more likely to be removed during the sedimentation phase.

To quantify the distribution of the entering MPFs into the AS and the effluent, a model of the concentration of MPFs in the SBR sludge was developed. The modeled concentration showed a decreasing trend, but slower than the decrease actually observed, and did not approach a horizontal asymptote. Both differences can be partly addressed to the low recovery rate of MPFs recovery rate of the effluent collection. To improve the fit of the model, further refinements would be needed: the quantification of the exact recovery rate of the effluent collection phase, the quantification of the recovery rate of the sludge collection phase, the monitoring of eventual variations of MPFs concentration in the tap water. The analyses of the positive contribution of the model showed that, due to atmospheric deposition and especially the tap water used to prepare the SW, it is very difficult to reach lower concentrations.

The second aim was to assess the proportion between natural and synthetic fibers in the SBR. 88% of the suspected MPFs recovered from the initial sludge sample were natural fibers, confirming the findings of previous studies. The high proportion of natural fibers amongst suspected MPFs underlined the urge

for the definition of a more reliable procedure to visually distinguish natural and plastic microfibers. The final adaptation of the H_2SO_4 digestion protocol was successful in eliminating natural fibers from the sample. Even though the results of the test were very promising, further studies are needed to better understand the effect of the adapted digestion protocol to the MPFs, with particular attention to nylon, rayon and spandex, which are soluble or partially soluble in H_2SO_4 (70%).

Finally, various authors stated that the lack of uniformity in the methods used for sampling and detection can lead to inconsistent results which are difficult to compare. Rapid, efficient and reliable protocols for the study of MPs are urgently needed. Meanwhile, the comparison amongst different studies of concentration trends must be preferred over the comparison of single measurements.

References

1. AATCC, A.A. of T.C. and C., 2018. Test Method for Fiber Analysis: Quantitative.
2. Avio, C.G., Gorbi, S., Milan, M., Benedetti, M., Fattorini, D., D'Errico, G., Pauletto, M., Bargelloni, L., Regoli, F., 2015a. Pollutants bioavailability and toxicological risk from microplastics to marine mussels. Environ. Pollut. 198, 211–222. https://doi.org/10.1016/j.envpol.2014.12.021
3. Avio, C.G., Gorbi, S., Regoli, F., 2015b. Experimental development of a new protocol for extraction and characterization of microplastics in fish tissues: First observations in commercial species from Adriatic Sea. Mar. Environ. Res. 111, 18–26. https://doi.org/10.1016/j.marenvres.2015.06.014
4. Babuponnusami, A., Muthukumar, K., 2014. A review on Fenton and improvements to the Fenton process for wastewater treatment. J. Environ. Chem. Eng. https://doi.org/10.1016/j.jece.2013.10.011
5. Bernardo, P., Drioli, E., 2010. Membrane Technology: Latest Applications in the Refinery and Petrochemical Field, in: Comprehensive Membrane Science and Engineering. Elsevier Inc., pp. 211–239. https://doi.org/10.1016/B978-0-08-093250-7.00054-2
6. Bretas Alvim, C., Mendoza-Roca, J.A., Bes-Piá, A., 2020. Wastewater treatment plant as microplastics release source – Quantification and identification techniques. J. Environ. Manage. 255. https://doi.org/10.1016/j.jenvman.2019.109739
7. Carbery, M., O'Connor, W., Palanisami, T., 2018. Trophic transfer of microplastics and mixed contaminants in the marine food web and implications for human health. Environ. Int. https://doi.org/10.1016/j.envint.2018.03.007
8. Carr, S.A., Liu, J., Tesoro, A.G., 2016. Transport and fate of microplastic particles in wastewater treatment plants. Water Res. 91, 174–182. https://doi.org/10.1016/j.watres.2016.01.002
9. Chahal, C., van den Akker, B., Young, F., Franco, C., Blackbeard, J., Monis, P., 2016. Pathogen and Particle Associations in Wastewater: Significance and Implications for Treatment and Disinfection Processes. Adv. Appl. Microbiol. 97, 63–119. https://doi.org/10.1016/bs.aambs.2016.08.001
10. Cocca, M., Di Pace, E., Errico, M.E., Gentile, G., Montarsolo, A., Mossotti, R., 2018. Proceedings of the International Conference on Microplastic Pollution in the Mediterranean Sea. Int. Conf. Microplastic Pollut. Mediterr. Sea 22, 238. https://doi.org/10.1007/978-3-319-71279-6
11. Cole, M., Lindeque, P.K., Halsband, C., Galloway, T.S., 2011. Microplastics as contaminants in the marine environment: A review. Mar. Pollut. Bull. https://doi.org/10.1016/j.marpolbul.2011.09.025
12. Cole, M., Webb, H., Lindeque, P.K., Fileman, E.S., Halsband, C., Galloway, T.S., 2014. Isolation of microplastics in biota-rich seawater samples and marine organisms. Sci. Rep. 4, 1–8. https://doi.org/10.1038/srep04528
13. Conkle, J.L., Báez, C.D., Valle, D., Turner, J.W., 2018. Are We Underestimating Microplastic

Contamination in Aquatic Environments? Environ. Manage. 61, 1–8. https://doi.org/10.1007/s00267-017-0947-8

14. DAM, D. de A. del M., 2019. EDAR CARRAIXET - DAM [WWW Document]. URL https://www.dam-aguas.es/portfolio-posts/edar-carraixet/ (accessed 5.3.20).
15. De Souza Machado, A.A., Lau, C.W., Till, J., Kloas, W., Lehmann, A., Becker, R., Rillig, M.C., 2018. Impacts of Microplastics on the Soil Biophysical Environment. Environ. Sci. Technol. 52, 9656–9665. https://doi.org/10.1021/acs.est.8b02212
16. Dehaut, A., Cassone, A.L., Frère, L., Hermabessiere, L., Himber, C., Rinnert, E., Rivière, G., Lambert, C., Soudant, P., Huvet, A., Duflos, G., Paul-Pont, I., 2016. Microplastics in seafood: Benchmark protocol for their extraction and characterization. Environ. Pollut. 215, 223–233. https://doi.org/10.1016/j.envpol.2016.05.018
17. Dowarah, K., Patchaiyappan, A., Thirunavukkarasu, C., Jayakumar, S., Devipriya, S.P., 2020. Quantification of microplastics using Nile Red in two bivalve species Perna viridis and Meretrix meretrix from three estuaries in Pondicherry, India and microplastic uptake by local communities through bivalve diet. Mar. Pollut. Bull. 153. https://doi.org/10.1016/j.marpolbul.2020.110982
18. Dris, R., Gasperi, J., Rocher, V., Saad, M., Renault, N.A.A., Tassin, B.A., 2015. Microplastic contamination in an urban area: a case study in Greater Paris. Environ. Chem. https://doi.org/10.1071/EN14167ï
19. Duan, L., Jiang, W., Song, Y., Xia, S., Hermanowicz, S.W., 2013. The characteristics of extracellular polymeric substances and soluble microbial products in moving bed biofilm reactor-membrane bioreactor. Bioresour. Technol. 148, 436–442. https://doi.org/10.1016/j.biortech.2013.08.147
20. Dümichen, E., Eisentraut, P., Bannick, C.G., Barthel, A.K., Senz, R., Braun, U., 2017. Fast identification of microplastics in complex environmental samples by a thermal degradation method. Chemosphere 174, 572–584. https://doi.org/10.1016/j.chemosphere.2017.02.010
21. Enders, K., Lenz, R., Beer, S., Stedmon, C.A., 2017. Extraction of microplastic from biota: recommended acidic digestion destroys common plastic polymers. ICES J. Mar. Sci. 74, 326–331. https://doi.org/10.1093/icesjms/fsw173
22. EPRO, 2016. Plastics – the Facts 2016 An analysis of european plastics production, demand and waste data, Plastics – the Facts 2016.
23. EPSAR, E. de S. d'Aigues, 2018. Cuenca del Carraixet [WWW Document]. URL http://www.epsar.gva.es/sanejament/instalaciones/edar.aspx?id=8
24. Ferrer-Polonio, E., White, K., Mendoza-Roca, J.A., Bes-Piá, A., 2018. The role of the operating parameters of SBR systems on the SMP production and on membrane fouling reduction. J. Environ. Manage. 228, 205–212. https://doi.org/10.1016/j.jenvman.2018.09.036

25. Frias, J.P.G.L., Nash, R., 2019. Microplastics: Finding a consensus on the definition. Mar. Pollut. Bull. 138, 145–147. https://doi.org/10.1016/j.marpolbul.2018.11.022
26. GESAMP, 2015. Sources, fate and effects of microplastics in the marine environment: a global assessment". Reports Stud. GESAMP. https://doi.org/10.13140/RG.2.1.3803.7925
27. Gies, E.A., LeNoble, J.L., Noël, M., Etemadifar, A., Bishay, F., Hall, E.R., Ross, P.S., 2018. Retention of microplastics in a major secondary wastewater treatment plant in Vancouver, Canada. Mar. Pollut. Bull. 133, 553–561. https://doi.org/10.1016/j.marpolbul.2018.06.006
28. Harrison, J.P., Ojeda, J.J., Romero-González, M.E., 2012. The applicability of reflectance micro-Fourier-transform infrared spectroscopy for the detection of synthetic microplastics in marine sediments. Sci. Total Environ. 416, 455–463. https://doi.org/10.1016/j.scitotenv.2011.11.078
29. He, P., Chen, L., Shao, L., Zhang, H., Lü, F., 2019. Municipal solid waste (MSW)landfill: A source of microplastics? -Evidence of microplastics in landfill leachate. Water Res. 159, 38–45. https://doi.org/10.1016/j.watres.2019.04.060
30. Hermabessiere, L., Dehaut, A., Paul-Pont, I., Lacroix, C., Jezequel, R., Soudant, P., Duflos, G., 2017. Occurrence and effects of plastic additives on marine environments and organisms: A review. Chemosphere. https://doi.org/10.1016/j.chemosphere.2017.05.096
31. Hernandez, E., Nowack, B., Mitrano, D.M., 2017. Polyester Textiles as a Source of Microplastics from Households: A Mechanistic Study to Understand Microfiber Release during Washing. Environ. Sci. Technol. 51, 7036–7046. https://doi.org/10.1021/acs.est.7b01750
32. Hidalgo-Ruz, V., Gutow, L., Thompson, R.C., Thiel, M., 2012. Microplastics in the Marine Environment: A Review of the Methods Used for Identification and Quantification. https://doi.org/10.1021/es2031505
33. Hidayaturrahman, H., Lee, T.G., 2019. A study on characteristics of microplastic in wastewater of South Korea: Identification, quantification, and fate of microplastics during treatment process. Mar. Pollut. Bull. 146, 696–702. https://doi.org/10.1016/j.marpolbul.2019.06.071
34. Hurley, R.R., Lusher, A.L., Olsen, M., Nizzetto, L., 2018. Validation of a Method for Extracting Microplastics from Complex, Organic-Rich, Environmental Matrices. https://doi.org/10.1021/acs.est.8b01517
35. Institute of Chemistry University of Tartu, 2018. Textile fibres – Database of ATR-FT-IR spectra of various materials [WWW Document]. URL http://lisa.chem.ut.ee/IR_spectra/textile-fibres/ (accessed 5.21.20).
36. Jiang, Y., Yang, K., Shang, Y., Zhang, H., Wei, L., Wang, H., 2019. Response and recovery of aerobic granular sludge to pH shock for simultaneous removal of aniline and nitrogen. Chemosphere 221, 366–374. https://doi.org/10.1016/j.chemosphere.2018.12.207

37. Jin, Q., Kirk, M.F., 2018. pH as a Primary Control in Environmental Microbiology: 1. Thermodynamic Perspective. Front. Environ. Sci. 6, 21. https://doi.org/10.3389/fenvs.2018.00021

38. Joannis, C., Ruban, G., Gromaire, M.C., Bertrand-Krajewski, J.L., Chebbo, G., 2008. Reproducibility and uncertainty of wastewater turbidity measurements. Water Sci. Technol. https://doi.org/10.2166/wst.2008.292

39. Karami, A., Golieskardi, A., Choo, C.K., Romano, N., Ho, Y. Bin, Salamatinia, B., 2017. A high-performance protocol for extraction of microplastics in fish. Sci. Total Environ. 578, 485–494. https://doi.org/10.1016/j.scitotenv.2016.10.213

40. Kim, K.S., Yoo, J.S., Kim, S., Lee, H.J., Ahn, K.H., Kim, I.S., 2007. Relationship between the electric conductivity and phosphorus concentration variations in an enhanced biological nutrient removal process. Water Sci. Technol. 55, 203–208. https://doi.org/10.2166/wst.2007.053

41. Kole, P.J., Löhr, A.J., Van Belleghem, F., Ragas, A., 2017. Wear and Tear of Tyres: A Stealthy Source of Microplastics in the Environment. Int. J. Environ. Res. Public Health 14, 1265. https://doi.org/10.3390/ijerph14101265

42. Lares, M., Ncibi, M.C., Sillanpää, Markus, Sillanpää, Mika, 2018. Occurrence, identification and removal of microplastic particles and fibers in conventional activated sludge process and advanced MBR technology. Water Res. 133, 236–246. https://doi.org/10.1016/j.watres.2018.01.049

43. Lasch, P, Lasch, Peter, 2012. Spectral pre-processing for biomedical vibrational spectroscopy and microspectroscopic imaging Spectral Pre-processing for Vibrational Spectroscopy Spectral Pre-processing for Biomedical Vibrational Spectroscopy and Microspectroscopic Imaging 117, 100–114. https://doi.org/10.1016/j.chemolab.2012.03.011

44. Lee, H., Kim, Y., 2018. Treatment characteristics of microplastics at biological sewage treatment facilities in Korea. Mar. Pollut. Bull. 137, 1–8. https://doi.org/10.1016/j.marpolbul.2018.09.050

45. Li, X., Chen, L., Mei, Q., Dong, B., Dai, X., Ding, G., Zeng, E.Y., 2018. Microplastics in sewage sludge from the wastewater treatment plants in China. Water Res. 142, 75–85. https://doi.org/10.1016/j.watres.2018.05.034

46. Li, X., Mei, Q., Chen, L., Zhang, H., Dong, B., Dai, X., He, C., Zhou, J., 2019. Enhancement in adsorption potential of microplastics in sewage sludge for metal pollutants after the wastewater treatment process. Water Res. https://doi.org/10.1016/j.watres.2019.03.069

47. Liu, X., Yuan, W., Di, M., Li, Z., Wang, J., 2019. Transfer and fate of microplastics during the conventional activated sludge process in one wastewater treatment plant of China. Chem. Eng. J. 362, 176–182. https://doi.org/10.1016/j.cej.2019.01.033

48. Löder, M.G.J., Imhof, H.K., Ladehoff, M., Löschel, L.A., Lorenz, C., Mintenig, S., Piehl, S., Primpke, S., Schrank, I., Laforsch, C., Gerdts, G., 2017. Enzymatic Purification of Microplastics in Environmental

Samples. https://doi.org/10.1021/acs.est.7b03055

49. Löder, M.G.J., Kuczera, M., Mintenig, S., Lorenz, C., Gerdts, G., 2015. Focal plane array detector-based micro-Fourier-transform infrared imaging for the analysis of microplastics in environmental samples. Environ. Chem. 12, 563–581. https://doi.org/10.1071/EN14205

50. Long, Z., Pan, Z., Wang, W., Ren, J., Yu, X., Lin, L., Lin, H., Chen, H., Jin, X., 2019. Microplastic abundance, characteristics, and removal in wastewater treatment plants in a coastal city of China. Water Res. 155, 255–265. https://doi.org/10.1016/j.watres.2019.02.028

51. Lusher, A.L., Hurley, R.R., Vogelsang, C., Nizzetto, L., Olsen, M., 2018. Mapping microplastics in sludge. https://doi.org/10.13140/RG.2.2.25277.56804

52. Magni, S., Binelli, A., Pittura, L., Avio, C.G., Della Torre, C., Parenti, C.C., Gorbi, S., Regoli, F., 2019. The fate of microplastics in an Italian Wastewater Treatment Plant. Sci. Total Environ. 652, 602–610. https://doi.org/10.1016/j.scitotenv.2018.10.269

53. Magnusson, K., Norén, F., 2014. Screening of microplastic particles in and down-stream a wastewater treatment plant.

54. Mahon, A.M., O'connell, B., Healy, M.G., O'connor, I., Officer, R., Nash, R., Morrison, L., 2016. Microplastics in Sewage Sludge: Effects of Treatment. https://doi.org/10.1021/acs.est.6b04048

55. MSFD Technical Subgroup on Marine Litter, 2013. Guidance on Monitoring of Marine Litter in European Seas. https://doi.org/10.2788/99475

56. Munno, K., Helm, P.A., Jackson, D.A., Rochman, C., Sims, A., 2018. Impacts of temperature and selected chemical digestion methods on microplastic particles. Environ. Toxicol. Chem. 37, 91–98. https://doi.org/10.1002/etc.3935

57. Murphy, F., Ewins, C., Carbonnier, F., Quinn, B., 2016. Wastewater Treatment Works (WwTW) as a Source of Microplastics in the Aquatic Environment. https://doi.org/10.1021/acs.est.5b05416

58. Najafpour, G.D., 2015. Chapter 19: Biological Treatment, in: Biochemical Engineering and Biotechnology. Elsevier, pp. 557–595. https://doi.org/10.1016/b978-0-444-63357-6.00019-5

59. Ngo, P.L., Pramanik, B.K., Shah, K., Roychand, R., 2019. Pathway, classification and removal efficiency of microplastics in wastewater treatment plants. Environ. Pollut. 255. https://doi.org/10.1016/j.envpol.2019.113326

60. Ni, B.-J., 2013. Formation, Characterization and Mathematical Modeling of the Aerobic Granular Sludge, 1st ed, PhD thesis. Springer-Verlag Berlin Heidelberg. https://doi.org/10.1007/978-3-642-31281-6

61. Norén, F., 2007. Small plastic particles in Coastal Swedish waters, KIMO Sweden.

62. Nuelle, M.T., Dekiff, J.H., Remy, D., Fries, E., 2014. A new analytical approach for monitoring microplastics in marine sediments. Environ. Pollut. 184, 161–169. https://doi.org/10.1016/j.envpol.2013.07.027

63. Ou, H., Zeng, E.Y., 2018. Occurrence and fate of microplastics in wastewater treatment plants, in: Microplastic Contamination in Aquatic Environments: An Emerging Matter of Environmental Urgency. https://doi.org/10.1016/B978-0-12-813747-5.00010-2

64. Prata, J.C., da Costa, J.P., Duarte, A.C., Rocha-Santos, T., 2019a. Methods for sampling and detection of microplastics in water and sediment: A critical review. TrAC - Trends Anal. Chem. 110, 150–159. https://doi.org/10.1016/j.trac.2018.10.029

65. Prata, J.C., Reis, V., Matos, J.T.V., da Costa, J.P., Duarte, A.C., Rocha-Santos, T., 2019b. A new approach for routine quantification of microplastics using Nile Red and automated software (MP-VAT). Sci. Total Environ. 690, 1277–1283. https://doi.org/10.1016/j.scitotenv.2019.07.060

66. Renner, G., Nellessen, A., Schwiers, A., Wenzel, M., Schmidt, T.C., Schram, J., 2019. Data preprocessing & evaluation used in the microplastics identification process: A critical review & practical guide. TrAC - Trends Anal. Chem. https://doi.org/10.1016/j.trac.2018.12.004

67. Renner, G., Schmidt, T.C., Rgen Schram, J., 2017. A New Chemometric Approach for Automatic Identification of Microplastics from Environmental Compartments Based on FT-IR Spectroscopy. Anal. Chem. 89, 12045–12053. https://doi.org/10.1021/acs.analchem.7b02472

68. Rolsky, C., Kelkar, V., Driver, E., Halden, R.U., 2020. Municipal sewage sludge as a source of microplastics in the environment. Curr. Opin. Environ. Sci. Heal. https://doi.org/10.1016/j.coesh.2019.12.001

69. Rummel, C.D., Jahnke, A., Gorokhova, E., Kühnel, D., Schmitt-Jansen, M., 2017. Impacts of Biofilm Formation on the Fate and Potential Effects of Microplastic in the Aquatic Environment. https://doi.org/10.1021/ACS.ESTLETT.7B00164

70. Shim, J., Hee, S., Ab, H., Eo, S., Ab, E., 2017. Identification methods in microplastic analysis: a review. https://doi.org/10.1039/c6ay02558g

71. Shim, W.J., Hong, S.H., Eo, S., 2018. Marine microplastics: Abundance, distribution, and composition, in: Microplastic Contamination in Aquatic Environments: An Emerging Matter of Environmental Urgency. Elsevier, pp. 1–26. https://doi.org/10.1016/B978-0-12-813747-5.00001-1

72. Shim, W.J., Song, Y.K., Hong, S.H., Jang, M., 2016. Identification and quantification of microplastics using Nile Red staining. Mar. Pollut. Bull. 113, 469–476. https://doi.org/10.1016/j.marpolbul.2016.10.049

73. Siegfried, M., Koelmans, A.A., Besseling, E., Kroeze, C., 2017. Export of microplastics from land to sea. A modelling approach. Water Res. 127, 249–257. https://doi.org/10.1016/j.watres.2017.10.011

74. Simon, M., van Alst, N., Vollertsen, J., 2018. Quantification of microplastic mass and removal rates at wastewater treatment plants applying Focal Plane Array (FPA)-based Fourier Transform Infrared (FT-IR) imaging. Water Res. 142, 1–9. https://doi.org/10.1016/j.watres.2018.05.019

75. Sun, J., Dai, X., Wang, Q., van Loosdrecht, M.C.M., Ni, B.J., 2019. Microplastics in wastewater treatment plants: Detection, occurrence and removal. Water Res. https://doi.org/10.1016/j.watres.2018.12.050

76. Sussarellu, R., Suquet, M., Thomas, Y., Lambert, C., Fabioux, C., Pernet, M.E.J., Goïc, N. Le, Quillien, V., Mingant, C., Epelboin, Y., Corporeau, C., Guyomarch, J., Robbens, J., Paul-Pont, I., Soudant, P., Huvet, A., 2016. Oyster reproduction is affected by exposure to polystyrene microplastics. Proc. Natl. Acad. Sci. U. S. A. 113, 2430–2435. https://doi.org/10.1073/pnas.1519019113

77. Tagg, A.S., Sapp, M., Harrison, J.P., Jesús, J., Ojeda, J.J., 2015. Identification and Quantification of Microplastics in Wastewater Using Focal Plane Array-Based Reflectance Micro-FT-IR Imaging. https://doi.org/10.1021/acs.analchem.5b00495

78. Talvitie, J., Mikola, A., Koistinen, A., Setälä, O., 2017a. Solutions to microplastic pollution – Removal of microplastics from wastewater effluent with advanced wastewater treatment technologies. Water Res. 123, 401–407. https://doi.org/10.1016/j.watres.2017.07.005

79. Talvitie, J., Mikola, A., Setälä, O., Heinonen, M., Koistinen, A., 2017b. How well is microlitter purified from wastewater? – A detailed study on the stepwise removal of microlitter in a tertiary level wastewater treatment plant. Water Res. 109, 164–172. https://doi.org/10.1016/j.watres.2016.11.046

80. Turner, A., Holmes, L.A., 2015. Adsorption of trace metals by microplastic pellets in fresh water. Environ. Chem. 12, 600. https://doi.org/10.1071/EN14143

81. von Friesen, L.W., Granberg, M.E., Hassellöv, M., Gabrielsen, G.W., Magnusson, K., 2019. An efficient and gentle enzymatic digestion protocol for the extraction of microplastics from bivalve tissue. Mar. Pollut. Bull. 142, 129–134. https://doi.org/10.1016/j.marpolbul.2019.03.016

82. Xu, S., Fan, A., Wang, H., Zhang, X., Wang, X., 2020. Raman-based Nanoscale Thermal Transport Characterization: A Critical Review. Int. J. Heat Mass Transf. 154, 119751. https://doi.org/10.1016/j.ijheatmasstransfer.2020.119751

83. Yang, L., Li, K., Cui, S., Kang, Y., An, L., Lei, K., 2019. Removal of microplastics in municipal sewage from China's largest water reclamation plant. Water Res. 155, 175–181. https://doi.org/10.1016/j.watres.2019.02.046

84. Zhao, S., Danley, M., Ward, J.E., Li, D., Mincer, T.J., 2017. An approach for extraction, characterization and quantitation of microplastic in natural marine snow using Raman microscopy †. https://doi.org/10.1039/c6ay02302a

85. Ziajahromi, S., Neale, P.A., Rintoul, L., Leusch, F.D.L., 2017. Wastewater treatment plants as a pathway for microplastics: Development of a new approach to sample wastewater-based microplastics. Water Res. 112, 93–99. https://doi.org/10.1016/j.watres.2017.01.042

86. Zitko, V., Hanlon, M., 1991. Another source of pollution by plastics: Skin cleaners with plastic scrubbers.

Mar. Pollut. Bull. 22, 41–42. https://doi.org/10.1016/0025-326X(91)90444-W

87. Zubris, K.A. V., Richards, B.K., 2005. Synthetic fibers as an indicator of land application of sludge. Environ. Pollut. 138, 201–211. https://doi.org/10.1016/j.envpol.2005.04.013